AD______________

AWARD NUMBER DAMD17-97-1-7180

TITLE: Cell Cycle of the BRCA1 Gene Product

PRINCIPAL INVESTIGATOR: David Livingston

CONTRACTING ORGANIZATION: Dana Farber Cancer Institute
Boston, Massachusetts 02115

REPORT DATE: September 1998

TYPE OF REPORT: Annual

PREPARED FOR: Commander
U.S. Army Medical Research and Materiel Command
Fort Detrick, Maryland 21702-5012

DISTRIBUTION STATEMENT: Approved for public release; distribution unlimited

REPORT DOCUMENTATION PAGE

Form Approved
OMB No. 0704-0188

1. AGENCY USE ONLY *(Leave blank)*

2. REPORT DATE
September 1998

3. REPORT TYPE AND DATES COVERED
Annual (15 Aug 97 - 14 Aug 98)

4. TITLE AND SUBTITLE
Cell Cycle of the BRCA1 Gene Product

5. FUNDING NUMBERS
DAMD17-97-1-7180

6. AUTHOR(S)
Livingston, David

7. PERFORMING ORGANIZATION NAME(S) AND ADDRESS(ES)
Dana Farber Cancer Institute
Boston, Massachusetts 02115

8. PERFORMING ORGANIZATION REPORT NUMBER

9. SPONSORING / MONITORING AGENCY NAME(S) AND ADDRESS(ES)
U.S. Army Medical Research and Materiel Command
ATTN: MCMR-RMI-S
504 Scott Street
Fort Detrick, Maryland 21702-5012

10. SPONSORING / MONITORING AGENCY REPORT NUMBER

11. SUPPLEMENTARY NOTES

12a. DISTRIBUTION / AVAILABILITY STATEMENT
Approved for public release; distribution unlimited

12b. DISTRIBUTION CODE

13. ABSTRACT *(Maximum 200 words)*

This proposal is aimed at understanding the function of BRCA1 through analysis of its cell cycle behavior. We found that BRCA1 colocalizes in S phase/G2 foci with hRad51, a protein with key roles in homologous recombination. The proteins also colocalized in primary human spermatocytes, suggesting a role for BRCA1 in meiotic recombination. An endogenous BRCA1-Rad51 complex was detected in somatic cells. We found that BRCA1 underwent specific phosphorylation following DNA damage. In response to some DNA damaging agents, BRCA1 and Rad51 were recruited to replication areas of the S phase nucleus, suggesting an interaction with damaged, replicating DNA.

A second major hereditary breast cancer gene product, BRCA2, can also interact with Rad51. We have developed reagents for working with hBRCA2, and identified a specific biochemical interaction between BRCA1 and BRCA2. BRCA2 colocalized with BRCA1 in nuclear foci during S/G2 phases of the somatic cell cycle, both before and after DNA damage, and in meiotic cells. This suggests that BRCA1 and BRCA2 operate, at least in part, on a common pathway involved in homologous recombination. Further, the results indicate that defects in the proper regulation of homologous recombination may contribute to the etiology of early-onset breast cancer.

14. SUBJECT TERMS
Breast Cancer

15. NUMBER OF PAGES
60

16. PRICE CODE

17. SECURITY CLASSIFICATION OF REPORT	18. SECURITY CLASSIFICATION OF THIS PAGE	19. SECURITY CLASSIFICATION OF ABSTRACT	20. LIMITATION OF ABSTRACT
Unclassified	Unclassified	Unclassified	Unlimited

FOREWORD

Opinions, interpretations, conclusions and recommendations are those of the author and are not necessarily endorsed by the U.S. Army.

____ Where copyrighted material is quoted, permission has been obtained to use such material.

____ Where material from documents designated for limited distribution is quoted, permission has been obtained to use the material.

____ Citations of commercial organizations and trade names in this report do not constitute an official Department of Army endorsement or approval of the products or services of these organizations.

DL In conducting research using animals, the investigator(s) adhered to the "Guide for the Care and Use of Laboratory Animals," prepared by the Committee on Care and use of Laboratory Animals of the Institute of Laboratory Resources, national Research Council (NIH Publication No. 86-23, Revised 1985).

DL For the protection of human subjects, the investigator(s) adhered to policies of applicable Federal Law 45 CFR 46.

DL In conducting research utilizing recombinant DNA technology, the investigator(s) adhered to current guidelines promulgated by the National Institutes of Health.

DL In the conduct of research utilizing recombinant DNA, the investigator(s) adhered to the NIH Guidelines for Research Involving Recombinant DNA Molecules.

DL In the conduct of research involving hazardous organisms, the investigator(s) adhered to the CDC-NIH Guide for Biosafety in Microbiological and Biomedical Laboratories.

PI - Signature Date

TABLE OF CONTENTS

INTRODUCTION

Purpose and Scope of the Research

The objective of this research program is to obtain insight into the function of the hereditary breast-ovarian cancer gene, BRCA1. The initial goal was to determine the significance of BRCA1's localization to nuclear foci correlated with the DNA synthesis phase (S phase) of the cell cycle; to search for proteins which colocalize with BRCA1 in these foci; and to determine the biochemical and functional significance of BRCA1's colocalization with such proteins.

Background

The molecular basis of familial breast/ovarian cancer predisposition has been brought into focus recently with the cloning of two genes which, when carried in heterozygous mutant form in the germline, predispose an individual to these diseases (1, 2). Termed BRCA1 and BRCA2, mutations in one or other of the two genes can account for a significant proportion of cases of familial breast/ovarian cancers. The patterns of gene mutation, genetics of inheritance, and loss of the wild-type allele in tumors arising in familial cases, strongly imply that BRCA1 and BRCA2 are tumor suppressor genes (3-5). How these genes can protect against cancer, and how loss of function of these genes can predispose to cancer, are major questions addressed by this proposal. Progress in answering them has the potential to influence therapeutic approaches to cases of hereditary breast/ovarian cancer, and may provide insight into sporadic cases of these diseases.

The BRCA1 open reading frame predicts a polypeptide of 1863 amino acids (1). Analysis of disease-predisposing germline mutations in the BRCA1 gene indicate that truncation mutation is the major means of inactivating BRCA1. The most subtle disease-predisposing truncation mutation, Tyr1853->Term, deletes only the last eleven amino acids from the BRCA1 open reading frame (6). This implicates the very C terminus of BRCA1 in a tumor suppressor fuction. In addition, missense mutation can also inactivate BRCA1. Although probable disease-predisposing missense mutations in BRCA1 have been detected throughout the open reading frame, there is some concentration of this type of mutation in two structural motifs. These are: an amino-terminal zinc-binding RING domain, and a more loosely defined C terminal domain (present as two tandem repeats in BRCA1) termed BRCT (7-9). Missense mutation in the RING domain preferentially targets one of two zinc-binding cysteine residues (Cys61->Gly; Cys64->Gly) (5). This data strongly implicates the RING domain and the BRCT domain of BRCA1 in tumor suppressor function.

Recently, Richard Baer's group identified a novel gene whose product binds the BRCA1 RING domain in vivo and in vitro (10). Termed BARD1, the gene product is a polypeptide of ~100kDa, bearing some structural similarlty to BRCA1, in that it too possesses an amino terminal RING domain and two tandem repeated C terminal BRCT domains. The ability of BRCA1 to bind BARD1 is abolished in the two missense mutant forms of BRCA1 which lose BRCA1 RING domain function (Cys61->Gly; Cys64->Gly). Thus, the BARD1-BRCA1 interaction is also likely to be important for tumor suppression.

Various functions have been ascribed to the two BRCA1 BRCT domains, present as tandem repeats near the C terminus. This section of the BRCA1 polypeptide is generally acidic, which led to the suggestion that BRCA1 might be a transcription factor (1). Consistent with this, the C terminus (including the BRCT region), when fused to the DNA binding module of GAL4, was able to transactivate a GAL4 reporter gene (11, 12). This function was suppressed if the wild-type BRCA1 C terminus was replaced with various clinically-described missense mutants of this segment of BRCA1. This would appear to suggest a role for BRCA1 in transcription. In apparent support of such a role, BRCA1 was found to physically associate with components of the RNA polymerase II general transcriptional apparatus (also termed "holoenzyme") (13). Taken together, however, these data are also consistent with a role for BRCA1 in DNA repair, since various DNA repair elements are seen associated with the RNA polymerase II "holoenzyme" (14).

The BRCA1 mRNA is ubiquitously expressed in both human and mouse tissue. A relationship between BRCA1 and proliferation is seen in the elevated levels of BRCA1 in rapidly proliferating tissues of developing mouse embryos, and in the induction of the BRCA1 mRNA at the G1/S border in cultures human cell lines (15-17). Analysis of mice bearing homozygous targeted mutations of BRCA1 in the germline revealed a further, paradoxical, relationship between BRCA1 and proliferation. In particular, BRCA1 -/- embryos died around the time of gastrulation, with an apparent proliferation deficit (18, 19). One study found that mRNA levels of the cell cycle inhibitor p21 were greatly elevated in such embryos, prior to cell death (18). The paradoxical phenotype of BRCA1 -/- mice may be understandable in the light of more recent data, which points to a role for BRCA1 in the maintenance of genome integrity (20, 21). This is dealt with in the section immediately following this one.

BODY

Evidence of a role for BRCA1 in genome integrity maintenance came from our work analyzing BRCA1 immunolocalization within the nulceus of cells in the S/G2 phase of the cell cycle. BRCA1 immunostaining revealed characteristic nuclear foci ("dots") in every human cell line examined (22). We found that these foci also contain hRad51 (20), the human homolog of the S. cerevisiae Rad51 recombinase, itself a close structural and functional homolog of the bacterial RecA protein. All Rad51/RecA species examined to date are necessary for efficient homologous recombination processing of DNA in vivo and in vitro (23-25). In S. cerevisiae, Rad51 mutants reveal profound defects in two processes closely linked to homologous recombination - double-stranded break repair and meiotic recombination (26). Interestingly, mice bearing homozygous mutations of Rad51 in the germline are approximate phenocopies of BRCA1-/- mice, revealing an early deficit in proliferation with early embryonic lethality (27).

Consistent with the colocalization of BRCA1 with Rad51 in S/G2 cells, an endogenous complex containing the two proteins was detected in extracts of human cells. In addition, Rad51 and BRCA1 colocalized upon the axial element of the developing synaptonemal complex in primary human spermatocytes, strongly suggesting a role for BRCA1 in meiotic as well as mitotic recombination (20).

In support of a role for BRCA1 in DNA repair, or in processes connected with genome integrity maintenance, the BRCA1 S phase dots were found to be labile in the face of acute DNA damage. The dispersion of BRCA1 from S phase foci was accompanied by two temporally related phenomena. First, after hydroxyurea treatment or low dose UV treatment to cells, BRCA1 was found to have relocated onto subnuclear regions containing PCNA (a marker of replication areas). Second, BRCA1 underwent specific phosphorylation acutely after DNA damage of any kind in S phase (21). This phosphorylation was distinct from the known phosphorylation change which occurs in BRCA1 during the G1/S phase transition (21, 28). In its relocation onto PCNA$^+$ replication sites, BRCA1 was accompanied by both Rad51 and BARD1 (a BRCA1-associated protein - see above). This relocalization phenomenon could be interpreted as a DNA repair response, especially in view of the persistent association of BRCA1 with Rad51 under such circumstances. More broadly, the specific phosphorylation of BRCA1 after DNA damage in S phase is likely to indicate that BRCA1 is the target of one or more DNA structure-dependent cell cycle checkpoints (21).

Many features of BRCA2, including the phenotype of BRCA2-/- mice, suggest that it may cooperate with BRCA1 on a common biochemical pathway. One possible common element on such a pathway is Rad51. In order to address this question, we asked whether

BRCA1 and BRCA2 can interact in vivo. This entailed the development of a full set of reagents for working with BRCA2, including assembly of the full-length cDNA, development of methods for transient expression of BRCA2 after transfection into human cell lines; and development of a panel of polyclonal affinity-purified antibodies specific for BRCA2. BRCA1 and BRCA2 were found to co-exist in a common biochemical complex within naive cell extracts of several different cancer cell lines. A BRCA2-interacting surface on BRCA1 was identified within residues 1314-1863 of BRCA1 (29).

Subcellular localization studies, performed on multiple different human canecr cell lines, using two color immunofluorescence staining and confocal microscopy, revealed co-localization of BRCA2 with BRCA1 and Rad51 in S/G2 phase-correlated nuclear foci. In meiotic cells, the three proteins colocalized on the axial element of the developing synaptonemal complex. Following hydroxyurea or UV treament of S phase cells, BRCA2 was noted to relocalize to $PCNA^+$ regions of the somatic S phase cell nucleus, in a manner that retained its colocalization with BRCA1 and Rad51 (29).

NOTE: Further detailed information regarding Experimental methods, Results and Discussion are contained within three appendices (attached). Each takes the form of a publication arising from work conducted under the experimental plan:"Cell Cycle Analysis of the BRCA1 Gene Product".

Appendix 1: Scully, R., Chen, J., Plug, A., Xiao, Y., Weaver, D., Feunteun, J., Ashley, T., and Livingston, D. M. (1997). Association of BRCA1 with Rad51 in mitotic and meiotic cells. Cell *88*, 265-275.

Appendix 2: Scully, R., Chen, J., Ochs, R., Keegan, K., Hoekstra, M., Feunteun, J., and Livingston, D. M. (1997). Dynamic changes during S phase of BRCA1 subnuclear location and phosphorylation state are initiated by DNA damage. Cell *90*, 425-435.

Appendix 3: Chen, J., Silver, D.P., Walpita, D., Cantor, S.B., Gazdar, A.F., Tomlinson, G., Couch, F.J., Weber, B.L., Ashley, T., Livingston, D.M. and Scully, R. (1998). Stable Interaction between the Products of the BRCA1 and BRCA2 Tumor Suppressor Genes in Mitotic and Meiotic Cells. Molecular Cell *2*, 317-328.

CONCLUSIONS

The above work indicates that BRCA1, BRCA2 and Rad51 participate in a common DNA damage response pathway, likely connected with homologous recombination. This pathway, when disabled, appears to predispose to early onset breast cancer. Thus, other genes participating in this pathway may also be found to be hereditary breast cancer genes. Further, this pathway may also be implicated in sporadic cases of breast cancer.

REFERENCES

1. Miki, Y., Swensen, J., Shattuck-Eidens, D., Futreal, P. A., Harshman, K., Tavtigian, S., Liu, Q., Cochran, C., Bennett, L. M., Ding, W., Bell, R., Rosenthal, J., Hussey, C., Tran, T., McClure, M., Frye, C., Hattier, T., Phelps, R., Haugen-Strano, A., Katcher, H., Yakumo, K., Gholami, Z., Shaffer, D. & Stone, S. (1994) *Science* **266,** 66-71.

2. Wooster, R., Bignell, G., Lancaster, J. & al., e. (1995) *Nature* **378,** 789.

3. Smith, S. A., Easton, D. F., Evans, D. G. R. & Ponder, B. A. J. (1992) *Nature Genetics* **2,** 128-131.

4. Neuhausen, S. L. & Marshall, C. J. (1994) *Cancer Res.* **54,** 6069-6072.

5. Shattuck-Eidens, D., McClure, M., Simard, J., Labrie, F., Narod, S., Couch, F., Hoskins, K., Weber, B., Castilla, L., Erdos, M., Brody, L., Friedman, L., Ostermeyer, E., Szabo, C., King, M.-C., Jhanwar, S., Offit, K., Norton, L., Gilewski, T., Lubin, M., Osborne, M., Black, D., Boyd, M. & Steel, M. (1995) *JAMA* **273,** 535-541.

6. Friedman, L. S., Ostermeyer, E. A., Szabo, C. I., Dowd, P., Lynch, E. D., Rowell, S. E. & King, M.-C. (1994) *Nature Genetics* **8,** 399-404.

7. Koonin, V. F., Altschul, S. F. & Bork, P. (1996) *Nature Genet.* **13,** 266-267.

8. Bork, P., Hofmann, K., Bucher, P., Neuwald, A. F., Altschul, S. F. & Koonin, E. V. (1997) *FASEB J* **11,** 68-76.

9. Callebaut, I. & Mornon, J. P. (1997) *FEBS Lett* **400,** 25-30.

10. Wu, L. C., Wang, Z. W., Tsan, J. T., Spillman, M. A., Phung, A., Xu, X. L., Yang, M. C., Hwang, L. Y., Bowcock, A. M. & Baer, R. (1996) *Nature Genetics* **14,** 430-40.

11. Chapman, M. S. & Verma, I. M. (1996) *Nature* **382,** 678-679.

12. Monteiro, A. N. A., August, A. & Hanafusa, H. (1996) *Proc. Natl. Acad. Sci. USA* **93,** 13595-13599.

13. Scully, R., Anderson, S. F., Chao, D. M., Wei, W., Ye, L., Young, R. A., Livingston, D. M. & Parvin, J. D. (1997) *Proc. Natl. Acad. Sci. (U.S.A.)* **94,** 5605-5610.

14. Maldonado, E., Shiekhattar, R., Sheldon, M., Cho, H., Drapkin, R., Rickert, P., Lees, E., Anderson, C. W., Linn, S. & Reinberg, D. (1996) *Nature* **381,** 86-9.

15. Lane, T. F., Deng, C., Elson, A., Lyu, M. S., Kozak, C. A. & Leder, P. (1995) *Genes Dev.* **9,** 2712-2722.

16. Marquis, S. T., Rajan, J. V., Wynshaw-Boris, A., Xu, J. & Yin, G.-Y. (1995) *Nature Genetics* **11,** 17-26.

17. Gudas, J. M., Li, T., Nguyen, H., Jensen, D., Rauscher, F. J. I. & Cowan, K. H. (1996) *Cell Growth Differ.* **7,** 717-723.

18. Hakem, R., de la Pomba, J. L., Sirard, C., Mo, R., Woo, M., Hakem, A., Wakeham, A., Potter, J., Reitmair, A., Billia, F., Firpo, E., Hui, C. C., Roberts, J., Rossant, J. & Mak, T. W. (1996) *Cell* **85,** 1009-1023.

19. Liu, C. Y., Flesken-Nikitin, A., Li, S., Zeng, Y. & Lee, W.-H. (1996) *Genes Dev.* **10,** 1835-43.

20. Scully, R., Chen, J., Plug, A., Xiao, Y., Weaver, D., Feunteun, J., Ashley, T. & Livingston, D. M. (1997) *Cell* **88,** 265-275.

21. Scully, R., Chen, J., Ochs, R. L., Keegan, K., Hoekstra, M., Feunteun, J. & Livingston, D. M. (1997) *Cell* **90,** 425-435.

22. Scully, R., Ganesan, S., Brown, M., De Caprio, J. A., Cannistra, S. A., Feunteun, J., Schnitt, S. & Livingston, D. M. (1996) *Science* **272,** 123-125.

23. Radding, C. M. (1991) *J. Biol. Chem.* **266,** 5355-5358.

24. Sung, P. (1994) *Science* **265,** 1241-1243.

25. Baumann, P., Benson, F. E. & West, S. C. (1996) *Cell* **87,** 757-766.

26. Shinohara, A., Ogawa, H. & Ogawa, T. (1992) *Cell* **69,** 457-470.

27. Lim, D.-S. & Hasty, P. (1996) *Mol. Celll. Biol.* **16,** 7133-7143.

28. Chen, Y. M., Farmer, A. A., Chen, C. F., Jones, D. C., Chen, P. L. & Lee, W. H. (1996) *Cancer Research* **56,** 3168-3172.

29. Chen, J., Silver, D. P., Walpita, D., Cantor, S. B., Gazdar, A. F., Tomlinson, G., Couch, F. J., Weber, B. L., Ashley, T., Livingston, D. M. & Scully, R. (1998) *Molecular Cell* **2,** 317-328.

DAMD17-97-1-7180

APPENDIX 1

Cell

Number 2 January 24, 1997

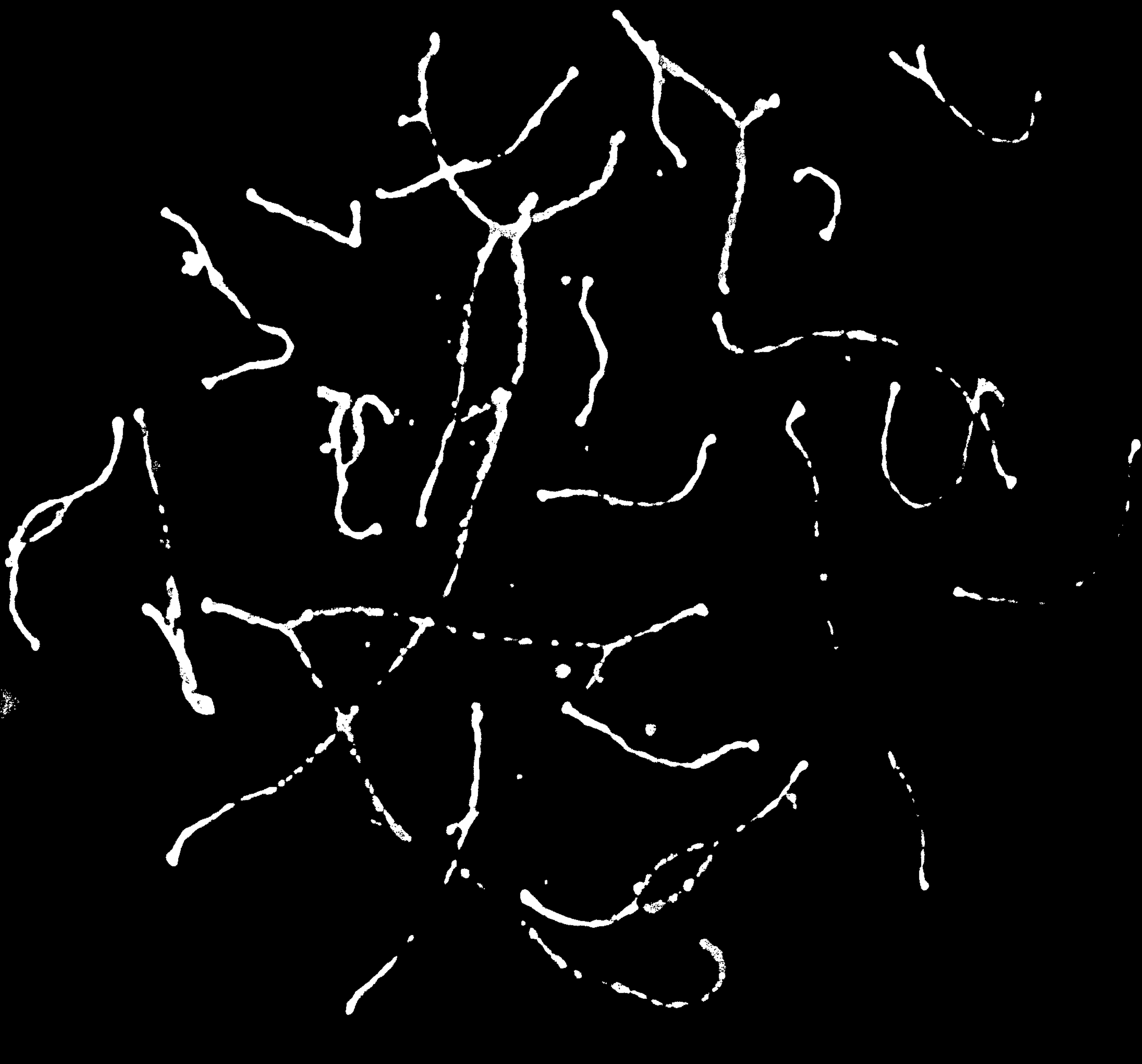

BRCA1 and Rad51 on Meiotic Chromosomes

Cell, Vol. 88, 265–275, January 24, 1997, Copyright ©1997 by Cell Press

Association of BRCA1 with Rad51 in Mitotic and Meiotic Cells

Ralph Scully,* Junjie Chen,*§
Annemieke Plug,†§ Yonghong Xiao,*
David Weaver,* Jean Feunteun,‡
Terry Ashley,† and David M. Livingston*
*The Dana-Farber Cancer Institute
Harvard Medical School
Boston, Massachusetts 02115
†Department of Genetics
Yale University School of Medicine
New Haven, Connecticut 06520-8005
‡Centre National de la Recherche Scientifique
Institut Gustave-Roussy
Cedex 94805 Villejuif
France

Summary

BRCA1 immunostaining reveals discrete, nuclear foci during S phase of the cell cycle. Human Rad51, a homolog of bacterial RecA, behaves similarly. The two proteins were found to colocalize in vivo and to coimmunoprecipitate. BRCA1 residues 758–1064 alone formed Rad51-containing complexes in vitro. Rad51 is also specifically associated with developing synaptonemal complexes in meiotic cells, and BRCA1 and Rad51 were both detected on asynapsed (axial) elements of human synaptonemal complexes. These findings suggest a functional interaction between BRCA1 and Rad51 in the meiotic and mitotic cell cycles, which, in turn, suggests a role for BRCA1 in the control of recombination and of genome integrity.

Introduction

Between 5% and 10% of all breast cancers and 10% of ovarian cancers can be attributed to mutations of highly penetrant, autosomal dominant susceptibility genes (Newman et al., 1988; Claus et al., 1991). One of these is *BRCA1*, which maps to 17q21 (Hall et al., 1990; Narod et al., 1991; reviewed in Feunteun and Lenoir, 1996). *BRCA1* mutations are responsible for almost all families with inherited breast and ovarian cancer and for approximately half of the families with breast cancer only (Easton et al., 1993). The detection of LOH affecting the wild-type *BRCA1* allele in tumors from *BRCA1* mutation carriers implies that *BRCA1* is a tumor suppressor gene (Smith et al., 1992; Neuhausen and Marshall, 1994).

The *BRCA1* cDNA encodes an 1863 residue polypeptide of as yet unknown biochemical function (Miki et al., 1994). The BRCA1 sequence includes an N-terminal RING domain (reviewed in Freemont, 1993; Saurin et al., 1996), a negatively charged region in its C terminus, and C-terminal sequences partially homologous to yeast RAD9 and to a cloned p53 binding protein (Koonin et al., 1996). The negatively charged segment may contribute to transcription-inducing activity of a GAL4–BRCA1 fusion protein (Chapman and Verma, 1996; Monteiro et al., 1996). Whether BRCA1 enacts a transcriptional control function is not yet known.

To date, more than 100 unique, naturally occurring *BRCA1* germline mutations have been identified (Castilla et al., 1994; Friedman et al., 1994; Simard et al., 1994; Shattuck-Eidens et al., 1995). Somatic *BRCA1* mutations have not been detected in sporadic breast cancer and are rare in sporadic ovarian cancer (Merajver et al., 1995). Approximately 90% of breast or ovarian cancer–linked *BRCA1* mutations leads to truncated products. The pattern of truncations and missense mutations suggests that multiple regions of the protein structure contribute to its tumor suppression function.

Multiple BRCA1-specific antibodies detect a protein migrating at ~220 kDa in various cell lines (Chen et al., 1995; Scully et al., 1996). This polypeptide comigrates with and has a peptide map indistinguishable from that of the 220 kDa clonal BRCA1 in vitro translation product (Chapman and Verma, 1996; Scully and Livingston, unpublished data). Several reports indicate that p220 BRCA1 is a nuclear protein in cultured cells and normal tissues (Chen et al., 1995; Chapman and Verma, 1996; Chen et al., 1996; Scully et al., 1996).

The developmental pattern of murine *BRCA1* expression (Lane et al., 1995; Marquis et al., 1995) and its cell cycle–regulated expression (Gudas et al., 1995; Gudas et al., 1996; Vaughn et al., 1996) suggest a relationship between BRCA1 function and cellular proliferation (e.g., in the mammary gland in response to ovarian hormones). Loss of BRCA1 function is a lethal event during murine embryogenesis (Gowen et al., 1996; Hakem et al., 1996; Liu et al., 1996). Some *BRCA1*$^{-/-}$ embryos revealed an early (~E7.5) proliferation block with elevated levels of p21 mRNA at E4 (Hakem et al., 1996).

There are also reports of growth- and transformation-suppressing behavior, as well as death of cells that acutely overproduce BRCA1 (Holt et al., 1996; Rao et al., 1996; Shao et al., 1996; Wilson et al., 1996). However, these studies do not reveal the mechanism underlying these effects.

We have reported that BRCA1 immunostaining is characterized by a "nuclear dot" pattern (Scully et al., 1996). As suggested by the work of Chen et al. (1996) and as defined below, BRCA1 nuclear dots appear in S phase of the cell cycle. Among nuclear proteins known to be characterized by dot-like staining is human Rad51 (hRad51), a homolog of bacterial RecA. hRad51 nuclear dots also appear in S phase (Tashiro et al., 1996).

hRad51 is a member of a protein family known to mediate DNA strand–exchange functions leading to normal recombination (Kowalczykowski, 1991; Radding, 1991; Sung, 1994; Sung and Robberson, 1995; Baumann et al., 1996). Although yeast, mutated for *RAD51*, cannot perform normal meiotic recombination and double-stranded break repair, they are viable (Shinohara et al., 1992). In contrast, mice bearing homozygous, loss-of-function *RAD51* mutations died early in embryogenesis. Moreover, like *BRCA1*$^{-/-}$ embryos, cells of *RAD51*$^{-/-}$ embryos revealed a proliferation defect, suggesting an

§These authors contributed equally to this work.

additional role for Rad51 in cell growth control (Lim and Hasty, 1996; Tsuzuki et al., 1996). Here, we report that BRCA1 and hRad51 colocalize in S phase cells, interact physically, and, in keeping with previous reports of the behavior of hRad51 (Ashley et al., 1995; Plug et al., 1996), share common space on the surfaces of zygotene and pachytene meiotic chromosomes. These observations identify a biochemical pathway involving BRCA1 and suggest that BRCA1 participates in nuclear processes that lead to normal chromosomal recombination and genome integrity control.

Results

S Phase Nuclear Dot Pattern of BRCA1

The identification of discrete, nuclear dot–like structures as loci of endogenous BRCA1 protein in multiple cell lines and diploid human fibroblasts has been established previously, using seven different BRCA1 monoclonal antibodies (MAb's) and an affinity-purified BRCA1 polyclonal Ab (Scully et al., 1996). BRCA1 nuclear dots were observed in only a fraction of asynchronous cells. The remaining cells revealed a weaker, more diffuse nuclear signal (data not shown). This suggested that the dot-like staining might be cell cycle–dependent. Serum starvation and synchronous release were used to synchronize populations of the breast cancer cell line, MCF7, which were then subjected to BRCA1 immunostaining. In cultures enriched for S phase cells (t = 24 hr population; see Figure 1), most cells scored positively for BRCA1 nuclear dots, while a G1-enriched population presented weaker and largely diffuse nuclear staining (t = 12 hr; see Figure 1 and see also Chen et al., 1996). Analysis of the same cultures with irrelevant MAb revealed no nuclear staining (Scully et al., 1996; data not shown). These and other results not shown here indicate that the BRCA1 nuclear dot pattern is S phase–specific.

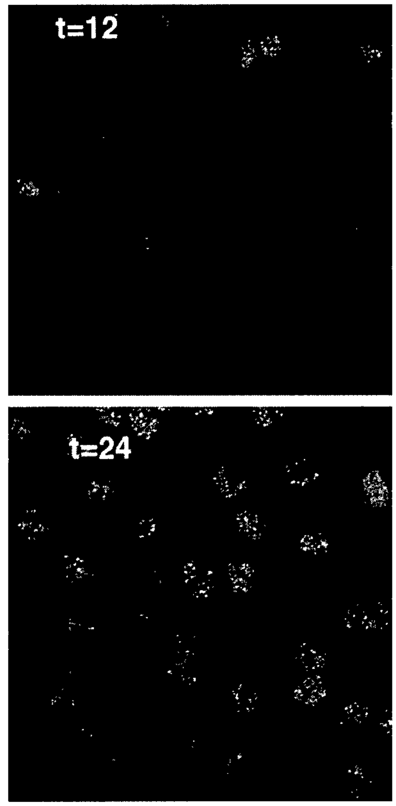

Figure 1. BRCA1 Nuclear Dot Pattern Arises in S Phase

MCF7 cells were serum-starved and released, as described in Experimental Procedures. The figure depicts immunostaining using BRCA1 MAb MS13. Identical results were obtained using two other BRCA1 MAb's (MS110 and AP16). (t = 12), cells 12 hr after serum release (83% G1, 9% S); (t = 24), cells 24 hr after serum release (30% G1, 62% S).

Colocalization of the BRCA1 and Rad51 Immunostaining Patterns in S Phase Nuclei

Rad51, a mammalian RecA homolog, has been shown previously to form S phase–specific nuclear foci (Tashiro et al., 1996). Given the apparent similarity in the timing of appearance of Rad51 and BRCA1 nuclear dots, we asked whether Rad51 and BRCA1 staining colocalize in the same structures. Two-color confocal immunostaining with a BRCA1 monoclonal antibody and an affinity-purified, rabbit polyclonal antiserum raised against clonal human Rad51 (Haaf et al., 1995; Plug et al., 1996) revealed significant, albeit not complete, colocalization of the BRCA1 and the Rad51 nuclear dot patterns (Figure 2). Figure 2 also illustrates cell-to-cell variability in colocalization between BRCA1 and Rad51 signals. In some cells, colocalization of dot signals was extensive (e.g., Figures 2D–2F). In others, the overlap was incomplete (e.g., Figures 2A–2C, top cell). This suggested that the colocalization of BRCA1 and Rad51 is conditional or transient, even in S phase cells. Similar colocalization results were obtained in WI38 and CV-1 cells. These observations raised the possibility that BRCA1 and Rad51 physically interact.

The specificity of the affinity-purified Rad51 antiserum was assessed. Immunoblotting of an MCF7 cell extract with this antiserum revealed a single band, migrating at 38 kDa, the expected size of hRad51 (data not shown). This band disappeared after preabsorbing the antiserum with clonal GST–hRad51 but not with 10-fold more unfused GST. The same was true for the nuclear immunofluorescence signal generated with this Ab. No reaction between this antiserum and authentic BRCA1 was detected by immunoblotting (data not shown).

Biochemical Evidence of an In Vivo BRCA1–Rad51 Interaction

MCF7, 293T, and HeLa cell immunoprecipitates generated with the BRCA1 MAb, SG11, contained endogenous, 38 kDa Rad51, as determined by immunoblotting (Figure 3A and data not shown). The Rad51 and BRCA1 signals detected in SG11 immunoprecipitates were suppressed by preincubation of this BRCA1 antibody with the immunizing BRCA1 peptide. Only a fraction of the ambient Rad51 coimmunoprecipitated with BRCA1 by this method. Although S phase extracts contained more BRCA1–Rad51 complexes than G1 extracts (data not shown), even in S phase–enriched fractions, there was incomplete coprecipitation of hRad51 with BRCA1. Whether this results from the presence of an excess of

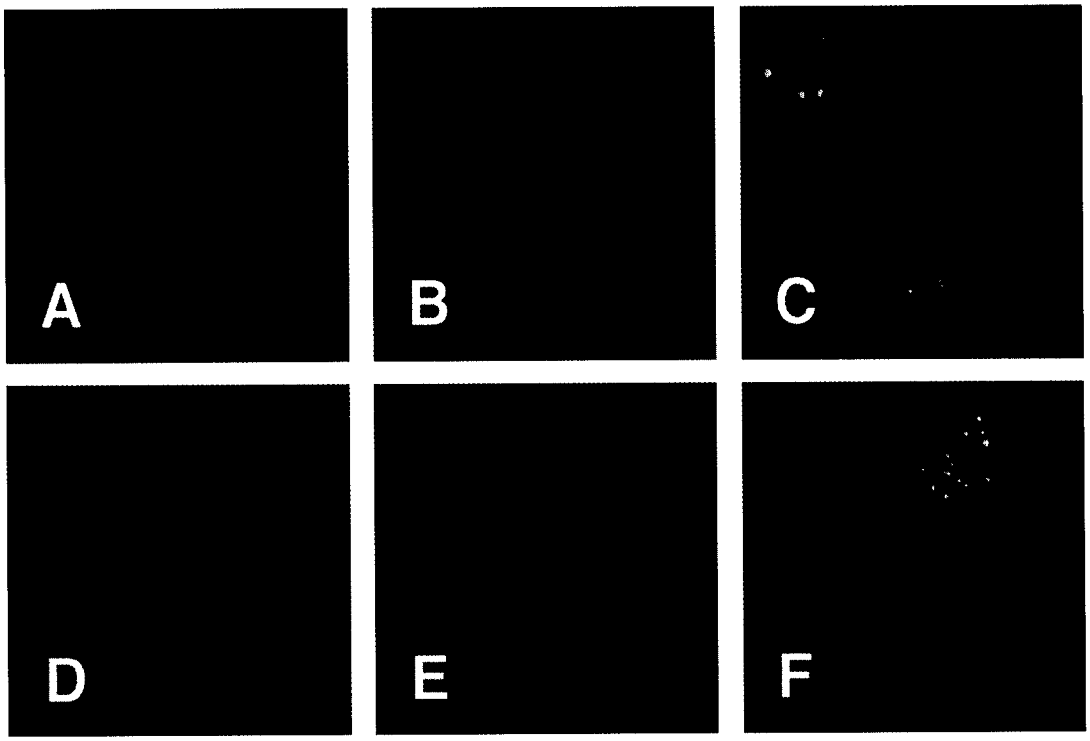

Figure 2. BRCA1 and Rad51 Colocalize in Discrete Nuclear Foci

MCF7 cells were double-stained with BRCA1 MAb MS13 (green) and anti-Rad51 (red). (A) and (D), BRCA1 stain; (B) and (E), Rad51 stain; and (C) and (F), composite BRCA1 and Rad51 stains. Where green and red signals overlap, a yellow pattern is seen, indicating colocalization of BRCA1 and Rad51.

(A–C) Staining of asynchronously growing MCF7 cells, depicting the location of BRCA1 and Rad51 in a BRCA1 dot-containing cell and in a cell exhibiting a more diffuse BRCA1 signal.

(D–E) Staining of serum-starved MCF7 cells, illustrating the rare (5%) S phase cell with a BRCA1 nuclear dot pattern.

Rad51 over BRCA1 and/or only a fraction of Rad51 is competent to bind, directly or indirectly, to BRCA1 is not known.

In an effort to confirm the existence of a physical interaction between BRCA1 and Rad51, we asked whether BRCA1 would complex with epitope-tagged, ectopic Rad51. Figure 3B shows that, after transient transfection of HA-tagged Rad51 into 293T cells, both endogenous BRCA1 and HA-tagged Rad51 were detected in an anti-BRCA1 immunoprecipitate. The coprecipitating band, identified as HA-Rad51, comigrated with bands precipitated from the same extract with either HA or Rad51 antibody. No such band precipitated from untransfected cells with anti-HA MAb (Figure 3B). In addition, transiently overproduced HA–E2F4 was not detected in BRCA1 immunoprecipitates, despite the fact that its concentration was similar to that of HA–Rad51 (data not shown). Hence, the BRCA1 MAb used here did not recognize the HA tag. Moreover, this BRCA1 MAb failed to recognize in vitro translated HA-tagged Rad51 synthesized in a wheat germ extract (data not shown). Hence, it did not appear to recognize Rad51 independently.

In a reciprocal experiment, anti-Rad51 immunoprecipitation of a HA-BRCA1-transfected 293T cell extract coprecipitated BRCA1 (Figure 3C). Despite the presence of higher levels of two HA-tagged control nuclear proteins—the p300 nuclear coactivator and the p130 pocket protein—in parallel transfections of the same cell line, neither protein was detected in anti-Rad51 immunoprecipitates (Figure 3C). Thus, further evidence of specific complex formation between Rad51 and BRCA1 was obtained in transiently transfected cells containing definitively tagged gene products.

BRCA1 Exon 11 Encodes Sequences That Mediate Rad51 Binding

Six overlapping BRCA1 fragments spanning the entire *BRCA1* open reading frame were synthesized as GST fusion proteins (Figures 4A and 4B). Approximately equal amounts of each protein, bound to glutathione-sepharose beads, were incubated with an extract of BJAB (Burkitt's lymphoma–derived) cells. Bead-bound proteins were recovered and separated electrophoretically. The separated proteins were immunoblotted for Rad51 (Figure 4C). GST–BRCA1 fragment #4, corresponding to BRCA1 residues 758–1064, which are encoded by a portion of exon 11, repeatedly bound a 38 kDa immunoreactive Rad51 comigrating band. Identical results were obtained using cell lines MCF7, 293T, and U2OS.

To distinguish between bona fide hRad51 and a comigrating 38 kDa band supplied by the bacterial extract, the same experiment was performed with an extract of ^{35}S-methionine-labeled MCF7 cells (Figure 4D). After incubation of the various bead-bound GST proteins with

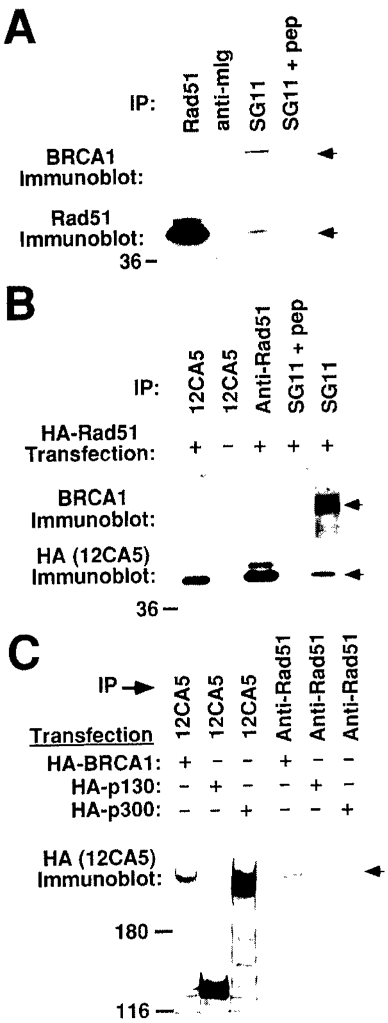

Figure 3. Coimmunoprecipitation of BRCA1 and Rad51

(A) Association in untransfected cells. MCF7 cultures were enriched for S phase (see Experimental Procedures). Extracts (5×10^6 cells per lane) were immunoprecipitated with the antibodies shown. Immunoprecipitated proteins were separated by SDS–PAGE and immunoblotted with MAb MS110 (anti-BRCA1, upper panel; arrow signals the migration position of p220 BRCA1 [Scully et al., 1996]) and with the Rad51 antiserum (arrow signals the presence of the 38 kDa protein). Control antibodies included the rabbit anti-mouse IgG secondary immunoprecipitation antibody ("anti-mIg") and MAb SG11 that had been preincubated with a 10-fold molar excess of the peptide against which it was raised.

(B) Coimmunoprecipitation of ectopic, HA-tagged Rad51 with BRCA1. 293T cells were transfected with an HA-Rad51 expression plasmid. Extracts of the transfected cultures ($\sim 10^7$ cells per lane) were subjected to immunoprecipitation 48 hr later. After SDS–PAGE, immunoblotting for p220 BRCA1 (using MAb MS110, upper panel) and for the HA tag (using MAb 12CA5, lower panel) was performed. Immunoblots of whole cell extracts clearly showed an HA-Rad51-specific doublet migrating at 40–42 kDa (data not shown). The absence of this doublet from an extract of untransfected cells indicated that the 40–42 kDa 12CA5$^+$ species depicted in the lower panel are HA–Rad51 products.

(C) Coimmunoprecipitation of ectopic HA-BRCA1 with Rad51. 293T cells were transfected, in parallel, with expression plasmids encoding HA–BRCA1, HA–p130, or HA–p300, as shown. Transfected cell extracts ($\sim 10^7$ cells per lane) were immunoprecipitated. After SDS–PAGE, anti-HA immunoblotting (using MAb 12CA5) was performed. Note that the nominal molecular weights of BRCA1 (220 kDa) and p300 (300 kDa) are not reflected in the relative migration rates of these proteins, which, even in the untagged state, migrate close to one another.

this extract and washing, we eluted the bead-bound proteins. After dilution of the individual eluates to reduce the ambient SDS concentration, the eluted proteins were reimmunoprecipitated with the Rad51 antiserum. A labeled 38 kDa band did reimmunoprecipitate from an eluate of the same lot of GST–BRCA1 #4 fragment-bound beads that yielded the Rad51 immunoreactive band in the earlier experiment (Figure 4C). No such band appeared in the eluates of GST beads alone. Hence, the protein recovered by the BRCA1 #4 fragment is Rad51 and originated in the mammalian and not the bacterial extract.

Taken together, the data indicate that *BRCA1* exon 11 encodes a sequence(s) that can serve as a specific binding site for Rad51. Whether the BRCA1 interaction with Rad51 is direct or depends upon BRCA1 binding to an intermediate protein(s) is not clear at present.

Presence of BRCA1 on Meiotic Chromosomes

The association of BRCA1 and Rad51 in mitotic cells and the known presence of Rad51 on synaptonemal complexes of various organisms (Bishop, 1994; Ashley et al., 1995; Terasawa et al., 1995; Plug et al., 1996) suggested that the two proteins might also colocalize during meiotic prophase. *BRCA1* mRNA is highly expressed in spermatocytes during meiotic prophase (Zabludoff et al., 1996).

The pairing of homologous chromosomes during meiosis is accompanied by the appearance of unique, meiosis-specific DNA- and protein-bearing structures, termed synaptonemal complexes. Following DNA replication in premeiotic S phase, meiotic chromosomes begin to condense and a protein-containing core, or axial element, forms between sister chromatids. As homologous chromosomes synapse in zygonema to form a bivalent, the axial elements align and are joined by transverse filaments. Finally, a discrete central element forms between the two axial elements, completing the structure of the synaptonemal complex. In the current study, we used an antibody to SCP3, a component of the axial/synaptic elements of this structure (Lammers et al., 1994), to visualize the progression of meiotic prophase.

In nuclei of zygotene spermatocytes obtained from fresh, human testis, BRCA1 staining (in red) was observed with three different MAb's (MS13, MS110, and SG11 [Scully et al., 1996]). Chromosomal axes doubly stained with MAb MS110 (red) and Ab to SCP3 (white) are shown in Figure 5. BRCA1 staining was detected in an uneven pattern. On those structures where the specific details of chromosomal anatomy were most clearly discernible, a significant fraction of the staining was noted along unsynapsed axial elements (small arrows, Figure 5A), as well as at axes that were in the process of synapsing (larger arrows, Figure 5A). BRCA1 staining was also detected on unsynapsed centromeric heterochromatin (arrowheads, Figure 5B), on remaining univalents (e.g., small arrow, Figure 5B), and at pairing forks (e.g., larger arrow, Figure 5B). Figure 5D highlights the

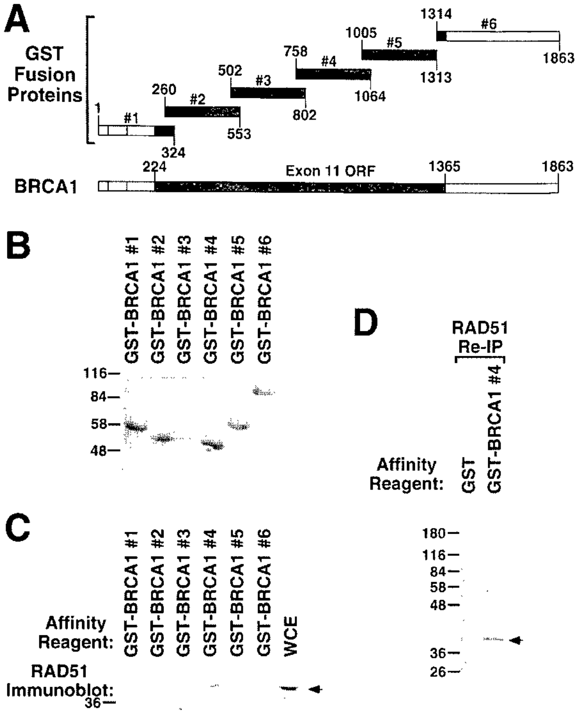

Figure 4. In Vitro Binding of a Segment of BRCA1 to Rad51

Six GST–BRCA1 fusion proteins were generated in E. coli. (A) The schematic diagram of these fusion proteins is not drawn to scale. BRCA1 exon 11 products are indicated by dense stippling. The amino-terminal BRCA1 RING domain is shown by light stippling. BRCA1 residues are marked relative to the translation initiation site.

(B) Synthesis of GST–BRCA1 fusion proteins in E. coli. Individual GST–BRCA1 fusion proteins were prepared as described in Experimental Procedures. The figure depicts a Coomassie blue–stained SDS acrylamide gel, showing the relative abundance of each fusion protein used in Figure 4C. Note that GST–BRCA1 protein #3 was consistently found to be unstable.

(C) Rad51 antiserum recognizes a 38 kDa protein bound to GST–BRCA1 #4. GST–BRCA1 affinity beads were incubated briefly with an unlabeled BJAB extract. After washing, bound proteins were electrophoresed and immunoblotted using the Rad51 antiserum as probe. The figure shows a 38 kDa band, comigrating with Rad51 detected in whole cell extracts (WCE), specifically associated with GST–BRCA1 #4.

(D) The 38 kDa protein bound to GST–BRCA1 #4 is a product of the human cell extract and can be reimmunoprecipitated with Rad51 antiserum. Beads containing GST–BRCA1 #4 and excess GST-containing affinity beads were incubated, in parallel, with extracts of ^{35}S-methionine-labeled MCF7. After washing, bound proteins were solubilized by boiling in SDS buffer. Diluted eluates were then immunoprecipitated with Rad51 antiserum, and the ensuing precipitates were analyzed by SDS-PAGE and autoradiography. The specific 38 kDa band (indicated with an arrow) was found in another experiment to comigrate with the 38 kDa Rad51 protein, as identified by immunoblotting. Furthermore, an anti-Rad51 reimmunoprecipitate from an initial anti-Rad51 precipitate of MCF7 cells yielded only a ^{35}S-labeled 38 kDa species (not shown).

existence of BRCA1 staining on unsynapsed axial elements (small arrows). Arrowheads mark examples of synapsed regions of the indicated synaptonemal complexes. Identical results were obtained with all three BRCA1 Ab's, strongly suggesting that the observed signals resulted from the presence of BRCA1.

Many fewer chromosomes revealed detectable BRCA1 staining in pachynema (Figure 5C). By contrast, BRCA1 staining persisted on the asynapsed X-axis during this period (Figure 5C). Indeed, as pachynema progressed, the BRCA1 signal seemed to be present in a less interrupted manner on late-synapsing autosomal axes (arrows, Figure 5C) and on the X chromosome (see Figure 6), which has no homolog in males. These data imply that the appearance of BRCA1 staining is a synchronous event during meiotic prophase.

The BRCA1 MAb MS13 was raised against a defined segment of the N-terminal region of the cloned protein (residues 1–304, Scully et al., 1996). As another test of specificity, we preincubated MAb MS13, in parallel, with each of two purified BRCA1 fragments. One was the initial MS13 immunogen. The other contained residues 1313–1863. These preincubated preparations were used, in parallel, to stain pachytene spermatocytes. Both Rad51 Ab and a second BRCA1 MAb, MS110, costained the unsynapsed axis of the X chromosome (data not shown). MAb MS13, preincubated with the C-terminal BRCA1 fragment, noted above, also stained the unsynapsed axis of the X chromosome (Figure 6B), which was simultaneously costained with SCP3 Ab (Figure 6A). In contrast, MAb MS13, preincubated with the relevant, immunizing N-terminal polypeptide, yielded no signal despite the presence of the X in that spread (Figures 6C [SCP3 staining] and 6D).

The same experiment was performed with MAb MS110 (which, like MS13, was raised against BRCA1 residues 1–304) with identical results (data not shown). MAb SG11, a third BRCA1 monoclonal Ab, led to a staining pattern identical to that of MS13 and MS110. However, as predicted, SG11 staining was blocked by preincubation with a C-terminal BRCA1 polypeptide containing the SG11 epitope (data not shown). Therefore, the immunostaining obtained with these MAb's likely reflects specific interactions of these MAb's with BRCA1.

A further indication of the specifity of the BRCA1 staining pattern is given by the failure of monoclonal antibodies specific to other nuclear proteins, such as the retinoblastoma protein and the nuclear coactivator, p300, to elicit any signal on human synaptonemal complexes. Furthermore, testis spreads, prepared in this manner, stained positively for DNA (with DAPI) throughout the nucleus. In S phase spermatocytes, nuclei also stained with Ab to the replication protein, RPA, throughout, indicating that the method of preparation does not extract non-SC-bound proteins from the spreads (A. Plug and T. Ashley, unpublished data). The unsynapsed/axial elements, therefore, appear to be the only sites of BRCA1 concentration in zygotene and pachytene spermatocytes.

Simultaneous BRCA1 and Rad51 Staining of Meiotic Chromosomes

Plug et al. (1996) showed that Rad51 is present in premeiotic S phase nuclear foci. During zygonema, Rad51 staining organizes into discrete structures along axial elements. Homologous synapsis is completed in early pachynema, and Rad51 foci remain evident along the

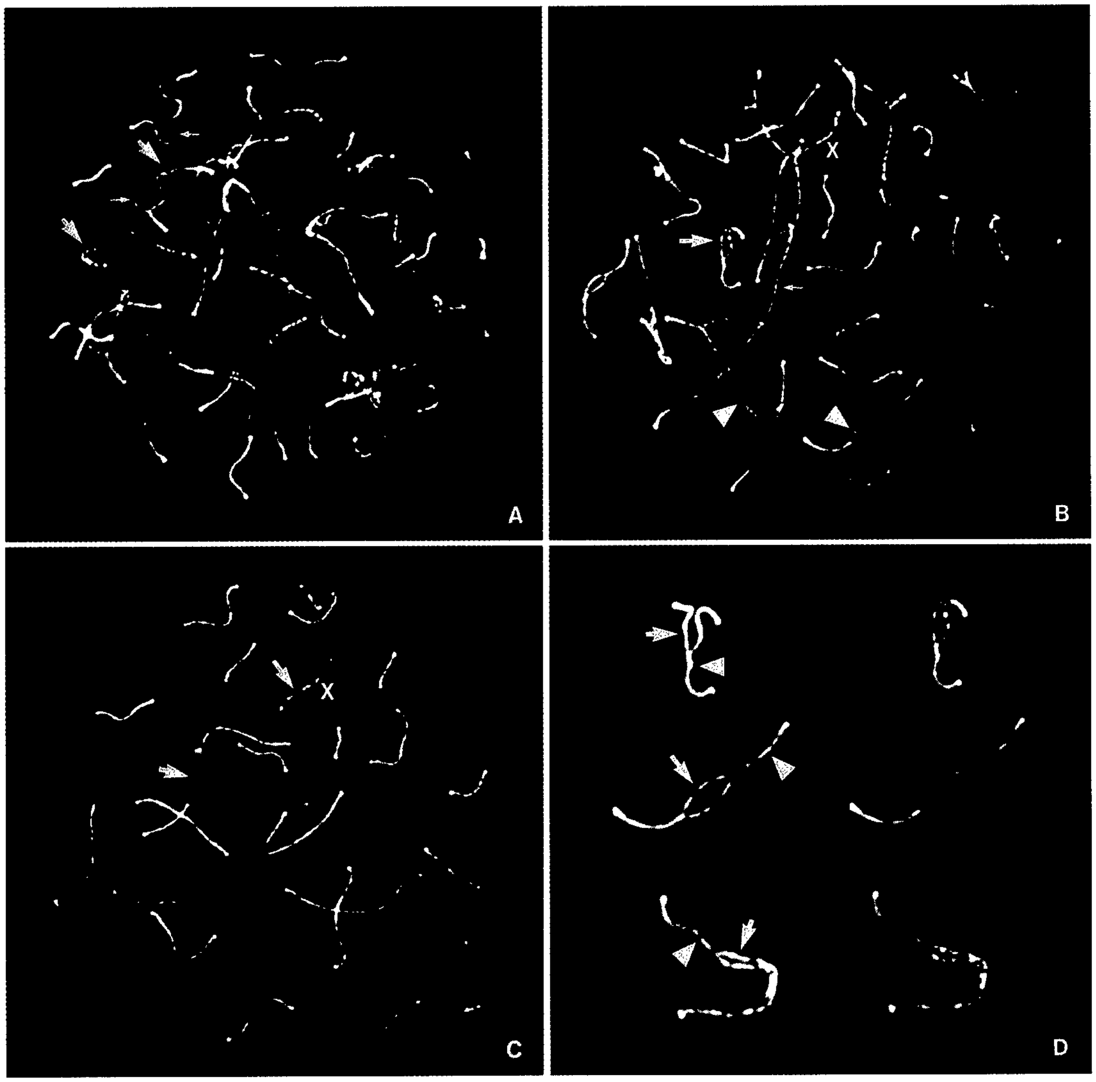

Figure 5. Localization of BRCA1 Staining to Meiotic Chromosomes

(A) Axial and synapsed segments (using Ab SCP3, white) in a human zygotene nucleus. BRCA1 (stained with MAb MS110, red) localized to discrete sites along unsynapsed axial elements (examples noted by small arrows) and axes that are in the process of synapsing (examples noted by larger arrows).

(B) Localization of BRCA1 to sites along unsynapsed axes of regions delayed in synapsis (examples noted by arrowheads), pairing forks (example noted by arrow), and remaining univalents (examples noted by small arrows).

(C) Pachytene nucleus showing the presence of BRCA1 staining on the unsynapsed X chromosome and a delayed pairing fork (arrows).

(D) BRCA1 staining on unsynapsed axial elements (enlarged images taken, in part, from [B]). Arrows indicate examples of unsynapsed segments; arrowheads indicate examples of synapsed regions. SCP3 staining (white) is shown on the left; SCP3 and BRCA 1 costaining (white and red, respectively) are shown on the right. The lowermost complexes of the three are from another zygotene spread, where BRCA1 staining was obtained with MS13.

length of the synaptonemal complex. Shortly after completion of synapsis of most chromosomes, Rad51 foci begin to disappear from the synaptonemal complex. In contrast, Rad51 foci remain associated with the unsynapsed axial element of the X chromosome in spermatocytes (Ashley et al., 1995; Plug et al., 1996). Rad51 foci also remain associated with a few autosomal axes in which synapsis is delayed (Plug et al., unpublished data). In coimmunostaining experiments, much of the BRCA1 staining (red, Figure 7B) and much, albeit not all, of the Rad51 staining (green, Figure 7A; composite image, Figure 7C) appeared in the same general locations on developing synaptonemal complexes during zygonema. In multiple spreads, some foci of Rad51 staining were not associated with a BRCA1 signal at all (Figure 7 and data not shown). One interpretation of the Rad51 and BRCA1 staining patterns, described above, is that a significant fraction of both the BRCA1 and the Rad51 staining, i.e., that which appears in the same general chromosomal locations, is concentrated at unsynapsed chromosomal sites.

Discussion

The data presented here show, for the first time, that BRCA1 associates with Rad51, a human homolog of

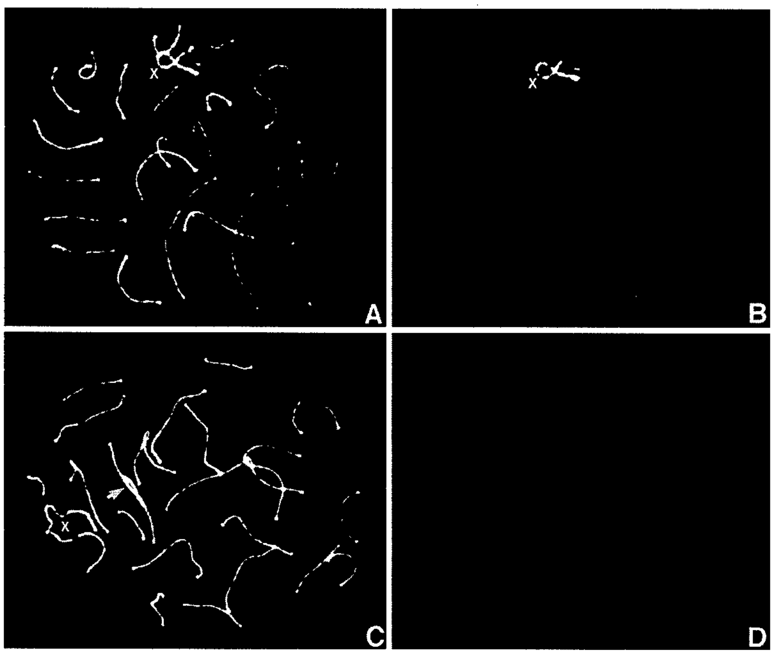

Figure 6. Specificity of BRCA1 Staining of Synaptonemal Complexes

(A) SCP3 staining of pachytene chromosomes.

(B) BRCA1 costaining of this spread with MAb MS13 that had been preincubated with a C-terminal GST–BRCA1 fusion protein, which lacks the MS13 epitope. BRCA1 staining is limited to the unsynapsed axes of the X chromosome.

(C) SCP3 staining of pachytene chromosomes. A prominent X-chromosomal axis is present.

(D) The same spread costained with MS13 preincubated with an N-terminal GST–BRCA1 fusion protein that contains the MS13 epitope.

bacterial RecA. In mitotic cells, this association was marked by colocalization in S phase nuclear foci and coimmunoprecipitation. Furthermore, during meiotic prophase in primary human spermatocytes, the proteins occupied the same general regions of developing synaptonemal complexes. These findings suggest a functional relationship between these two proteins. This conclusion was strengthened by the mapping of a Rad51 interaction domain to BRCA1 residues 758–1064, the site of at least one naturally occurring, loss-of-function missense mutation (Shattuck-Eidens et al., 1995).

Like Rad51, BRCA1 was detected in the nuclei of human spermatocytes on the axial (unsynapsed) elements of developing synaptonemal complexes. This is consistent with the prior observation that *BRCA1* mRNA levels are greatly elevated in zygotene/pachytene spermatocytes (Zabludoff et al., 1996). Since recombination, per se, occurs in synapsed regions, one might speculate that BRCA1 does not act directly in meiotic crossing-over. If that were true, it is possible that BRCA1 acts prior to the initiation of recombination, e.g., as an upstream regulator of this process. Alternatively, since its association with meiotic structures developed and ended synchronously, one could argue that it functions only when it is detected on the meiotic chromosome, e.g., during a period when the search for homologous sequences initiates and proceeds and/or when double-strand breaks appear (reviewed in Kleckner, 1996). The relatively synchronous manner in which BRCA1 appeared on meiotic chromosomes and formed dot structures in mitotic cells suggests a role in both mitotic and meiotic cell cycle control.

Recently, the *ATR* and *ATM* gene products were detected on mutually exclusive regions of the synaptonemal complex (Keegan et al., 1996). Like BRCA1, Atr was found on axial elements, together with Rad51. Atm, the product of another gene whose germ line inactivation may predispose to breast cancer (Swift et al., 1987), was present on synapsed regions. Atr is a homolog of Mec-1 (S. cerevisiae), Rad3 (S. pombe), and mei-41 (Drosophila), and mutations affecting these proteins lead to defects in DNA damage–induced cell cycle responses, radiation hypersensitivity, and defective meiosis (Al-Khodairy and Carr, 1992; Jiminez et al., 1992; Rowley et al., 1992; Cimprich et al., 1996). These large proteins are protein kinases, and, where studied, kinase function was essential to their normal biological activity (Bentley et al., 1996). This, in turn, suggests a role for these proteins in one or more signal transduction cascades, one product of which is proper meiotic and mitotic checkpoint control (reviewed in Carr, 1996).

The question of whether BRCA1 and Atr interact is now clearly relevant. Their similar locations on meiotic chromosomes, the known contribution of Atr to DNA damage control, and its possible role in meiotic cell cycle regulation (Keegan et al., 1996) suggest a related role for BRCA1. The Atr equivalent function in mitotic cells could be monitoring intersister chromatid interactions during S and G2 (Kleckner, 1996). One wonders, then, whether Atr and, possibly, BRCA1 participate in monitoring the progress of DNA replication and/or normal recombination-linked functions.

Tumorigenesis can arise from defects in DNA repair, e.g., in the case of hereditary nonpolyposis colon cancer. There, the defects lie in certain mismatch repair genes (reviewed in Kolodner, 1996). The products of some of these genes are also present on synaptonemal complexes and participate in normal meiosis (Baker et al., 1995; Baker et al., 1996; Edelmann et al., 1996). That BRCA1 and the product(s) of a second class of tumor suppressor genes that play a role in maintaining genome integrity are intimately associated with synaptonemal complexes raises the question of whether they communicate with one another.

What might be the outcome of a specific BRCA1 interaction with Rad51? In yeast, Rad51 participates in double-stranded break repair and meiotic recombination

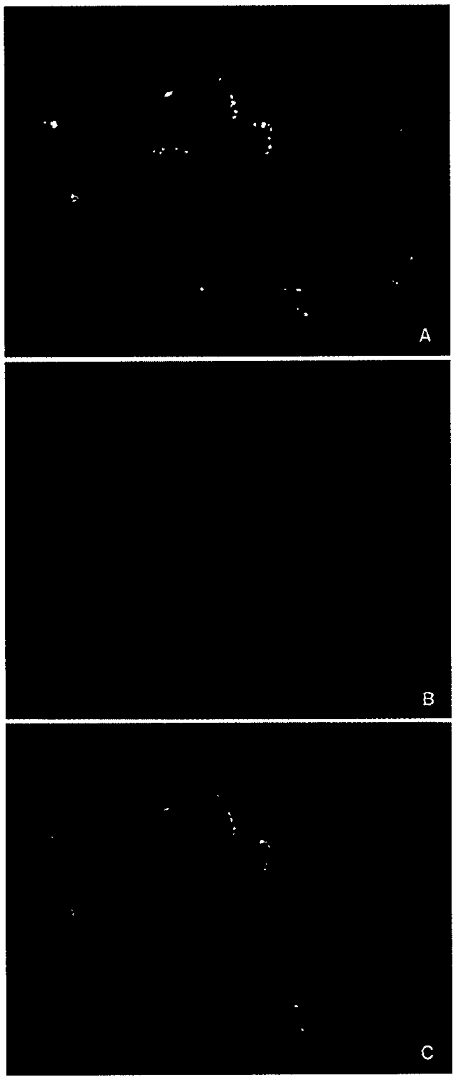

Figure 7. Colocalization of BRCA1 and Rad51 on Meiotic Chromosomes

(A) Rad51 immunostaining (green).

(B) BRCA1 immunostaining (red, MS13).

(C) Rad51 and BRCA1 costaining (colocalization is reflected by yellow images).

(Shinohara et al., 1992). Indeed, it must also play some role in the normal replication of mammalian embryonic cells, since *Rad51*$^{-/-}$ murine zygotes undergo early replication arrest (Lim and Hasty, 1996; Tsuzuki et al., 1996). Finally, RecA function is essential for the SOS response, a bacterial DNA damage control pathway dependent upon the activated transcription of certain genes (reviewed in Echols and Goodman, 1991).

Given these facts, one outcome of the Rad51–BRCA1 interaction could be orderly cell cycle progression, high fidelity DNA replication, and/or events that lead to the maintenance of genomic integrity. Indeed, BRCA1 breast tumors are characterized by a greater degree of genome plasticity than those arising in patients with mutations in the *BRCA2* gene (Marcus et al., 1996). Similarly, given the essential role of RecA in the SOS response and the apparent transcription activation function of certain BRCA1 fusion proteins (Chapman and Verma, 1996; Monteiro et al., 1996), one wonders whether BRCA1 plays a role in mediating a response to mammalian DNA damage in a Rad51/transcription–dependent manner. Notable in this regard is the finding of Reinberg and his coworkers of hRad51 in a fraction of RNA polymerase II holoenzyme (Maldonado et al., 1996).

Importantly, Rad51 and p53, another tumor suppressor with a central role in the response to DNA damage, interact, specifically, in vivo (Sturzbecher et al., 1996). There is a putative p53 interaction sequence in BRCA1 (Koonin et al., 1996) that is distinct from the apparent Rad51 interacting region of BRCA1. p53 also serves as an hereditary breast cancer–inducing gene in patients with the Li-Fraumeni Syndrome (Malkin et al., 1990).

On the face of it, the phenotype (i.e., cell cycle arrest) of *BRCA1* knockout embryos would seem to run counter to a proposed tumor suppressing role for this protein. On the other hand, if BRCA1 has a role in the maintenance of genome integrity, loss of its function might result in genome errors and the subsequent activation of checkpoint genome guardian functions, the outcome of which might be cell cycle arrest. Perhaps only those cells that are already defective in monitoring genome integrity and/or responding to a defect therein can escape the proliferation defect of BRCA1 loss. If this is the case, then loss of BRCA1 function, per se, may not initiate tumorigenesis, but rather accelerate its progression in cells that have already sustained damage to such a checkpoint function.

Interestingly, only trophoblast cells of *BRCA1* knockout embryos developed normally (Hakem et al., 1996). This tissue is unusual in that it normally undergoes endoreplication. If BRCA1 loss trips a normal S phase checkpoint, these cells may not be susceptible to it.

Rad51 loss is lethal in mice but not in yeast, a unicellular organism that may not be subjected to all of the same checkpoint and cell cycle controls as multicellular organisms. Interestingly, yeast also lack a *BRCA1* gene.

Experimental Procedures

Tissue Culture Methods and Preparation of Cell Extracts

Cells were cultured in DMEM-10% fetal bovine serum (FBS), or 10% Fetal Clone I (Hyclone labs). For synchronization studies of MCF7 cells, asynchronous cultures were cultivated for 24 hr in DMEM/0.05% BSA to induce G1 arrest. After release into 20% FBS, cell cycle progression was measured by FACS analysis. Maximum S phase enrichment was seen 24 hr after serum release. For transfection, a standard calcium phosphate precipitation method was used (Wigler et al., 1977). Immunoprecipitation (typically $\sim$2 μg Ab per reaction) and immunoblotting were performed as described previously (Scully et al., 1996), with the exception of the extraction buffer, which contained only NP-40 (0.5%) as detergent.

Immunostaining of Adherent Cells

Cells were fixed and permeablized as described previously (Eckner et al., 1994). Primary antibodies were incubated in a humidified atmosphere at 37°C for 20 min. Species-specific, fluorochrome-conjugated secondary antibodies (Jackson Immunoresearch) were incubated in a similar fashion. Immunofluorescence was recorded using a Zeiss confocal microscope.

Preparation and Immunostaining of Human Synaptonemal Complexes

Preparation of "spreads" of human spermatocytes was perfomed as described by Peters et al. (1997). Antibody incubation and detection were performed as described previously (Moens et al., 1987; Ashley et al., 1995). BRCA1 MAb's were detected with anti-mouse IgG rhodamine conjugate (Pierce), and SCP3 polyclonal antibodies with anti-rabbit IgG FITC conjugate (Pierce). Preparations were counterstained with 4′,6′ diamino-2-phenylindole (DAPI, Sigma), mounted in a DABCO (Sigma) antifade solution, and examined on a Zeiss Axioskop (63-X and 100-X, 1.2 Plan Neofluor oil immersion objective). Each fluorochrome image was captured separately as an 8-bit source image using a computer-assisted cooled CCD camera (Photometrics CH 220). The separate images were 24-bit pseudocolored and merged with custom software developed by Tim Rand (Ried et al., 1992).

Construction of *BRCA1* and *Rad51* Expression Vectors

To optimize in vivo expression of *BRCA1* cDNA, a rabbit β-globin intron was inserted into pcDNA3 (Invitrogen). The insert was generated by PCR from vector pSG5 (Stratagene), using the primers: 5′-GGGCCAAGCTTGCGTCTAGAGTCGATCCTGAGAACTTCAG GGTG-3′ and 5′-GGGGGATCCGCCCGGGCCAAGCTTGGGGTCGA CAGCAC<u>AATAA</u>CCAGCACGTTGCCC-3′. The pcDNA3 HindIII restriction site was converted to a unique NheI site using HindIII digestion, Klenow treatment, and religation. The insert was digested with XbaI and BamHI and subcloned into the NheI–BamHI sites of pcDNA3. Full sequencing of the insert showed that nucleotides AATAA (underlined above) had been replaced by the sequence AAA. No other errors were found. This vector was termed "pcDNA3β."

Derivation of the wild-type human cDNA for BRCA1 has been described previously (Scully et al., 1996). An amino-terminal HA-BRCA1 expression vector was generated by PCR of BRCA1 cDNA (using primers 5′-GGGGGATCCATGGATTTATCTGCTCTTCGCG-3′ and 5′-GGGTCAGAATTCAGCCTTTTCTACATTCATTCTGTC-3′). A BamHI–BstXI fragment of this product was subcloned into the same sites of a partial *BRCA1* cDNA, and the full-length cDNA was reassembled into pcDNA3β containing a previously subcloned HA tag-coding sequence (Krek et al., 1993) located between HindIII and BamHI sites. The PCR-derived part was confirmed correct by direct sequencing.

An amino-terminal HA-tagged *hRad51* expression construct was generated in a similar fashion. A full-length *hRad51* cDNA, housing a BamHI site immediately upstream of the open reading frame, was generated by using Pfu polymerase and PCR primers: 5′-GGG CCCGGATCCATGGCAATGCAGATGCAGC-3′ and 5′-GGGCCCCAA TTGGATATCATTCAGTCTTTGGCATCTCCCACTCC-3′. Restriction digests confirmed the identity of the cloned fragment, which was subcloned into BamHI–EcoRV sites of a pcDNA3/HA vector, as described above. Expression vectors for HA-p300 and HA-p130 have been described previously (Eckner et al., 1994; Vairo et al., 1995).

Construction and Expression of Bacterial GST-Fusion Proteins

Constructs corresponding to GST–BRCA1 #1–#5 (see text) were made using the vector pGEX-5X3 (Pharmacia). Inserts were generated by PCR using Pfu polymerase and the following pairs of primers: (#1) 5′-ATAGGATCCAAATGGATTTATCTGCTCTTCGC-3′ and 5′-ATAGTCGACTTCCAGCCCATCTGTTATGT-3′; (#2) 5′-ATAGGAT CCAGGGTAGTTCTGTTTCAAACTTG-3′ and 5′-ATAGTCGACCACT ATTAGTAATATTCATCACT-3′; (#3) 5′-ATAGGATCCGTAAAAGGAG ACCTACATCAG-3′ and 5′-ATAGTCGACTCACACATTTATTTGGTT CTG-3′; (#4) 5′-ATAGGATCCAAACTGAAAGATCTGTAGAGAGT-3′ and 5′-ATAGTCGACTGGAACCTATTTCATTAATAC-3′; and (#5) 5′-ATAGGATCCCATTCAATGTCACCTGAAAGA-3′ and 5′-ATAGTCGA CTGGGTGTTTGTATTTGCAGTCAA-3′.

GST–BRCA1 fragment #6 was described previously (Scully et al., 1996). GST–hRad51 was generated using the *Rad51* cDNA described above. Synthesis of GST fusion proteins and their partial purification on glutathione-sepharose beads was performed as described (Kaelin et al., 1992). Where GST fusion proteins were used for specificity controls, they were used as glutathione-eluted protein (10 μg per sample) or as affinity beads.

Acknowledgments

We are especially indebted to Drs. Nancy Kleckner, Bill Kaelin, Jim DeCaprio, Myles Brown, and Richard Kolodner for stimulating and helpful discussions. We are grateful to Drs. Adam Kibel and Jerome Ritchie for their expert help in obtaining testis tissue for these experiments. Drs. Charles Radding, Efim Golub, Gurucharan Reddy, and Oleg Kovalenko generously provided affinity-purified hRad51 antibody, and we thank them enthusiastically for it. We also thank Dr. Christa Heyting for her generosity in supplying SCP3 antibody and Mr. Phillipe Male for processing meiosis photographs. This work was supported by grants from the National Institutes of Health and the Dana-Farber Women's Cancer Program.

Received December 2, 1996; revised December 20, 1996.

References

Al-Khodairy, F., and Carr, A.M. (1992). DNA repair mutants defining G2 checkpoint pathways in Schizosaccharomyces pombe. EMBO J. *11*, 1343–1350.

Ashley, T., Plug, A.W., Xu, J., Solari, A.J., Reddy, G., Golub, E.I., and Ward, D.C. (1995). Dynamic changes in Rad51 distribution on chromatin during meiosis in male and female vertebrates. Chromosoma *104*, 19–28.

Baker, S.M., Bronner, C.E., Zhang, L., Plug, A.W., Robatzek, M., Warren, G., Elliott, E.A., Yu, J., et al. (1995). Male mice defective in the DNA mismatch repair gene PMS2 exhibit abnormal chromosome synapsis in meiosis. Cell *82*, 309–319.

Baker, S.M., Plug, A.W., Prolla, T.A., Bronner, C.E., Harris, A.C., Yao, X., Christie, D.-M., Monell, C., et al. (1996). Involvement of mouse Mlh1 in DNA mismatch repair and meiotic crossing over. Nat. Genet. *13*, 336–342.

Baumann, P., Benson, F.E., and West, S.C. (1996). Human Rad51 protein promotes ATP-dependent homologous pairing and strand transfer reactions in vitro. Cell *87*, 757–766.

Bentley, N.J., Holtzman, D.A., Keegan, K.S., Flaggs, G., DeMaggio, A.J., Ford, J.C., Hoekstra, M.F., and Carr, M. (1996). The Schizosaccharomyces pombe rad3 checkpoint gene. EMBO J., in press.

Bishop, D.K. (1994). RecA homologues Dmc1 and Rad51 interact to form multiple nuclear complexes prior to meiotic chromosome synapsis. Cell *79*, 1081–1092.

Carr, A.M. (1996). Checkpoints take the next step. Science *271*, 314–315.

Castilla, L.H., Couch, F.J., Erdos, M.R., Hoskins, K.F., Calzone, K., and Garber, J.E. (1994). Mutations in the BRCA1 gene in families with early-onset breast and ovarian cancer. Nat. Genet. *8*, 387–391.

Chapman, M.S., and Verma, I.M. (1996). Transcriptional activation by BRCA1. Nature *382*, 678–679.

Chen, Y., Chen, C.-F., Riley, D.J., Allred, D.C., Chen, P.-L., Von Hoff, D., Osborne, C.K., and Lee, W.-H. (1995). Aberrant subcellular localization of BRCA1 in breast cancer. Science *270*, 789–791.

Chen, Y.M., Farmer, A.A., Chen, C.F., Jones, D.C., Chen, P.L., and Lee, W.H. (1996). BRCA1 is a 220-kDa nuclear phosphoprotein that is expressed and phosphorylated in a cell cycle–dependent manner. Cancer Res. *56*, 3168–3172.

Cimprich, K.A., Shin, T.B., Keith, C.T., and Schreiber, S.L. (1996). cDNA cloning and gene mapping of a candidate human cell cycle checkpoint protein. Proc. Natl. Acad. Sci. USA *7*, 2850–2855.

Claus, E.B., Risch, N., and Thompson, W.D. (1991). Genetic analysis of breast cancer in the Cancer and Steroid Hormone Study. Am. J. Hum. Genet. *48*, 232–241.

Easton, D.F., Bishop, T., Ford, D., Crockford, G.P., and The Breast Cancer Linkage Consortium (1993). Genetic linkage analysis in familial breast and ovarian cancer: results from 214 families. Am. J. Hum. Genet. *52*, 678–701.

Echols, H., and Goodman, M.F. (1991). Fidelity mechanisms in DNA replication. Annu. Rev. Biochem. *60*, 477–511.

Eckner, R., Ewen, M.E., Newsome, D., Gerdes, M., DeCaprio, J.A., Lawrence, J.B., and Livingston, D.M. (1994). Molecular cloning and functional analysis of the adenovirus E1A-associated 300-kD protein (p300) reveals a protein with properties of a transcriptional adaptor. Genes Dev. *8*, 869–884.

Edelmann, W., Cohen, P.E., Kane, M., Lau, K., Morrow, B., Bennett, S., Umar, A., Kunkel, T., et al. (1996). Meiotic pachytene arrest in MLH1-deficient mice. Cell *85*, 1125–1134.

Feunteun, J., and Lenoir, G.M. (1996). BRCA1, a gene involved in inherited predisposition to breast and ovarian cancer. Biochem. Biophys. Acta *1242*, 177–180.

Freemont, P.S. (1993). The RING finger. Ann. NY Acad. Sci. *684*, 174–192.

Friedman, L.S., Ostermeyer, E.A., Szabo, C.I., Dowd, P., Lynch, E.D., Rowell, S.E., and King, M.-C. (1994). Confirmation of BRCA1 by analysis of germline mutations linked to breast and ovarian cancer in ten families. Nat. Genet. *8*, 399–404.

Gowen, L.C., Johnson, B.L., Latour, A.M., Sulik, K.K., and Koller, B.H. (1996). BRCA1 deficiency results in early embryonic lethality characterized by neuroepithelial abnormalities. Nat. Genet. *12*, 191–194.

Gudas, J.M., Li, T., Nguyen, H., Jensen, D., Rauscher, F.J.I., and Cowan, K.H. (1996). Cell cycle regulation of BRCA1 messenger RNA in human breast epithelial cells. Cell Growth Differ. *7*, 717–723.

Gudas, J.M., Nguyen, H., Li, T., and Cowan, K. (1995). Hormone-dependent regulation of BRCA1 in human breast cancer cells. Cancer Res. *55*, 4561–4565.

Haaf, T., Golub, E.I., Reddy, G., Radding, C.M., and Ward, D.C. (1995). Nuclear foci of mammalian Rad51 recombination protein in somatic cells after DNA damage and its localization in synaptonemal complexes. Proc. Natl. Acad. Sci. USA *92*, 2298–2302.

Hakem, R., de la Pomba, J.L., Sirard, C., Mo, R., Woo, M., Hakem, A., Wakeham, A., Potter, J., et al. (1996). The tumor suppressor gene *Brca1* is required for embryonic cellular proliferation in the mouse. Cell *85*, 1009–1023.

Hall, J.M., Lee, M.K., and Newmann, B. (1990). Linkage of early-onset breast cancer to chromosome 17q21. Science *250*, 1684–1689.

Holt, J.T., Thompson, M.E., Szabo, C., Robinson-Benion, C., Arteaga, C. L., King, M.-C., and Jensen, R.A. (1996). Growth retardation and tumor inhibition by BRCA1. Nat. Genet. *12*, 298–302.

Jiminez, G., Yucel, J., Rowley, R., and Subramani, S. (1992). The $rad3^{+}$ gene of Schizosaccharomyces pombe is involved in multiple checkpoint functions and in DNA repair. Proc. Natl. Acad. Sci. USA *87*, 4952–4956.

Kaelin, W.G., Jr., Krek, W, Sellers, W.R., DeCaprio, J.A., Ajchenbaum, F., Fuchs, C.S., Chittenden, T., Li, Y., Farnham, P.J., et al. (1992). Expression cloning of a cDNA encoding a retinoblastoma-binding protein with E2F-like properties. Cell *70*, 351–364.

Keegan, K.S., Holtzman, D.A., Plug, A.W., Christenson, E.R., Brainerd, E.E., Flaggs, G., Bentley, N.J., Taylor, E.M., et al. (1996). The Atr and Atm protein kinases associate with different sites along meiotically pairing chromosomes. Genes Dev. *10*, 2423–2437.

Kleckner, N. (1996). Meiosis: how could it work? Proc. Natl. Acad. Sci. USA *93*, 8167–8174.

Kolodner, R. (1996). Biochemistry and genetics of eukaryotic mismatch repair. Genes Dev. *10*, 1433–1442.

Koonin, V.F., Altschul, S.F., and Bork, P. (1996). BRCA1 protein products: functional motifs. Nat. Genet. *13*, 266–267.

Kowalczykowski, S.C. (1991). Biochemistry of genetic recombination: energetics and mechanism of DNA strand exchange. Annu. Rev. Biophys. Chem. *20*, 539–575.

Krek, W., Livingston, D.M., and Shirodkar, S. (1993). Binding to DNA and the retinoblastoma gene product promoted by complex formation of different E2F family members. Science *262*, 1557–1560.

Lammers, J.H.M., Offenberg, H.H., van Aalderen, M., Vink, A.C., Dietrich, A.J., and Heyting, C. (1994). The gene encoding a major component of the lateral element of the synaptonemal complex of the rat is related to X-linked lymphocyte-regulated genes. Mol. Cell. Biol. *14*, 1137–1146.

Lane, T.F., Deng, C., Elson, A., Lyu, M.S., Kozak, C.A., and Leder, P. (1995). Expression of BRCA1 is associated with terminal differentiation of ectodermally and mesodermally derived tissues in mice. Genes Dev. *9*, 2712–2722.

Lim, D.-S., and Hasty, P. (1996). A mutation in mouse rad51 results in an early embryonic lethal that is suppressed by a p53 mutation. Mol. Cell. Biol. *16*, 7133–7143.

Liu, C.Y., Flesken-Nikitin, A., Li, S., Zeng, Y., and Lee, W.-H. (1996). Inactivation of the mouse Brca1 gene leads to failure in the morphogenesis of the egg cylinder in early postimplantation development. Genes Dev. *10*, 1835–1843.

Maldonado, E., Shiekhattar, R., Sheldon, M., Cho, H., Drapkin, R., Rickert, P., Lees, E., Anderson, C.W., Linn, S., and Reinberg, D. (1996). A human RNA polymerase II complex associated with SRB and DNA-repair proteins. Nature *381*, 86–89.

Malkin, D., Li, F.P., Strong, L.C., Fraumeni, J.F., Jr., Nelson, C.E., Kim, D.H., Kassel, J., Gryka, M.A., Bischoff, F.Z., et al. (1990). Germ line p53 mutations in a familial syndrome of breast cancer, sarcomas, and other neoplasms. Science *250*, 1233–1238.

Marcus, J.N., Watson, P., Page, D.L., Narod, S.A., Lenoir, G., Tonin, P., Linder-Stephenson, L., et al. (1996). Hereditary breast cancer: pathobiology, prognosis, and BRCA1 and BRCA2 gene linkage. Cancer *77*, 697–709.

Marquis, S.T., Rajan, J.V., Wynshaw-Boris, A., Xu, J., and Yin, G.-Y. (1995). The developmental pattern of BRCA1 expression implies a role in differentiation of the breast and other tissues. Nat. Genet. *11*, 17–26.

Merajver, S.D., Pham, T.M., Caduff, R.F., Chen, M., Poy, E.L., Cooney, K.A., Weber, B.L., Collins, F.S., et al. (1995). Somatic mutations in the BRCA1 gene in sporadic ovarian tumors. Nat. Genet. *9*, 439–443.

Miki, Y., Swensen, J., Shattuck-Eidens, D., Futreal, P.A., Harshman, K., Tavtigian, S., Liu, Q., Cochran, C., et al. (1994). A strong candidate for the breast and ovarian cancer susceptibility gene BRCA1. Science *266*, 66–71.

Moens, P.B.C., Heyting, C., Dietrich, A.J., van Raamsdonk, W., and Chen, Q. (1987). Synaptonemal complex antigen localization and conservatation. J. Cell Biol. *105*, 93–103.

Monteiro, A.N.A., August, A., and Hanafusa, H. (1996). Evidence for a transcriptional activation function of BRCA1 C-terminal region. Proc. Natl. Acad. Sci. USA *93*, 13595–13599.

Narod, S.A., Feunteun, J., Lynch, H.T., Watson, P., Conway, T., Lynch, J., and Lenoir, G. (1991). Familial breast-ovarian cancer locus on chromosome 17q12–23. Lancet *338*, 82–83.

Neuhausen, S.L., and Marshall, C.J. (1994). Loss of heterozygosity in familial tumors from three BRCA1-linked kindreds. Cancer Res. *54*, 6069–6072.

Newman, B., Austin, M.A., Lee, M., and King, M.-C. (1988). Inheritance of breast cancer: evidence for autosomal dominant transmission in high risk families. Proc. Natl. Acad. Sci. USA *85*, 1–5.

Peters, A.H.F.M., Plug, A.W., van Vugt, M.J. and deBoer, P. (1997). Drying down method for spreading mammalian meiocytes from the male and female germline. Chromosoma *5*, 1–3.

Plug, A.W., Xu, J., Reddy, G., Golub, E.I., and Ashley, T. (1996). Presynaptic association of Rad51 protein with selected sites in meiotic chromatin. Proc. Natl. Acad. Sci. USA *93*, 5920–5924.

Radding, C.M. (1991). Helical interactions in homologous pairing and strand exchange driven by RecA protein. J. Biol. Chem. *266*, 5355–5358.

Rao, V.N., Shao, N., Ahmad, M., and Reddy, E.S. (1996). Antisense RNA to the putative tumor suppressor gene BRCA1 transforms mouse fibroblasts. Oncogene *12*, 523–528.

Ried, T., Baldini, A., Rand, T.C. and Ward, D.C. (1992). Simultaneous visualization of seven different DNA probes by in situ hybridization using combinatorial fluorescence and digital imaging microscopy. Proc. Natl. Acad. Sci. USA *89*, 1388–1392.

Rowley, R., Subramani, S., and Young, P.G. (1992). Checkpoint controls in Schizosaccharomyces pombe, rad 1. EMBO J. *11*, 1335–1342.

Saurin, A.J., Borden, K.L. B., Boddy, M.N., and Freemont, P.S. (1996). Does this have a familiar RING? Trends Biochem. Sci. *21*, 208–214.

Scully, R., Ganesan, S., Brown, M., De Caprio, J.A., Cannistra, S.A., Feunteun, J., Schnitt, S., and Livingston, D.M. (1996). Location of BRCA1 in human breast and ovarian cell lines. Science *272*, 123–125.

Shao, N.S., Chai, Y.L., Shyam, E., Reddy, P., and Rao, N.V. (1996). Induction of apoptosis by the tumor suppressor protein BRCA1. Oncogene *13*, 1–7.

Shattuck-Eidens, D., McClure, M., Simard, J., Labrie, F., Narod, S., Couch, F., Hoskins, K., Weber, B., et al. (1995). A collaborative survey of 80 mutations in the BRCA1 breast and ovarian cancer susceptibility gene. J. Am. Med. Assoc. *273*, 535–541.

Shinohara, A., Ogawa, H., and Ogawa, T. (1992). Rad51 protein involved in repair and recombination in Saccharomyces cerevisiae is a RecA-like protein. Cell *69*, 457–470.

Simard, J., Tonin, P., Durocher, F., Morgan, K., Rommens, J., and Gingras, S. (1994). Common origins of BRCA1 mutations in Canadian breast and ovarian cancer families. Nat. Genet. *8*, 392–398.

Smith, S.A., Easton, D.F., Evans, D.G.R., and Ponder, B.A.J. (1992). Allele losses in the region 17q12–q21 in familial breast and ovarian cancer non-randomly involve the wild-type chromosome. Nat. Genet. *2*, 128–131.

Sturzbecher, H.-W., Donzelmann, B., Henning, W., Knippschild, U., and Buchop, S. (1996). p53 is linked directly to homologous recombination processes via RAD51/RecA protein interaction. EMBO J. *15*, 1992–2002.

Sung, P. (1994). Catalysis of ATP-dependent homologous DNA pairing and strand exchange by yeast Rad51 protein. Science *265*, 1241–1243.

Sung, P., and Robberson, D.L. (1995). DNA strand exchange mediated by a Rad51–ssDNA nucleoprotein filament with polarity opposite to that of RecA. Cell *82*, 453–461.

Swift, M., Reitnauer, P.J., Morrell, D., and Chase, C.L. (1987). Breast and other cancers in families with Ataxia-Telangiectasia. N. Engl. J. Med. *316*, 1289–1294.

Tashiro, S., Kotomura, N., Shinohara, A., Tanaka, K., Ueda, K., and Kamada, N. (1996). S phase specific formation of the human Rad51 protein nuclear foci in lymphocytes. Oncogene *12*, 2165–2170.

Terasawa, M., Shinohara, A., Hotta, Y., Ogawa, H., and Ogawa, T. (1995). Localization of RecA-like recombination proteins on chromosomes of lily at various meiotic stages. Genes Dev. *9*, 925–934.

Tsuzuki, T., Fujii, Y., Sakumi, K., Tominaga, Y., Nakao, K., Sekiguchi, M., Matsushiro, A., Yoshimura, Y., and Morita, T. (1996). Targeted disruption of the Rad51 gene leads to lethality in embryonic mice. Proc. Natl. Acad. Sci. USA *93*, 6236–6240.

Vairo, G., Livingston, D.M., and Ginsberg, D. (1995). Functional interaction between E2F-4 and p130: evidence for distinct mechanisms underlying growth suppression by different retinoblastoma protein family members. Genes Dev. *9*, 869–881.

Vaughn, J.P., Davis, P.L., Jarboe, M.D., Huper, G., Evans, A.C., Wiseman, R.W., Berchuck, A., Iglehart, J.D., et al. (1996). BRCA1 expression is induced before DNA synthesis in both normal and tumor-derived breast cells. Cell Growth Differ. *7*, 711–715.

Wigler, M., Silverstein, S., Lee, L.S., Pellicer, A., Cheg, Y.C., and Axel, R. (1977). Transfer of purified herpes virus thymidine kinase gene to cultured mouse cells. Cell *11*, 223–232.

Wilson, C.A., Payton, M.N., Elliott, G.S., Buaas, F.W., Cajulis, E.E., Grosshans, D., Ramos, L., Reese, D.M., et al. (1996). Differential subcellular localization, expression and biological toxicity of BRCA1 and the splice variant BRCA1-Δ11b. Oncogene, in press.

Zabludoff, S.D., Wright, W.W., Harshman, K., and Wold, B.J. (1996). BRCA1 mRNA is expressed highly during meiosis and spermiogenesis but not during mitosis of male germ cells. Oncogene *13*, 649–653.

Cell, Vol. 90, 425–435, August 8, 1997, Copyright ©1997 by Cell Press DAMD17-97-1-7180

APPENDIX 2

Dynamic Changes of BRCA1 Subnuclear Location and Phosphorylation State Are Initiated by DNA Damage

Ralph Scully,* Junjie Chen,* Robert L. Ochs,† Kathleen Keegan,‡ Merl Hoekstra,‡ Jean Feunteun,§ and David M. Livingston*
*The Dana-Farber Cancer Institute
Harvard Medical School
Boston, Massachusetts 02115
†The Scripps Research Institute
La Jolla, California 92037
‡ICOS Corporation
Bothell, Washington 98021
§Centre National de la Recherche Scientifique
Institut Gustave-Roussy
Cedex 94805 Villejuif
France

Summary

BRCA1 localizes to discrete nuclear foci (dots) during S phase. Hydroxyurea-mediated DNA synthesis arrest of S phase MCF7 cells led to a loss of BRCA1 from these structures. Ultraviolet light, mitomycin C, or gamma irradiation produced a similar effect but with no concurrent arrest of DNA synthesis. BARD1 and Rad51, two proteins associated with the BRCA1 dots, behaved similarly. Loss of the BRCA1 foci was accompanied by a specific, dose-dependent change(s) in the state of BRCA1 phosphorylation. Three distinct DNA damaging agents preferentially induced this change in S phase. The S phase BRCA1 phosphorylation response to DNA damage occurred in cells lacking, respectively, two DNA damage-sensing protein kinases, DNA-PK and Atm, implying that neither plays a prime role in this process. Finally, after BRCA1 dot dispersal, BRCA1, BARD1, and Rad51 accumulated, focally, on PCNA$^+$ replication structures, implying an interaction of BRCA1/BARD1/Rad51 containing complexes with damaged, replicating DNA. Taken together, the data imply that the BRCA1 S phase foci are dynamic physiological elements, responsive to DNA damage, and that BRCA1-containing multiprotein complexes participate in a replication checkpoint response.

Introduction

BRCA1 is a tumor suppressor gene that maps to human chromosome 17q 21.3 (Futreal et al., 1994; Hall et al., 1990; Miki et al., 1994; Neuhausen and Marshall, 1994; Smith et al., 1992). When one copy of *BRCA1* is inactivated in the germ line, affected individuals are predisposed to developing breast, ovarian, and other malignant tumors (reviewed in Feunteun and Lenoir, 1996). Until recently, there has been little understanding of how its product operates as a tumor suppressor or in any other capacity.

BRCA1 is an 1863 residue nuclear polypeptide which appears in discrete, nuclear foci (dots) during S phase (Chen et al., 1996; Scully et al., 1996, 1997a). These structures contain at least two other proteins, Rad51 and BARD1, both of which form complexes with BRCA1 in vivo (Scully et al., 1997a; Wu et al., 1996; R. Baer, personal communication and data presented below).

The *BRCA1* gene is widely expressed in developing embryos, with a marked preference for replicating cells (Lane et al., 1995; Marquis et al., 1995). It is essential for early embryonic proliferation and development (Gowen et al., 1996; Hakem et al., 1996; Liu et al., 1996). Recently, its full-length product was found to interact, directly or indirectly, with Rad51, a major participant in eukaryotic double-strand break repair and homologous recombination (Shinohara et al., 1992; Baumann et al., 1996; Scully et al., 1997a). BRCA1/Rad51 interactions have been identified in both mitotic and meiotic cells (Scully et al., 1997a), where Rad51 contributes to meiotic recombination (Ashley et al., 1995; Bishop, 1994; Terasawa et al., 1995). These observations imply that BRCA1 and Rad51 communicate physiologically and further suggest that BRCA1 functions in the maintenance of genome integrity.

In keeping with these findings, Sharan et al. (1997) have reported that another familial breast cancer tumor suppressor gene product, BRCA2, can interact with Rad51, and that murine embryos lacking wild-type *BRCA2* exhibit radiation sensitivity. Collectively, these data suggest that loss of functional BRCA1 or BRCA2 are mutagenic events, and, thereby, accelerate neoplastic transformation. Interestingly, BRCA1 and BARD1 each contain a C-terminal "BRCT" domain, which is found in many DNA repair and cell cycle checkpoint proteins (Bork et al., 1997; Callebaut and Mornon, 1997; Koonin et al., 1996). The generic function of the BRCT domain is not clear. However, this segment of BRCA1 has both transactivation (Chapman and Verma, 1996; Monteiro et al., 1996) and growth suppression properties (Humphrey et al., 1997) and may play a part in docking BRCA1 onto the RNA polymerase II holoenzyme (Scully et al., 1997b).

Although these observations are consistent with a role for BRCA1 in DNA repair and the maintenance of genome stability, there is little evidence that speaks to a dynamic function of BRCA1 in this regard. Here we report that BRCA1/Rad51/BARD1 containing S phase nuclear foci are sensitive to the integrity of the genome, undergoing a major structural change in the face of genotoxic insult. This response to DNA damage is accompanied by a specific change in BRCA1 phosphorylation and by the relocation of BRCA1, BARD1, and Rad51 to sites of "abnormal" (nonduplex) DNA structure in S phase cells. These findings suggest that BRCA1 participates in an S phase, DNA damage-dependent cell cycle checkpoint response.

Results

Disruption of BRCA1 S Phase Nuclear Foci by DNA Damage

A proportion of BRCA1 is localized to nuclear foci in S phase cells. These structures were not detected in

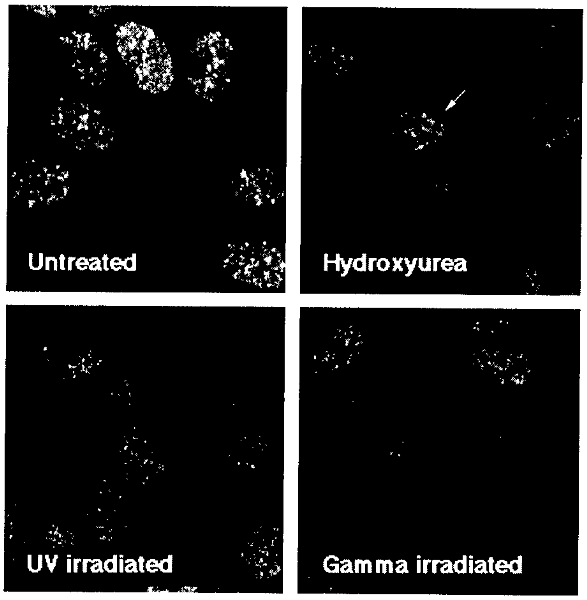

Figure 1. DNA Damage Disperses BRCA1 S Phase Focal Staining

S phase MCF7 cells were treated with DNA damaging agents, as indicated. Immunostaining for BRCA1 was performed using mAb MS13. Cells received either no treatment, HU 1 mM, UV 10 Jm^{-2}, or 5000 Rads and were harvested 1 hr later. The arrow indicates a rare cell in an HU-treated culture which retains some focal staining for BRCA1.

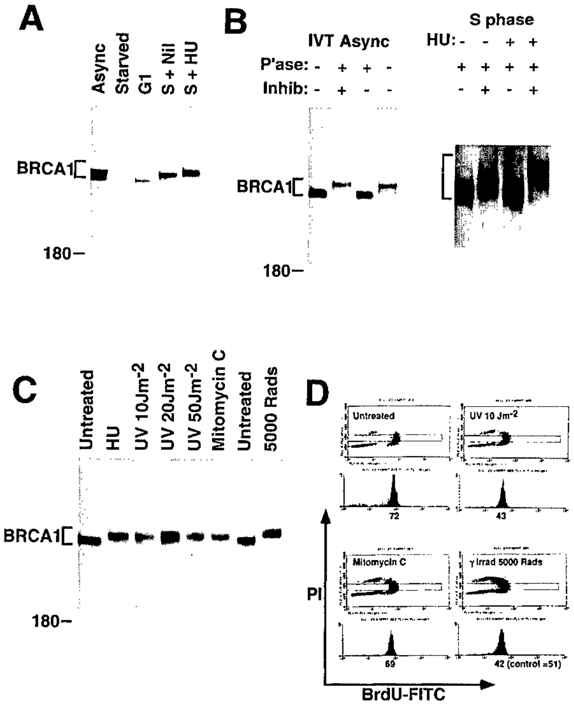

Figure 2. Specific Phosphorylation of BRCA1 following DNA Damage

(A) Cell cycle variation in BRCA1 gel mobility. MCF7 extracts were immunoblotted for BRCA1 using mAb MS110. Migration of BRCA1 is indicated. Async, asynchronous culture (58% G1, 30% S); starved, cells after 24 hr of serum starvation (90% G1, 2.5% S); G1, cells 12 hr after release into high serum (86% G1, 7% S); S + Nil, cells 24 hr after release into high serum (40% G1, 54% S); S + HU, identically treated S phase cells (in parallel) cultured after 24 hr of serum refeeding in HU for 1 hr before harvesting.

(B) Changes in mobility are due to changes in phosphorylation of BRCA1. BRCA1 IPs were treated with λ-phosphatase (see Experimental Procedures) ± phosphatase inhibitors, as indicated, and then immunoblotted for BRCA1. IVT, in vitro translated wild-type BRCA1. Left panel, MCF7 cells were asynchronous. Right panel, similar treatment of S phase MCF7 cells ± HU, as indicated. BRCA1 species are bracketed.

(C) Phosphorylation of BRCA1 in S phase after DNA damage. S phase MCF7 cells were exposed to the treatments shown for 1 hr prior to harvesting. Cell extracts were then immunoblotted for BRCA1.

(D) Cell cycle analysis on samples from (C). BrdU staining and cell cycle FACS analysis were performed as described in Experimental Procedures. To quantitate BrdU incorporation in S phase cells, a FACS gate was used to exclude G1 and G2 populations. Under each panel, the histogram gives the mean BrdU fluorescence intensity of gated (S phase) cells, in arbitrary units. HU-treated S phase cells, which had arrested DNA synthesis, had a mean BrdU fluorescence intensity of 13 in the same experiment.

multiple cell lines during G1, when a less intense nucleoplasmic BRCA1 immunostaining signal was observed (Scully et al., 1997a). They can be detected using many different BRCA1-specific Abs, raised to distinct epitopes, using any of several different fixation methods, or in living cells containing green fluorescent protein (GFP)-tagged BRCA1 (Scully et al., 1996; R. S., D. M. L., J. A. DeCaprio, and P. A. Silver, unpublished observations). Further, BRCA1 foci exist in mouse fibroblast nuclei as shown by immunofluorescence with anti-murine BRCA1 (X. Wu and D. M. L., unpublished observations). Hence, they are general BRCA1 phenomena.

Since BRCA1 is suspected of playing a role in genome integrity maintenance, we asked whether the S phase BRCA1 dots were altered in S phase cells after DNA damage and/or when DNA synthesis is interrupted. Hydroxyurea (HU) was used to induce DNA synthesis arrest of S phase cultures of the human breast cancer cell line, MCF7. BRCA1 immunostaining of HU-treated cells, performed with any of three different BRCA1 monoclonal antibodies, revealed overt dispersal of BRCA1 nuclear foci (Figure 1). Given the likelihood that HU treatment of S phase cells mimics DNA damage (Allen et al., 1994; Carr, 1995; Sanchez et al., 1996; Sun et al., 1996), we asked whether other DNA damaging agents affect the integrity of the S phase BRCA1 dots. Treatment with ultraviolet (UV) irradiation, mitomycin C, or gamma irradiation also led to dispersal of the dots within 1 hr (Figure 1 and data not shown). Untreated or mock-treated S phase cells revealed typical BRCA1 dots (Figure 1 and data not shown). Thus, dispersal of BRCA1 S phase foci might represent a cellular response to DNA damage. A few cells retained BRCA1 foci after HU or UV treatment (e.g., cell indicated by an arrow in Figure 1). The nature of these foci is discussed below (Figures 5 and 6 and accompanying text).

Cell Cycle–Specific Phosphorylation of BRCA1

In an effort to understand the mechanisms governing the migration of BRCA1 into and out of S phase foci, we sought biochemical correlates of the different BRCA1 nuclear immunofluorescence patterns. Immunoblotting for p220 BRCA1 in asynchronous MCF7 cells revealed a doublet (Figure 2A). Each band of the doublet reacted with BRCA1 monoclonal antibodies (mAbs), MS13, MS110, SG11, and AP16 (data not shown and Figure 2B). Serum-starved MCF7 cells contained reduced levels of BRCA1 (Figure 2A). Cells released into G1 for 12 hr produced an enrichment of the faster migrating band of the doublet (Figure 2A). In contrast, 24 hr after release into high serum, when most cells were in S phase, there was a further increase in BRCA1 protein level, represented primarily by the slower migrating form of the protein (Figure 2A). Similar observations concerning the migration of G1 and S phase associated forms of BRCA1 have been made by Ruffner and Verma (1997).

A parallel culture of S phase MCF7 cells was treated with HU for 1 hr. Immunoblotting revealed the presence of a form of BRCA1 that was not detected in untreated cycling cells but which migrated more slowly than the BRCA1 present in untreated S phase cells (Figure 2A). Thus, endogenous "p220" BRCA1 was detectable in at least three different forms: a rapidly migrating, G1-associated form; a more slowly migrating, S phase form; and an even more slowly migrating form, noted in HU-treated S phase cells.

Thus, BRCA1 might undergo regulated post-translational modifications, such as phosphorylation. Consistent with this, phosphatase treatment of BRCA1 immunoprecipitates (IPs) altered the gel mobility of BRCA1 (Figure 2B). IPs of BRCA1 from asynchronous MCF7 cells, using the C-terminal mAb, SG11, were aliquoted into three fractions. The first was treated with λ-phosphatase in the presence of phosphatase inhibitors; the second with λ-phosphatase in the absence of inhibitors; and the third was left untreated. IPs were immunoblotted using the N-terminal BRCA1 mAb, MS110. Phosphatase treatment in the absence of inhibitors resulted in collapse of the BRCA1 doublet into a single band which comigrated with in vitro synthesized, clonal BRCA1 (Figure 2B). Phosphatase treatment in the presence of inhibitors did not perturb the BRCA1 doublet relative to untreated IPs (Figure 2B), ruling out nonspecific effects of the phosphatase preparation. Similarly, phosphatase treatment of BRCA1 IPs, prepared from HU-treated S phase cells, led to its comigration with the phosphatase-treated BRCA1 species detected in naive S phase cells (Figure 2B). These results strongly suggest that the differential gel mobility of the three forms of BRCA1, noted in G1, S phase, and HU-treated S phase cells, is due to differential phosphorylation.

HU treatment of S phase cells, therefore, led to three measured events: DNA synthesis arrest, dispersal of BRCA1 foci, and phosphorylation of BRCA1. DNA synthesis arrest following brief (2 hr) HU exposure was found to be reversible. Removal of HU after this time led to the resumption of full DNA synthesis. Furthermore, both the BRCA1 foci and the faster migrating S phase BRCA1 band reappeared, while the slower HU-associated band disappeared (data not shown). Therefore, within the time limits of this experiment, all three effects of HU were reversible.

Phosphorylation of BRCA1 after DNA Damage in S Phase without Arrest of Scheduled DNA Synthesis

Exposure of S phase MCF7 cells to UV irradiation, mitomycin C, or gamma irradiation was found to retard the migration of the S phase BRCA1 band, similar to the effect of HU treatment (Figure 2C). This effect, coupled with the above noted dispersal of BRCA1 S phase foci (Figure 1), indicated a similarity between the effect of these DNA damaging agents and HU. However, in contrast to HU-treated cells, the response of S phase cells to two of these three DNA damaging agents did not include acute DNA synthesis arrest. Specifically, mitomycin C–treated and gamma-irradiated S phase MCF7 cells showed no impairment of BrdU incorporation compared with untreated controls, at a time when BRCA1 had already undergone the relevant DNA damage-induced phosphorylation (Figures 2C and 2D). UV treatment led to a dose-dependent inhibition of BrdU uptake, with only a modest impairment of DNA synthesis detectable in cells treated with 10 Jm^{-2}, but near total DNA synthesis arrest seen at 50 Jm^{-2} (Figure 2D and data not shown). Ten joules per square meter did, however, lead to the supershift of the S phase band, as seen following treatment with HU, mitomycin, or gamma irradiation (Figure 2C).

The finding of continued BrdU incorporation into S phase cells that had sustained acute DNA damage could be interpreted as unscheduled DNA synthesis (i.e., repair synthesis) in the context of an arrest of scheduled DNA synthesis. Although some repair process might be expected to be occurring at this time (e.g., to permit resolution of abnormal DNA structures at replication forks), the data are incompatible with the idea that scheduled DNA synthesis itself had ceased. First, BrdU incorporation during repair synthesis should be much less efficient than during normal DNA replication (Li et al., 1996), whereas near normal DNA synthesis levels were noted after acute exposure to mitomycin C, gamma irradiation, or 10 Jm^{-2} UV. Second, if the BrdU incorporation detected were a manifestation of repair synthesis alone, a higher density of DNA lesions should produce a higher level of BrdU incorporation. However, the reverse was true for UV treatment, where increasing doses led to progressive impairment of BrdU incorporation efficiency. Therefore, 1 hr after treatment with either UV irradiation (10 Jm^{-2}), mitomycin C, or gamma irradiation, scheduled DNA synthesis had not yet ceased. Therefore, DNA damage-associated BRCA1 phosphorylation can occur in S phase cells without arrest of scheduled DNA synthesis.

Although three DNA damaging agents and HU had disparate effects upon scheduled DNA synthesis, the feature common to all these treatments is their ability to induce DNA lesions, rather than their effect on the replication machinery per se. HU treatment might be predicted to produce, at least transiently, "abnormal" (i.e., nonduplex) DNA structures at arrested replication forks. The simplest model to explain these phenomena would be one in which "abnormal" DNA structures, generated in S phase, trigger a signaling cascade, one outcome of which is specific BRCA1 phosphorylation.

Time Course of the Response to UV Irradiation

These results suggest a relationship between DNA damage-associated phosphorylation of BRCA1 and dispersal of the BRCA1 dots. This was explored further, using UV as the stimulus. The phosphorylation status of BRCA1 was followed at 10-min intervals following a pulse of 10 Jm^{-2}, administered to S phase MCF7 cells. A significant alteration in BRCA1 gel mobility was apparent 20–30 min after treatment (Figure 3A). In a similar experiment, the time course of dispersal of BRCA1 foci was followed at 5-min intervals, by scoring, at each time point, four randomly selected confocal microscopic fields for the percentage of cells containing BRCA1 foci. Significant dispersal of BRCA1 foci was not detected until 25 min after the UV pulse (Figure 3B). Thus, at this UV dose (and also at higher doses, data not shown), there was a close temporal correlation between damage-induced phosphorylation of BRCA1 and dispersal of the BRCA1 foci.

Hydroxyurea, Mitomycin C, and UV Treatments Preferentially Target BRCA1 in S Phase

The data, noted above, raise the question of whether BRCA1 is targeted for phosphorylation by DNA damage only in S phase. The migration pattern of MCF7 in asynchronous or G1-enriched cells provided a means to address this question. We had noted (Figure 2A) that there is a faster migrating form of p220 BRCA1 enriched in G1 MCF7 cells and detectable in asynchronous cultures. Asynchronous MCF7 cells were subjected to treatment with HU, UV, or gamma irradiation. One hour later they were harvested and immunoblotted for BRCA1. Consistently, HU treatment or low-dose UV (10 Jm^{-2}) treatment induced the predicted BRCA1 gel shift of the upper (S phase correlated) but not the lower (G1 correlated) BRCA1 band (data not shown). In contrast, gamma irradiation (5000 Rads) appeared to displace both forms of BRCA1. This implied that low-dose UV or HU treatment might produce phosphorylation of BRCA1 in S phase but not in G1.

To test this notion directly, we prepared G1-synchronized MCF7 cells by serum starvation followed by 7 hr of incubation in high serum. These synchronized cells were then exposed to HU, UV, mitomycin C, or gamma irradiation and harvested 1 hr later, while still in G1. Immunoblotting for BRCA1 in unperturbed control G1 cells revealed the presence of the faster-migrating, G1 form of BRCA1, albeit at levels lower than in S phase cells (Figure 3C, left panel). Strikingly, neither HU, mitomycin C, nor low-dose UV treatment (10 Jm^{-2}) led to a change in the mobility of the G1 band (Figure 3C, right panel). Under identical conditions, the S phase band shifted (compare Figures 2C and 3C). Higher doses of UV led to a dose-dependent shift in the G1 form of BRCA1 (Figure 3C) as did gamma irradiation (5000 Rads).

This preferential S phase targeting of BRCA1 for phosphorylation, following HU, low dose UV, or mitomycin C, could be interpreted in two ways. First, the sensor(s) of abnormal DNA structure, or their subsequent amplificatory cascades, might operate differently between S phase and G1. Second, the S phase preference for BRCA1 phosphorylation after UV/mitomycin C could be an attribute of the BRCA1 protein itself, rather than of the signals impinging on it. A hint that the former might be correct came from examination of the response to

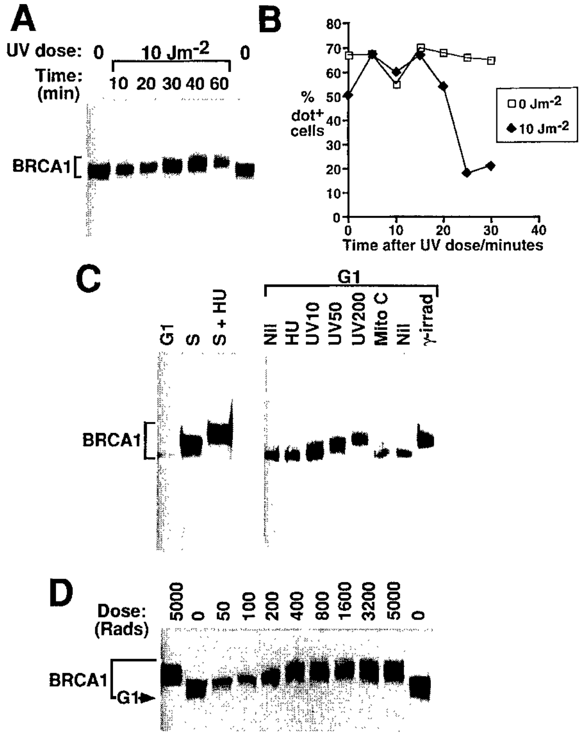

Figure 3. Time Course and Cell Cycle Specificity of the BRCA1/DNA Damage Response

(A) Time course of phosphorylation change after UV irradiation. S phase enriched MCF7 cells were exposed to 10 Jm^{-2} UV light, harvested at the time points indicated, and immunoblotted for BRCA1. The shift in BRCA1 migration is seen ~20–30 min after UV exposure.

(B) Time course of BRCA1 focus dispersal following UV exposure. In a protocol identical to that employed in A, S phase MCF7 cells were exposed to 10 Jm^{-2} UV light (filled diamonds), or mock treated (open squares), and were harvested at the time points indicated. Each coverslip was stained for BRCA1, and cells in four randomly selected confocal fields were scored for the presence or absence of BRCA1 nuclear foci. One hundred and fifteen to 185 cells were scored per time point. Results are presented as the percentage of cells scoring positive for BRCA1 foci.

(C) S phase specificity of the BRCA1 damage response. MCF7 cells were released from serum starvation into G1 for 7 hr. After treatment with DNA damaging agents, as shown, cells were harvested 1 hr later (while still in G1) and immunoblotted for BRCA1. Extracts of S phase MCF7 and HU-treated S phase cells were analyzed in parallel to show the relative migration of the G1, G1/damage, S and S/damage forms of BRCA1. Note that HU, mitomycin C, and low-dose UV treatment (10 Jm^{-2}) each failed to shift the G1 form of BRCA1 under conditions in which the S phase form had undergone damage-induced phosphorylation (compare with Figure 2C).

(D) BRCA1 gel migration change after ionizing radiation. Asynchronously growing MCF7 cells were exposed to metered doses of gamma irradiation, harvested 1 hr later, and then immunoblotted for BRCA1. The lower (G1) band of BRCA1, indicated with an arrow, was noted to disappear at 50 Rads, whereas the S phase band shifted only at doses above 200 Rads.

gamma irradiation. When asynchronous MCF7 cells were exposed to a range of doses of gamma irradiation, the emergence of BRCA1 species migrating slower than the S phase band was apparent only at doses above 200 Rads (Figure 3D). In contrast, exposure to 50 Rads was sufficient to displace the G1 form of the protein (Figure 3D). Therefore, gamma irradiation appeared to

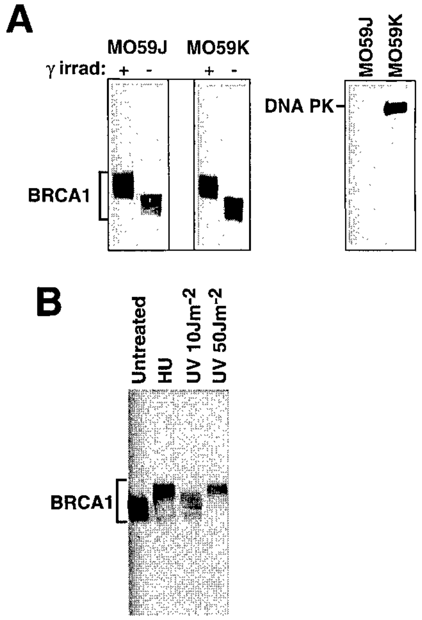

Figure 4. BRCA1 Damage Response in DNA-PK and ATM Mutant Cell Lines

(A) Asynchronously growing human glioma cell lines, MO59J (DNA-PK null) and MO59K (DNA-PK wild type) were exposed to 5000 Rads, or mock treated, and harvested 1 hr later. Immunoblotting for BRCA1 is shown in the left panel, and for DNA-PK in the right panel.

(B) Response of AT fibroblasts to HU and UV treatment. Asynchronous cultures of the AT primary human diploid fibroblast culture, GM02052B, were exposed to DNA damaging agents as shown, harvested 1 hr later, and immunoblotted for BRCA1.

provide an exception to the above-noted preference for S phase in signaling from DNA damage to BRCA1. This suggests that cell cycle specificity in the BRCA1 DNA damage response is a property of the particular sensors of and signaling arising from DNA damage, rather than of the BRCA1 protein itself.

DNA-Dependent Protein Kinase and the Ataxia Telangiectasia Gene Product Are Not Required for DNA Damage-Induced BRCA1 Phosphorylation in S Phase

Genetic and biochemical approaches suggest a role for the PIK family of nuclear protein kinases in linking the detection of DNA damage to cell cycle responses (Bentley et al., 1996; Cimprich et al., 1996; Hari et al., 1995; Hartley et al., 1995; Keith and Schreiber, 1995; Morrow et al., 1995; Savitsky et al., 1995). This family of proteins includes the catalytic subunit of DNA-dependent protein kinase (p460 DNA-PK), Atm, and Atr. Initially, we asked whether a functional copy of DNA-PK was necessary for detection of the BRCA1 DNA damage-phosphorylation response. The human glioma cell line, MO59, has two derivatives, one of which (MO59K) is wild-type for p460 DNA-PK. The other (MO59J) does not express its gene (Lees-Miller et al., 1995). Using gamma irradiation as the stimulus, we asked whether the two cell lines could each respond to DNA damage by phosphorylating BRCA1. Indeed, the two cell lines mounted indistinguishable responses to gamma irradiation (Figure 4A and data not shown). Immunoblotting of whole cell extracts was used to confirm the expression of p460 DNA-PK in MO59K cells and its absence from MO59J cells (Figure 4A). BRCA1 phosphorylation after HU or UV treatment was also detected in both cell lines, and the response to each of these stimuli was indistinguishable between MO59J and MO59K cells (data not shown). These results exclude p460 DNA-PK as a necessary component of the DNA damage-BRCA1 phosphorylation pathway.

To investigate a potential role for Atm, we analyzed primary cultures of Atm homozygous mutant fibroblasts. Both HU and UV exposure elicited a clear retardation in the migration of the S phase BRCA1 band (Figure 4B). A similar response to gamma irradiation was also noted (data not shown), although a quantitative effect of Atm on the DNA damage-BRCA1 signaling pathway has not yet been ruled out.

Recruitment of BRCA1 to PCNA- and DNA-Containing Nuclear Structures after DNA Damage in S Phase

Close examination of the BRCA1 immunostaining pattern after HU treatment or UV irradiation revealed that the frequency of cells, within S phase cultures, containing BRCA1 nuclear foci, although substantially reduced, was not zero (Figures 1 and 3B). In a small proportion of cells, there were characteristic small, punctate BRCA1 dots. In yet others, a qualitatively different BRCA1 focal pattern was detected (see below). The reasons for the presence of these different BRCA1 focal staining patterns became clear when cells were double stained for BRCA1 and proliferating cell nuclear antigen (PCNA), as detailed below.

Under some fixation conditions, PCNA immunostaining is seen only in cells synthesizing DNA, and given that its staining pattern changes during S phase, it can be used as an S phase temporal marker (Bravo, 1986; Bravo and Macdonald-Bravo, 1987). In early/mid–S phase cells, PCNA immunostaining is in a multifocal/diffusely nuclear pattern. In late S phase, the staining pattern changes dramatically and becomes "nodular." Importantly, throughout S phase, the immunostaining pattern of BrdU incorporation into replication forks clearly overlies the PCNA stain (Bravo and Macdonald-Bravo, 1987; Nakamura et al., 1986; Figure 5A). We confirmed, by the use of a mimosine block and release protocol, that these changes in PCNA morphology are similarly correlated with the stage of S phase in MCF7 cells (data not shown).

In synchronized cells, BRCA1 foci first appear in S phase. This raised the question of whether BRCA1 foci coincide with PCNA foci. This was addressed using two-color immunostaining followed by confocal microscopy. Images in Figure 5B depict unperturbed, S phase MCF7 cells doubly stained for BRCA1 (green, fluorescein isothiocyanate [FITC]) and PCNA (red, rhodamine). In repeated experiments, the two immunostaining patterns were found to be distinct, even when the PCNA pattern resembled the nodular one reported for late S phase cells (Bravo and Macdonald-Bravo, 1987; Nakamura et al., 1986). Thus, in conventionally cycling S phase cells, there was no immunocytochemical indication that

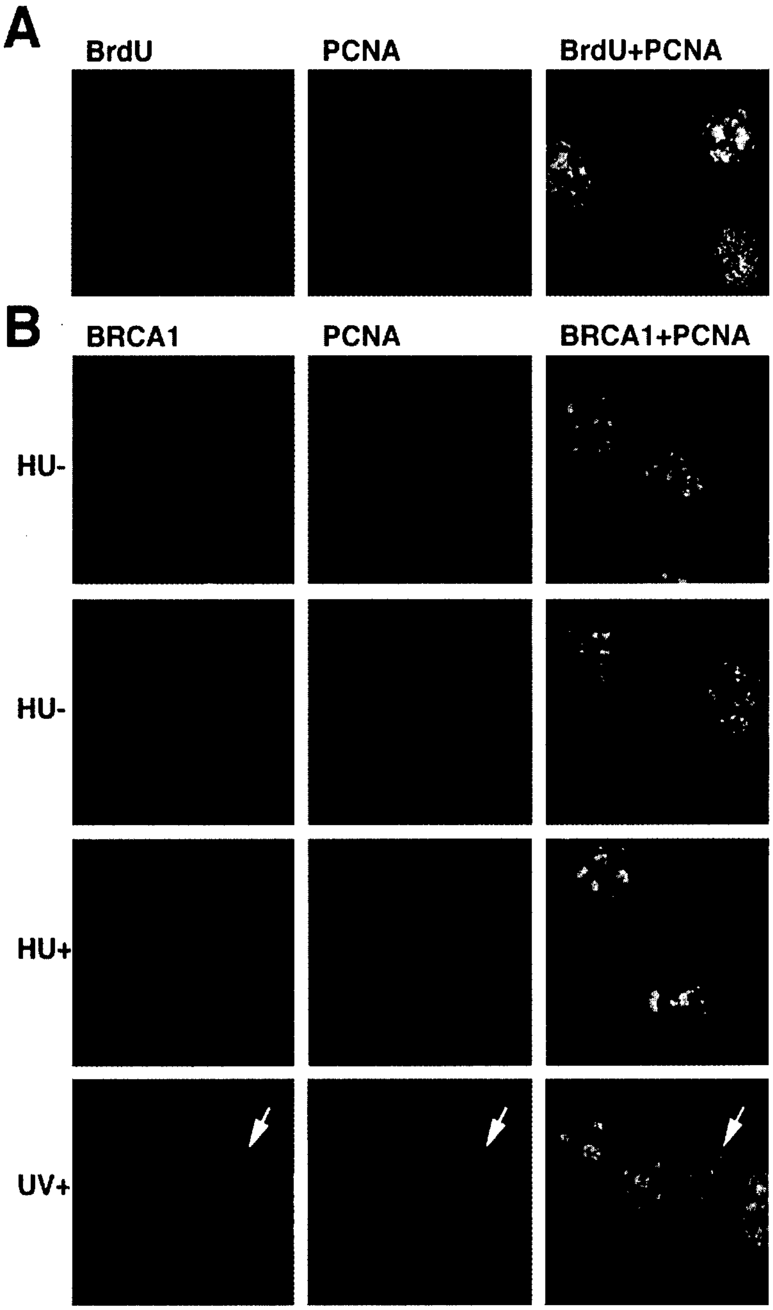

Figure 5. Recruitment of BRCA1 to Replication Structures after HU or UV Treatment

(A) In S phase cells, PCNA immunostaining can be used to locate sites of DNA synthesis. Panels depict S phase MCF7 cells, pulsed with BrdU prior to fixation, double stained with anti-BrdU mAb (green), and anti-PCNA Ab ("AK" serum, red). Where colocalization of the two images is seen, the signal appears in the right hand panel as a yellow signal.

(B) Recruitment of BRCA1 to replication structures after HU treatment. In untreated S phase cells ("HU−"), BRCA1 foci (mAb MS13, green) were not significantly coincident with PCNA (AK Ab, red) in either early S phase (upper row) or late S phase (second row). In contrast, in HU-treated cells ("HU+," third row), BRCA1 colocalizes extensively with PCNA in late S phase nuclei, as shown by the yellow overlap signal of green and red. Similar results were obtained in UV treated cells ("UV+," lowest row). The arrow points to a cell carrying BRCA1 dots and no PCNA staining. This may be a G2 cell.

BRCA1 focally accumulates at replication forks. Further, a small proportion of cells was noted to be positive for BRCA1 foci and negative for PCNA. This population was found to be enriched in late S phase cultures (data not shown), suggesting that the presence of BRCA1 foci is also a feature of some G2 cells.

In contrast, when HU- or UV-treated S phase cultures were similarly examined, a striking colocalization of the BRCA1 staining pattern and the PCNA staining pattern was noted in those rare, late S phase cells in which PCNA immunostaining was clearly nodular or focal (Figure 5B and data not shown). In the majority of S phase nuclei, where the PCNA pattern was diffuse, the BRCA1 stain was also diffuse (data not shown). The overt relocation of BRCA1 to $PCNA^+$ structures after DNA damage suggests that BRCA1 is recruited to replication forks after HU or UV treatment of S phase cells. By contrast, the small subset of nuclei scoring positive for BRCA1 dots but negative for PCNA (presumed G2 cells, as noted above) were not perturbed by either HU or UV treatment (e.g., "UV^+" panel in Figure 5B, cell indicated by an arrow).

Colocalization of BRCA1, BARD1, and Rad51 before and after DNA Damage in S Phase

Two proteins associated with BRCA1 in S phase foci—Rad51 and BARD1—were examined during the DNA damage response. Consistent with the described physical interaction between BRCA1 and BARD1 (Wu et al., 1996), BARD1 immunostaining, reflected by binding of multiple antibodies to BARD1, colocalized with BRCA1 in S phase nuclear dots (Figure 6A). This result was

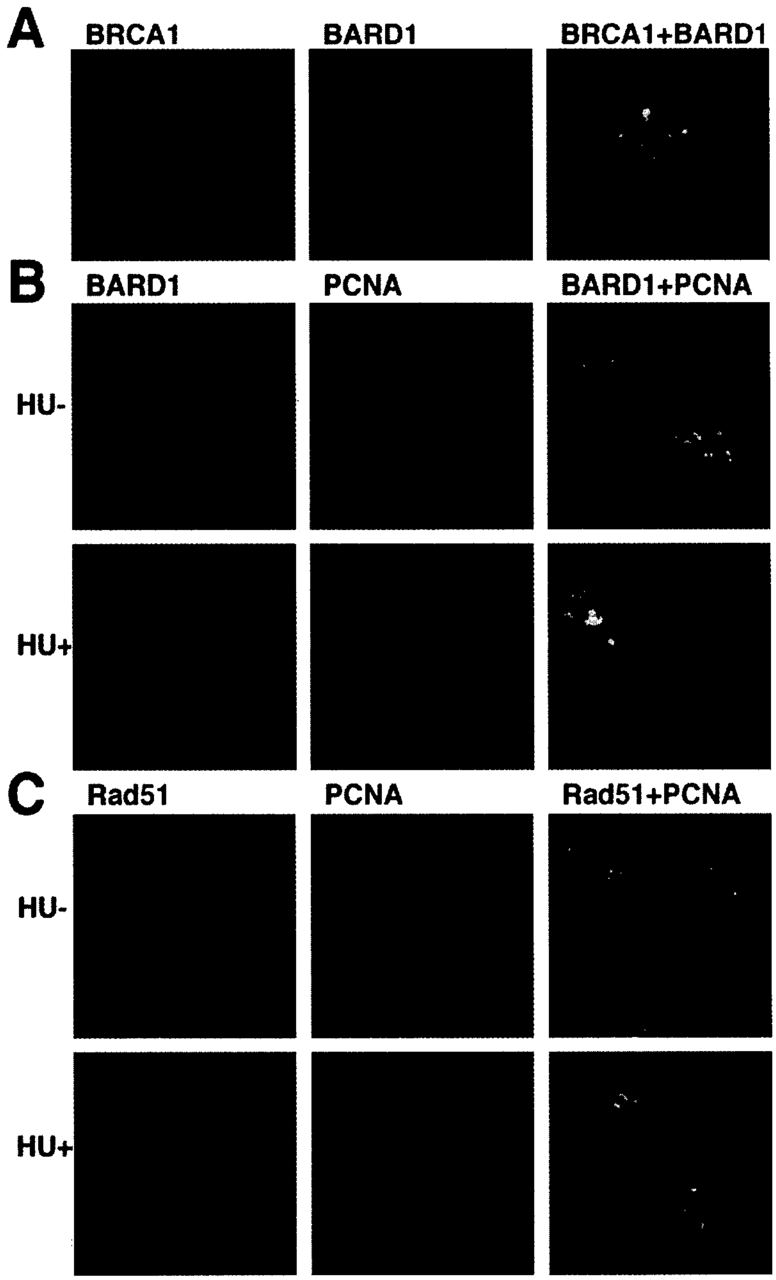

Figure 6. Recruitment of BARD1 and Rad51 to Replication Structures after DNA damage

(A) Colocalization of BRCA1 and BARD1 in S phase nuclear foci. Untreated S phase MCF7 cells, stained with BRCA1 mAb MS13 (green, FITC) and BARD1 Ab (rhodamine, red). Where the two nuclear dot signals overlap, a yellow signal was detected.

(B) Recruitment of BARD1 to replication structures after HU treatment. The upper panel depicts untreated S phase MCF7 cells ("HU−") double stained for BARD1 (using affinity purified polyclonal antiserum to BARD1, red) and PCNA (using mAb PC10, green). No significant colocalization of the green and red signals was noted. The lower panel shows the same, two-color immunstaining experiment, performed on HU-treated MCF7 cells ("HU+"). Where BARD1 and PCNA signals overlap, a yellow color was noted in the right-hand panel.

(C) Recruitment of Rad51 to replication structures after HU treatment. Similar treatments as for (B). Cells were double stained for Rad51 (using affinity purified polyclonal antiserum to Rad51, green) and PCNA (using "AK" antiserum, red), as described in Experimental Procedures. After HU treatment ("HU+"), but not in untreated cells ("HU−"), significant colocalization of Rad51 and PCNA is seen as a yellow overlap.

first obtained by Richard Baer and coworkers (personal communication). S phase ($PCNA^+$) nuclei were examined for BARD1 and Rad51 before and after HU or UV treatment. As was noted for BRCA1, undamaged cells revealed no significant colocalization of either Rad51 or BARD1 with PCNA (Figures 6B and 6C, see HU−). After HU or UV exposure, however, colocalization was seen on PCNA nodules (Figures 6B and 6C, see HU+). In the majority of S phase nuclei, where the PCNA stain was diffuse, Rad51 and BARD1 stains were also found to have become diffuse (data not shown). Thus, BRCA1 and two known associated proteins, BARD1 and Rad51, both concentrate in PCNA-containing, replicating structures after DNA damage. Like BRCA1 dots, BARD1 and Rad51 foci appeared to persist into G2 (data not shown). In addition, as was noted above for BRCA1 foci in G2, the BARD1/Rad51 G2 foci were not perturbed by either UV or HU treatment (data not shown).

These findings strengthen the notion that BRCA1 relocalizes to replication forks after DNA damage, since it does so in the company of two known physiological partners. Hence, either multiprotein BRCA1-containing complexes leave the dots after DNA damage, or the underlying subnuclear structure which constitutes the substance of the S phase foci, itself, undergoes disassembly after DNA damage.

Discussion

These experiments identify the p220 BRCA1 protein as a participant in a DNA damage response of cycling cells, thereby fulfilling the prediction that BRCA1 participates in the maintenance of genome integrity (Scully et al., 1997a). Within 1 hr of treatment of cells with various DNA damaging agents, two effects were noted in the behavior of the BRCA1 protein. First, S phase cells lost the characteristic BRCA1 nuclear foci. Second, the protein underwent a specific change(s) in phosphorylation. Third, BRCA1 was now associated with PCNA/replicating DNA-containing structures. The timing of these events was closely correlated, suggesting that they are different manifestations of the same cellular response. Taken together, these findings allow one to construct a functional model of BRCA1 behavior, at least during S phase.

First, the BRCA1 dots, which clearly contain BRCA1-containing complexes, given the colocalization of both Rad51 and BARD1, appear to be dynamic physiological structures. Their integrity is, at a minimum, tied to the integrity of the genome. DNA damage leads to signals, transmitted over a measurable period of time, which result in the loss of BRCA1 containing protein/protein complexes from these structures, if not the loss of the structures themselves. These signals do not depend upon the cessation of DNA synthesis for accurate transmission and are, hence, not a specific result of replication arrest. Whether the dots are active in the absence of genome damage, playing an as yet unknown role in the replication process (and/or in postreplication events) or whether they are simply repositories of proteins that are active in the damage (and possibly other stress) response(s) is not clear. That BRCA1 appears to disperse from the dots after genome damage strongly suggests that BRCA1 itself plays a role in the response to DNA damage. Such a conclusion strongly supports the earlier speculation put forward on the occasion of the first detection of BRCA1/Rad 51 complexes (Scully et al., 1997a). Thus, the BRCA1/Rad51/BARD1 nuclear dots are an example of multiprotein-containing nuclear structures whose integrity is modified by modifiers of genome integrity.

Second, in parallel with the loss of the BRCA1 dots, DNA damage led to a specific alteration in the state of BRCA1 phosphorylation. The timing of the two events was similar, and both events were reversible in HU-treated cells, implying that they are linked and that both are reflections of the existence of unrepaired DNA damage. These findings indicate that BRCA1 is a substrate of one or more kinases activated specifically by DNA damage. They, therefore, place BRCA1 on an S phase DNA damage-initiated signaling pathway. G1 cells were able to respond with specific BRCA1 phosphorylation events following DNA damage, but there were clear differences in the substance of the responses between G1 and S phase cells. Whether the protein contributes to the enaction of both G1 and S (and possibly G2) checkpoint responses remains to be seen.

One class of genes implicated in such signaling pathways encode the "PIK" kinases, Atm, Atr, and p460 DNA-PK, each of which shows extensive conservation between yeast, drosophila and human (Bentley et al., 1996; Cimprich et al., 1996; Hari et al., 1995; Hartley et al., 1995; Keith and Schreiber, 1995; Morrow et al., 1995; Savitsky et al., 1995). Genetic analysis has suggested a role for Atm in multiple cell cycle checkpoints (Painter and Young, 1980; reviewed in Elledge, 1996). The yeast homologs of Atr, rad3^{sp}, and MEC1^{sc}, have been clearly implicated in S phase and other DNA damage checkpoints (Bentley et al., 1996; Paulovich and Hartwell, 1995). DNA-PK functions in double-stranded break repair and VDJ recombination (reviewed in Lieber et al., 1997). In addition, the products of these genes are protein kinases and they interact with yet other protein kinases. This combined evidence suggests that the "PIK" kinases are signal transducers, e.g., linking DNA damage with cell cycle events (reviewed in Elledge, 1996). Our observations on BRCA1 suggest that its phosphorylation after DNA damage might be an assay for the activity of one or more "PIK" kinases. There are data in the literature consistent with a model in which BRCA1 and Atr and, possibly, Atm interact on meiotic chromosomes (Keegan et al., 1996; Scully et al., 1997a).

The availability of tissue from ataxia-telangiectasia patients has provided cultured primary cells lacking Atm function. For each modality of DNA damage examined—HU treatment, UV, or ionizing radiation—S phase BRCA1 mobility slowed within 1 hr of exposure. Thus, Atm is not absolutely required for S phase DNA damage-induced phosphorylation of BRCA1. Whether the same is true for G1 cells is unclear at present. Similarly, p460 DNA-PK deficient cells responded normally to this same spectrum of DNA damaging agents. This implies that DNA-PK is not an absolute requirement for the S phase effect as well. The components of the S phase DNA damage/BRCA1 signaling pathway, therefore, remain to be identified. Based upon what is known from analyses of Drosophila and yeast, Atr must be considered a potential participant in this pathway. At present, however, there are no cell lines known to be functionally null for Atr.

Finally, BRCA1 appears to relocalize to replicating DNA structures after DNA damage. The interpretation of these observations can only be speculated upon at present. HU and UV induced the same relocalization behavior in BRCA1 (also in Rad51 and BARD1), again suggesting that the responses provoked by these two agents have fundamental similarities. One interpretation of these phenomena is that, in each case, a DNA repair process is initiated at the replication fork. In the case of UV-induced damage, DNA replication may be accompanied by a recombinational DNA damage response (Fornace, 1983; Friedberg et al., 1995). In the case of HU treatment, the replication fork likely contains a high density of "abnormal," or nonduplex, DNA structures, which might provoke a DNA damage response. If such speculations hold true, one might deduce that BRCA1 has an affinity for sites of specialized DNA structure, a conclusion supported by its localization to the axial element of the developing synaptonemal complex (Kleckner, 1996; Scully et al., 1997a).

If BRCA1 is recruited to certain abnormal DNA structures as part of a DNA damage response, a role for BRCA1 in DNA repair seems likely. This might or might not be linked to an inferred role of BRCA1 in transcription regulation, as evidenced by its transactivation domain and by its stable association with the RNA polymerase II holoenzyme (Scully et al., 1997b). Two paradigms, which are not mutually exclusive, could be considered.

First, BRCA1 may play a DNA repair role, even in the context of the RNA polymerase II holoenzyme, perhaps analogous to some components of TFIIH (reviewed in Bhatia et al., 1996). Second, BRCA1 may be truly bifunctional (or multifunctional), serving as both a factor in the processing of abnormal DNA structures and as a participant in the signaling which results in the activation of certain genes which follow DNA damage. The p53 tumor suppressor protein likely operates in such a bifunctional manner (reviewed in Ko and Prives, 1996).

How do these observations reflect upon the function of the BRCA1 dots in undamaged cells? One might speculate that the BRCA1 S/G2 phase dots are sites specialized for the processing of replicating or replicated DNA. It is worth noting, at this point, that BRCA1 is active during both the mitotic and meiotic cell cycle and interacts with developing synaptonemal complexes (Scully et al., 1997a). Given the functional parallel between meiotic interhomolog and mitotic intersister interactions (Kleckner, 1996), one wonders whether function in the BRCA1 dots is connected with intersister interactions.

Similarly obscure at present is the relationship that might exist between the mechanisms governing the behavior of BRCA1 in a replication checkpoint pathway and the tissue specificity of its role in tumor suppression. The connection may become clearer from a better understanding of the biology of breast and ovarian epithelium.

Experimental Procedures

Tissue Culture Methods

Cells were cultured in Dulbecco's modified Eagle's medium (DMEM)–10% fetal bovine serum (FBS). MCF7 cells were synchronized as described previously (Scully et al., 1997a). For late G1 synchronization, mimosine (200 μM final concentration) was added to MCF7 cells for 16 hr. Release into S phase produced tight synchrony through this segment of the cycle, allowing preparation of early or late S phase cultures.

DNA Damaging Agents

Cells were exposed to genotoxic agents and, unless otherwise stated, harvested 1 hr later. HU (Sigma) treatment was added to a final concentration of 1 mM. Mitomycin C (Sigma) was added to a final concentration of 20 μg/ml. UV doses were delivered in a single pulse using a Stratalinker (Stratagene). Prior to pulsing, medium was removed, being replaced immediately after treatment. Gamma irradiation was delivered using a Gammacell 1000 apparatus.

Immunoblotting and Immunoprecipitation of BRCA1

Cell extracts were prepared in EBC buffer (50 mM Tris, pH 8, 120 mM NaCl, 0.5% Nonidet P-40 [NP-40]), with the addition of 50 mM NaF, 1 mM sodium orthovanadate, 100 μg/ml polymethylsulfonyl fluoride (PMSF), 20 μg/ml aprotinin, and 10 μg/ml leupeptin. One hundred micrograms of whole cell extract were loaded per lane. To detect changes in the mobility of p220 BRCA1, prolonged 5 or 6% SDS-polyacrylamide gel electrophoresis (SDS-PAGE) was used (e.g., 100 V for 16 hr). Transfer to nitrocellulose was performed using a semidry transfer method (Novablot, Pharmacia), in 50 mM Tris base, 40 mM glycine, 0.37 g/l SDS, 20% methanol (for 3 hr at 1.5 mA/cm2). After blocking with 5% nonfat dried milk in TBS-T (20 mM Tris, pH 8, 0.9% NaCl, 0.05% Tween 20) with sodium azide (0.1%), the primary antibody, MS110 (Scully et al., 1996; Oncogene Science), was used at 2 μg/ml in PBS/1% nonfat dried milk/0.1% azide, for 1 hr at room temperature. The secondary antibody was peroxidase-conjugated goat anti-mouse IgG (H+L, Jackson Immunoresearch), at 1:10,000 in 1% nonfat milk/TBS-T. Signals were developed by ECL (Amersham). IP of BRCA1 was performed as described previously (Scully et al., 1997a).

Phosphatase Treatment of Immunoprecipitates

BRCA1 IPs were washed in extraction buffer in the absence of phosphatase inhibitors. Parallel samples were resuspended in λ-phosphatase buffer (New England Biolabs) either in the presence or absence of the phosphatase inhibitors, NaF (50 mM final concentration) and sodium orthovanadate (2 mM final concentration). After heating samples to 30°C for 1 min, 500 U of λ-phosphatase (New England Biolabs) was added to each sample, followed by incubation at 30°C for 1 hr. Samples were separated by SDS-PAGE and immunoblotted for BRCA1. In the same experiments, in vitro translation of the BRCA1 cDNA was performed using a TNT kit (Promega).

Antibodies, Immunostaining, and Confocal Microscopy

Cells were fixed for 10 min in PBS-buffered 3% paraformaldehyde/2% sucrose solution, followed by 5 min permeablization on ice in Triton buffer (0.5% Triton X-100 in 20 mM HEPES, pH 7.4, 50 mM NaCl, 3 mM MgCl, 300 mM sucrose). Alternatively, to visualize replication forks using PCNA Ab, methanol acetone (70%:30% v/v) fixation for 15 min at −20°C was performed. The latter coverslips were air dried and rehydrated in PBS prior to immunostaining. Methanol/acetone fixation produced poor results with the Rad51 Ab. To visualize replication forks in this case, cells were permeablized in Triton buffer (above) prior to paraformaldehyde fixation, to elute away the soluble PCNA fraction (a modification of Li et al., 1996).

BRCA1 was visualized using mAbs- MS13, MS110, or AP16 (Scully et al., 1996). PCNA was visualized using AK antiserum at 1:5000, or with PCNA mAb PC10 (Santa Cruz) at 1:100. BARD1 was visualized using an affinity-purified rabbit polyclonal antiserum to residues 141–388 of the gene product. This was shown to colocalize with BARD1-specific mAbs, confirming the identity of the signal. Cross-reactivity between this antiserum and BRCA1 protein was sought but not detected. Rad51 Ab was generated by immunization of rabbits with GST-Rad51 fusion protein. After absorption of anti-GST Abs, affinity purification was performed by standard methods using an aminolink column (Pierce) coupled to GST-Rad51. All secondary antibodies used were species-specific fluorochrome-conjugated Abs from Jackson Immunoresearch, used at 1:200 throughout.

Two-color immunostaining for BrdU and PCNA was performed as follows. Methanol-acetone fixed cells were stained with PCNA antiserum "AK" (from R. Ochs), followed by secondary Ab. After post-fixing in paraformaldehyde/sucrose solution (above) for 10 min at room temperature, cells were incubated for 5 min in 2 N HCl to expose incorporated BrdU. After multiple phosphate-buffered saline (PBS) washes, fluorescein isothiocyanate (FITC)-conjugated anti-BrdU mAb (Becton Dickenson) was used to develop a BrdU incorporation signal.

All antibody incubations were performed at 37°C for 20 min. Under the conditions used, no significant signal attributable to secondary antibody, alone, was detected. All images were collected by confocal microscopy (Zeiss) and processed using Adobe Photoshop software.

Cell Cycle Analysis

Cells were pulsed with BrdU (Boehringer-Mannheim) for 10 min prior to harvesting. Aliquots of harvested plates were trypsinized, neutralized, washed in PBS, and fixed in cold 70% ethanol while vortexing. After storage on ice, cells were vortexed into 2 N HCl/0.5% Tween-20. After 30 min of incubation, cells were washed twice in PBS/HEPES, pH 7.4, to restore physiological pH, and incubated with 50 μl of PBS/1% BSA/0.5% Tween-20 and 20 μl of FITC-conjugated anti-BrdU mAb (Becton-Dickenson), for 30 min at room temperature. After further washes, cells were incubated in 70 μM propidium diiodide dissolved in 38 mM sodium citrate, in the presence of DNAase-free RNAase (2.5 μg/ml final concentration, Boehringer-Mannheim) for 30 min at 37°C. Samples were analyzed immediately thereafter by FACS (Becton-Dickenson).

Acknowledgments

We are indebted to numerous colleagues whose generosity in sharing reagents and thoughts made this work possible. In particular, we thank Dr. Richard Baer for generously making available antibodies to BARD1 and for informing us of his results revealing colocalization of BARD1 and BRCA1 in dots; Drs. David Weaver and Kurt Auger for gifts of cell lines; Dr. David Hill for antibody to DNA-PK; and Drs. Myles Brown, James DeCaprio, Mark Ewen, William Kaelin, and Richard Kolodner for critical and stimulating discussions.

Received June 11, 1997; revised July 1, 1997.

References

Allen, J.B., Zhou, Z., Siede, W., Friedberg, E.C., and Elledge, S.J. (1994). The SAD1/RAD53 protein kinase controls multiple checkpoints and DNA damage-induced transcription in yeast. Genes Dev. *8*, 2401–2415.

Ashley, T., Plug, A.W., Xu, J., Solari, A.J., Reddy, G., et al. (1995). Dynamic changes in Rad51 distribution on chromatin during meiosis in male and female vertebrates. Chromosoma *104*, 19–28.

Baumann, P., Benson, F.E., and West, S.C. (1996). Human Rad51 protein promotes ATP-dependent homologous pairing and strand transfer reactions in vitro. Cell *87*, 757–766.

Bentley, N.J., Holtzman, D.A., Keegan, K.S., Flaggs, G., DeMaggio, A.J., et al. (1996). The Schizosaccharomyces pombe rad3 checkpoint gene. EMBO J. *15*, 6641–6651.

Bhatia, P.K., Wang, Z., and Friedberg, E.C. (1996). DNA repair and transcription. Curr. Opin. Genet. Dev. *6*, 146–150.

Bishop, D.K. (1994). RecA homologues Dmc1 and Rad51 interact to form multiple nuclear complexes prior to meiotic chromosome synapsis. Cell *79*, 1081–1092.

Bork, P., Hofmann, K., Bucher, P., Neuwald, A.F., Altschul, S.F., and Koonin, E.V. (1997). A superfamily of conserved domains in DNA damage-responsive cell cycle checkpoint proteins. FASEB J. *11*, 68–76.

Bravo, R. (1986). Synthesis of the nuclear protein cyclin (PCNA) and its relationship with DNA replication. Exp. Cell. Res. *163*, 287–293.

Bravo, R., and Macdonald-Bravo, H. (1987). Existence of two populations of cyclin/proliferating cell nuclear antigen during the cell cycle: association with DNA replication sites. J. Cell. Biol. *105*, 1549–1554.

Callebaut, I., and Mornon, J.P. (1997). From BRCA1 to RAP1: a widespread BRCT module closely associated with DNA repair. FEBS Lett. *400*, 25–30.

Carr, A.M. (1995). DNA structure checkpoints in fission yeast. Semin. Cell Biol. *6*, 65–72.

Chapman, M.S., and Verma, I.M. (1996). Transcriptional activation by BRCA1. Nature *382*, 678–679.

Chen, Y.M., Farmer, A.A., Chen, C.F., Jones, D.C., Chen, P.L., and Lee, W.H. (1996). BRCA1 is a 220-kDa nuclear phosphoprotein that is expressed and phosphorylated in a cell cycle-dependent manner. Cancer Res. *56*, 3168–3172.

Cimprich, K.A., Shin, T.B., Keith, C.T., and Schreiber, S.L. (1996). cDNA cloning and gene mapping of a candidate human cell cycle checkpoint protein. Proc. Natl. Acad. Sci. USA *7*, 2850–2855.

Elledge, S.J. (1996). Cell cycle checkpoints: preventing an identity crisis. Science *274*, 1664–1672.

Feunteun, J., and Lenoir, G.M. (1996). BRCA1, a gene involved in inherited predisposition to breast and ovarian cancer. Biochim. Biophys. Acta *1242*, 177–180.

Fornace, A.J., Jr. (1983). Recombiation of parent and daughter strand DNA after UV-irradiation in mammalian cells. Nature *304*, 552–554.

Friedberg, E.C., Walker, G.C., and Siede, W. (1995). DNA Repair and Mutagenesis. (Washington: ASM Press).

Futreal, P.A., Liu, Q., Shattuck-Eidens, D., Cochran, C., Harshmann, K., et al. (1994). BRCA1 mutations in primary breast and ovarian carcinomas. Science *266*, 120–122.

Gowen, L.C., Johnson, B.L., Latour, A.M., Sulik, K.K., and Koller, B.H. (1996). BRCA1 deficiency results in early embryonic lethality characterized by neuroepithelial abnormalities. Nature Genet. *12*, 191–194.

Hakem, R., de la Pomba, J.L., Sirard, C., Mo, R., Woo, M., et al. (1996). The tumor suppressor gene *Brca1* is required for embryonic cellular proliferation in the mouse. Cell *85*, 1009–1023.

Hall, J.M., Lee, M.K., and Newmann, B. (1990). Linkage of early-onset breast cancer to chromosome 17q21. Science *250*, 1684–1689.

Hari, K.L., Santerre, A., Sekelsky, J.J., McKim, K.S., Boyd, J.B., and Hawley, R.S. (1995). The mei-41 gene of D. melanogaster is a structural and functional homolog of the human ataxia telangiectasia gene. Cell *82*, 815–821.

Hartley, K.O., Gell, D., Smith, G.C., Zhang, H., Divecha, N., et al. (1995). DNA-dependent protein kinase catalytic subunit: a relative of phosphatidylinositol 3-kinase and the ataxia telangiectasia gene product. Cell *82*, 849–856.

Humphrey, J.S., Salim, A., Erdos, M.R., Collins, F.S., Brody, L.C., and Klausner, R.D. (1997). Human *BRCA1* inhibits growth in yeast: potential use in diagnostic testing. Proc. Natl. Acad. Sci. USA *94*, 5820–5825.

Keegan, K.S., Holtzman, D.A., Plug, A.W., Christenson, E.R., Brainerd, E.E., et al. (1996). The Atr and Atm protein kinases associate with different sites along meiotically pairing chromosomes. Genes Dev. *10*, 2423–2437.

Keith, C.T., and Schreiber, S.L. (1995). PIK-related kinases: DNA repair, recombination, and cell cycle checkpoints. Science *270*, 50–51.

Kleckner, N. (1996). Meiosis: How could it work? Proc. Natl. Acad. Sci. USA *93*, 8167–8174.

Ko, L.J., and Prives, C. (1996). p53: puzzle and paradigm. Genes Dev. *10*, 1054–1072.

Koonin, V.F., Altschul, S.F., and Bork, P. (1996). BRCA1 protein products: functional motifs. Nature Genet. *13*, 266–267.

Lane, T.F., Deng, C., Elson, A., Lyu, M.S., Kozak, C.A., and Leder, P. (1995). Expression of BRCA1 is associated with terminal differentiation of ectodermally and mesodermally derived tissues in mice. Genes Dev. *9*, 2712–2722.

Lees-Miller, S.P., Godbout, R., Chan, D.W., Weinfeld, M., Day, R.S.I., et al. (1995). Absense of p350 subunit of DNA-activated protein kinase from a radiosensitive human cell line. Science *267*, 1183–1185.

Li, R., Hannon, G.J., Beach, D., and Stillman, B. (1996). Subcellular distribution of p21 and PCNA in normal and repair-deficient cells following DNA damage. Curr. Biol. *6*, 189–199.

Lieber, M.R., Grawunder, U., Wu, X., and Yaneva, M. (1997). Tying loose ends: roles of Ku and DNA-dependent protein kinase in the repair of double-strand breaks. Curr. Opin. Genet. Dev. *7*, 99–104.

Liu, C.Y., Flesken-Nikitin, A., Li, S., Zeng, Y., and Lee, W.-H. (1996). Inactivation of the mouse Brca1 gene leads to failure in the morphogenesis of the egg cylinder in early postimplantation development. Genes Dev. *10*, 1835–1843.

Marquis, S.T., Rajan, J.V., Wynshaw-Boris, A., Xu, J., and Yin, G.-Y. (1995). The developmental pattern of BRCA1 expression implies a role in differentiation of the breast and other tissues. Nature Genet. *11*, 17–26.

Miki, Y., Swensen, J., Shattuck-Eidens, D., Futreal, P.A., Harshman, K., et al. (1994). A strong candidate for the breast and ovarian cancer susceptibility gene BRCA1. Science *266*, 66–71.

Monteiro, A.N.A., August, A., and Hanafusa, H. (1996). Evidence for a transcriptional activation function of BRCA1 C-terminal region. Proc. Natl. Acad. Sci. USA *93*, 13595–13599.

Morrow, D.M., Tagle, D.A., Shiloh, Y., Collins, F.S., and Hieter, P. (1995). TEL1, an S. cerevisiae homolog of the human gene mutated in ataxia telangiectasia, is functionally related to the yeast checkpoint gene MEC1. Cell *82*, 831–840.

Nakamura, H., Morita, T., and Sato, C. (1986). Structural organizations of replicon domains during DNA synthetic phase in the mammalian nucleus. Exp. Cell Res. *165*, 291–297.

Neuhausen, S.L., and Marshall, C.J. (1994). Loss of heterozygosity in familial tumors from three BRCA1-linked kindreds. Cancer Res. *54*, 6069–6072.

Painter, R.B., and Young, B.R. (1980). Radiosensitivity in ataxia telangiectasia: a new explanation. Proc. Natl. Acad. Sci. USA *77*, 7315–7317.

Paulovich, A.G., and Hartwell, L.H. (1995). A checkpoint regulates the rate of progression through S phase in S. cerevisiae in response to DNA damage. Cell *82*, 841–847.

Ruffner, H., and Verma, I. (1997). BRCA1 is a cell cycle-regulated nuclear phosphoprotein. Proc. Natl. Acad. Sci. USA *94*, 7138–7143.

Sanchez, Y., Desany, B.A., Jones, W.J., Liu, Q., Wang, B., and Elledge, S.J. (1996). Regulation of RAD53 by the ATM-like kinases MEC1 and TEL1 in yeast cell cycle checkpoint pathways. Science *271*, 357–360.

Savitsky, K., Bar-Shira, A., Gilad, S., Rotman, G., Ziv, Y., et al. (1995). A single ataxia telangiectasia gene with a product similar to PI-3 kinase. Science *268*, 1749–1753.

Scully, R., Ganesan, S., Brown, M., De Caprio, J.A., Cannistra, S.A., et al. (1996). Location of BRCA1 in human breast and ovarian cell lines. Science *272*, 123–125.

Scully, R., Chen, J., Plug, A., Xiao, Y., Weaver, D., et al. (1997a). Association of BRCA1 with Rad51 in mitotic and meiotic cells. Cell *88*, 265–275.

Scully, R., Anderson, S.F., Chao, D.M., Wei, W., Ye, L., et al. (1997b). BRCA1 is a component of the RNA polymerase II holoenzyme. Proc. Natl. Acad. Sci. USA *94*, 5605–5610.

Sharan, S.K., Morimatsu, M., Albrecht, U., Lim, D.-S., Regel, E., et al. (1997). Embryonic lethality and radiation hypersensitivity mediated by Rad51 in mice lacking BRCA2. Nature *386*, 804–810.

Shinohara, A., Ogawa, H., and Ogawa, T. (1992). Rad51 protein involved in repair and recombination in Saccharomyces cerevisiae is a RecA-like protein. Cell *69*, 457–470.

Smith, S.A., Easton, D.F., Evans, D.G.R., and Ponder, B.A.J. (1992). Allele losses in the region 17q12-q21 in familial breast and ovarian cancer non-randomly involve the wild-type chromosome. Nature Genet. *2*, 128–131.

Sun, Z., Fay, D.S., Marini, F., Foiani, M., and Stern, D.F. (1996). Spk1/Rad53 is regulated by Mec1-dependent protein phosphorylation in DNA replication and damage checkpoint pathways. Genes Dev. *10*, 395–406.

Terasawa, M., Shinohara, A., Hotta, Y., Ogawa, H., and Ogawa, T. (1995). Localization of RecA-like recombination proteins on chromosomes of lily at various meiotic stages. Genes Dev. *9*, 925–934.

Wu, L.C., Wang, Z.W., Tsan, J.T., Spillman, M.A., Phung, A., et al. (1996). Identification of a RING protein that can interact in vivo with the BRCA1 gene product. Nature Genet. *14*, 430–440.

Molecular Cell, Vol. 2, 1–20, September, 1998, Copyright ©1998 by Cell Press 08-1! APPENDIX 3

Stable Interaction between the Pro of the *BRCA1* and *BRCA2* Tumor Suppressor Genes in Mitotic and Meiotic Cells

Junjie Chen,* Daniel P. Silver,* Deepika Walpita,† Sharon B. Cantor,* Adi F. Gazdar,‡ Gail Tomlinson,‡ Fergus J. Couch,‖ Barbara L. Weber,§ Terry Ashley,† David M. Livingston,*# and Ralph Scully*
*The Dana Farber Cancer Institute
Harvard Medical School
Boston, Massachusetts 02115
†Department of Genetics
Yale University School of Medicine
New Haven, Connecticut 06520
‡Hamon Center for Therapeutic Oncology Research
University of Texas Southwestern Medical Center
Dallas, Texas 75235
§Department of Medicine
University of Pennsylvania
Philadelphia, Pennsylvania 19104
‖Department of Laboratory Medicine and Pathology
Mayo Clinic and Foundation
Rochester, Minnesota 55905

Summary

BRCA1 and BRCA2 account for most cases of familial, early onset breast and/or ovarian cancer and encode products that each interact with hRAD51. Results presented here show that BRCA1 and BRCA2 coexist in a biochemical complex and colocalize in subnuclear foci in somatic cells and on the axial elements of developing synaptonemal complexes. Like BRCA1 and RAD51, BRCA2 relocates to PCNA⁺ replication sites following exposure of S phase cells to hydroxyurea or UV irradiation. Thus, BRCA1 and BRCA2 participate, together, in a pathway(s) associated with the activation of double-strand break repair and/or homologous recombination. Dysfunction of this pathway may be a general phenomenon in the majority of cases of hereditary breast and/or ovarian cancer.

Introduction

BRCA1 or *BRCA2* germline mutations predispose women to early onset, familial breast cancer (Hall et al., 1990; Narod et al., 1991; Miki et al., 1994; Wooster et al., 1994, 1995; Tavtigian et al., 1996). Disease risk is inherited as an autosomal dominant trait (Newman et al., 1988; Claus et al., 1991). The majority of tumors arising in *BRCA1*- or *BRCA2*-linked family members show loss of heterozygosity (LOH) at the relevant loci with retention of the mutant allele (reviewed in Zhang et al., 1998). Thus, the behavior of these two genes follows the Knudson model of tumor suppressor genetics.

The *BRCA1* and *BRCA2* products are large nuclear proteins, whose primary amino acid sequences yield few clues to their function. An exception is a motif at the C terminus of BRCA1, termed BRCT (Koonin et al., 1996). BRCT is a relatively common feature of proteins involved in DNA repair and/or in cell cycle checkpoint function (Koonin et al., 1996; Bork et al., 1997; Callebaut and Mornon, 1997). Although there is some similarity between the exon structures of *BRCA1* and *BRCA2*, there is no appreciable sequence homology between the proteins.

There is evidence suggesting that *BRCA1* and *BRCA2* function in an analogous manner (reviewed in Zhang et al., 1998). Both gene products interact with hRAD51 in vivo (Scully et al., 1997a; Sharan et al., 1997). RAD51 plays a key role in homologous recombination and double-strand break repair (Radding, 1991; Shinohara et al., 1992; Sung, 1994; Sung and Robberson, 1995; Baumann et al., 1996). In the developing mouse embryo, the patterns of *BRCA1*, *RAD51*, and *BRCA2* gene expression are almost identical (Lane et al., 1995; Marquis et al., 1995; Rajan et al., 1997; Sharan et al., 1997). In human cell lines, the expression of each gene increases as cells enter S phase, suggesting that at least some of the biological function(s) of these genes are exerted during or following DNA replication (Gudas et al., 1995, 1996; Rajan et al., 1996; Vaughn et al., 1996; Chen et al., 1997; Blackshear et al., 1998).

BRCA1, *BRCA2*, or *RAD51* nullizygous mice all reveal early embryonic lethality, associated with a proliferation deficit (Gowen et al., 1996; Hakem et al., 1996; Lim and Hasty, 1996; Liu et al., 1996; Tsuzuki et al., 1996; Ludwig et al., 1997; Sharan et al., 1997; Suzuki et al., 1997). Death occurs at E6.5 in *RAD51*, E7.5 in *BRCA1*, and E8.5 in *BRCA2* nullizygotes. Preceding death of either *BRCA1* or *BRCA2* nullizygotes, there is increased expression of the DNA damage-responsive, cell cycle inhibitor, p21 (Hakem et al., 1996; Connor et al., 1997; Suzuki et al., 1997). For *RAD51*, *BRCA1*, and *BRCA2*, the lethal nullizygous phenotype is partially suppressed by coincident, homozygous *p53* germline mutation (Lim and Hasty, 1996; Hakem et al., 1997; Ludwig et al., 1997). Homozygous *p21* germline mutations also partially suppress the *BRCA1* or *BRCA2* nullizygous phenotype (Hakem et al., 1997). Hence, viability of these embryos is likely limited by activation of the p53-mediated checkpoint control system with subsequent nonproliferation.

These observations imply that BRCA1 and BRCA2 function in related pathways. If these pathways were linked to genome integrity control, abnormal DNA structures might emerge as a consequence of their dysfunction (Scully et al., 1997a). Abnormal DNA structures, in turn, might lead to DNA damage-dependent, p53/p21-mediated cell cycle arrest, leading to the genetic relationships noted above. Consistent with this model, *BRCA2* nullizygous embryos exhibited X-ray supersensitivity (Sharan et al., 1997). Cells of *BRCA2* mutant mice reveal inefficient repair of DNA breaks and aberrant chromosomal structures (Connor et al., 1997; Patel et al., 1998). They are also hypersensitive to DNA-adducting agents (Patel et al., 1998). These findings suggest a role for BRCA2 in recombinational responses to DNA damage, as was suggested for BRCA1 (Scully et al., 1997a, 1997c). Moreover, the cells of *BRCA1*- and

#To whom correspondence should be addressed.

MASTER PROOF

08-19-98 16:24:23 0808415114

BRCA2-deficient tumors are especially aneuploid (Marcus et al., 1996), consistent with both loci participating in the maintenance of genome stability.

Here we report the interaction of endogenous BRCA2 with endogenous BRCA1 in cultured human cell lines, their nuclear colocalization, and similar responses of these proteins to DNA damage. These data indicate that endogenous BRCA1 and BRCA2 coexist in a biochemical complex, suggesting their joint participation in at least one DNA damage pathway that is frequently inactivated in hereditary breast and ovarian cancer.

Results

Characterization of Anti-BRCA2 Antibodies

Three affinity-purified polyclonal rabbit antibodies (Ab), anti-BRCA2A, -2B, and -2C were raised against GST BRCA2 proteins encoding aa 1425–1973, 2422–2976, and 3245–3418, respectively. To learn whether these antibodies recognize endogenous BRCA2, blots of U2OS cell extracts were probed with the BRCA1 mAb, MS110, or a BRCA2 Ab (Figure 1A, left panel). All three BRCA2 antibodies recognized a protein larger than BRCA1 (400 kDa; see Figure 1A, and data not shown). To learn whether the 400 kDa protein was hBRCA2, we generated a full-length cDNA encoding hBRCA2 fused to an N-terminal influenza hemagglutinin (HA) epitope. The abundance of the 400 kDa protein, detected by immunoblotting with anti-BRCA2, was significantly increased in cells transfected with an HA-BRCA2 expression plasmid (Figure 1B, left panel). HA antibody also immunoprecipitated a 400 kDa protein from transfected cells but not from untransfected cells (data not shown), suggesting that this protein is HA-tagged, full-length BRCA2. HA-BRCA2 comigrated with the 400 kDa protein precipitated by BRCA2 antibody from untransfected cell extracts (Figure 1B, right panel).

To determine whether BRCA2 antibody can immunoprecipitate intact BRCA2, extracts of untransfected cells or cells transfected with HA-BRCA2 were immunoprecipitated with a control anti-mIgG Ab or anti-BRCA2C (Figure 1C). Blotted immunoprecipitates were probed with anti-HA mAb (12CA5). The 400 kDa protein was detected by anti-HA immunoblotting only in transfected cell extracts, and it was also immunoprecipitated by anti-BRCA2 antibody, thereby showing that the BRCA2 antiserum can immunoprecipitate hBRCA2 (Figure 1C).

CAPAN-1 is a human pancreatic carcinoma cell line that carries a 6174delT BRCA2 mutation and has lost the wild-type *BRCA2* allele (Goggins et al., 1996). This mutation should result in the loss of BRCA2 residues 1982–3418 and the concomitant disappearance of the anti-BRCA2B (residues 2422–2976) and 2C epitopes (residues 3245–3418). An IP/immunoblotting protocol was used with anti-BRCA2C to search for BRCA2 in various human cell lines, including CAPAN-1. Full-length BRCA2 proteins were detected in 293T, MCF-7, HCC1937, and U2OS cells, but not in CAPAN-1 (Figure 1D, upper left panel), implying that anti-BRCA2C Ab recognizes intact, endogenous BRCA2. While anti-BRCA2B also failed to recognize truncated BRCA2 in CAPAN-1 cells (Figure 1D, upper right panel), anti-BRCA2A, raised against a more N-terminal region of BRCA2, did recognize this fast-migrating BRCA2 species (Figure 1D, upper right panel; Figure 3B). The 220 kDa BRCA1 protein levels in CAPAN-1 cells were similar to those detected in the control cell lines 293T, MCF-7, and U2OS (Figure 1D, lower panel).

HCC1937 was established from the primary infiltrating breast ductal carcinoma of a 24-year-old female who had a germline BRCA1 mutation, insert C at nt 5382 (G. T. et al., unpublished data). HCC1937 has lost the wild-type *BRCA1* allele. The mutant sequence predicts a frameshift in codon 1756 of the *BRCA1* ORF, leading to the synthesis of a 210 kDa truncated product lacking the BRCA1 C terminus. Consistent with this, HCC1937 extracts revealed no full-length BRCA1 protein (Figure 1D, lower panel). HCC1937 extracts did, however, contain low levels of a 210 kDa BRCA1 species (Figure 1D, lower right panel). The BRCA2 levels in HCC1937 cells were similar to those in 293T, MCF-7, and U2OS extracts (Figure 1D, upper left panel).

Association of BRCA1 and BRCA2 In Vivo

MCF7 cell extracts were subjected to immunoprecipitation using multiple BRCA1 Abs, each raised against a different region of BRCA1 (Figure 2A). While an E1A mAb, M73, and control rabbit IgG failed to precipitate BRCA1 or BRCA2, all BRCA1 Abs coimmunoprecipitated BRCA1 and BRCA2 (Figure 2A, left panel). Identical results were obtained with 293T or U2OS extracts (data not shown). Each BRCA1 Ab recognized in vitro translated BRCA1, but not in vitro translated BRCA2 (data not shown), indicating that they do not recognize BRCA2 directly. These observations suggest that endogenous BRCA1 and BRCA2 interact, directly or indirectly.

To test further for evidence of BRCA1/2 antibody cross-reactivity, we investigated the coimmunoprecipitation of BRCA1 and BRCA2 in HCC1937 cells. The mAb, SG11, was raised against the C-terminal 17 residues of BRCA1 (Scully et al., 1996). As noted above, this epitope should be absent from the 210 kDa truncated *BRCA1* product detected in HCC1937 cells. While monoclonal antibodies against more N-terminal epitopes of BRCA1 immunoprecipitated this truncated form of BRCA1, SG11 did not (Figure 2A, right panel and data not shown). In addition, unlike SG11, MS13, a mAb raised against an N-terminal segment of BRCA1 (Scully et al., 1996), also coimmunoprecipitated BRCA2 from HCC1937 extracts (Figure 2A, right panel). These results rule out the possibility that SG11 cross-reacts with BRCA2. They also suggest that the extreme C terminus of BRCA1 is not required for the proposed BRCA1/BRCA2 interaction.

In search of additional evidence that BRCA1 and BRCA2 can form a complex in vivo, we generated a full-length *BRCA1* cDNA bearing an N-terminal myc epitope. Myc-tagged BRCA1 and HA-tagged BRCA2 were transiently transfected, individually and together, into 293T cells. A myc mAb, 9E10, coimmunoprecipitated HA-BRCA2 from cells cotransfected with both expression vectors, but not from cells transfected with HA-BRCA2, alone (Figure 2B). A BRCA1 mutant (Mut) with an 11-residue truncation of its extreme C terminus (Y1853term) also coprecipitated with BRCA2 in these assays (Figure

MASTER PROOF (SH)

08-19-98 16:24:23 0808415114

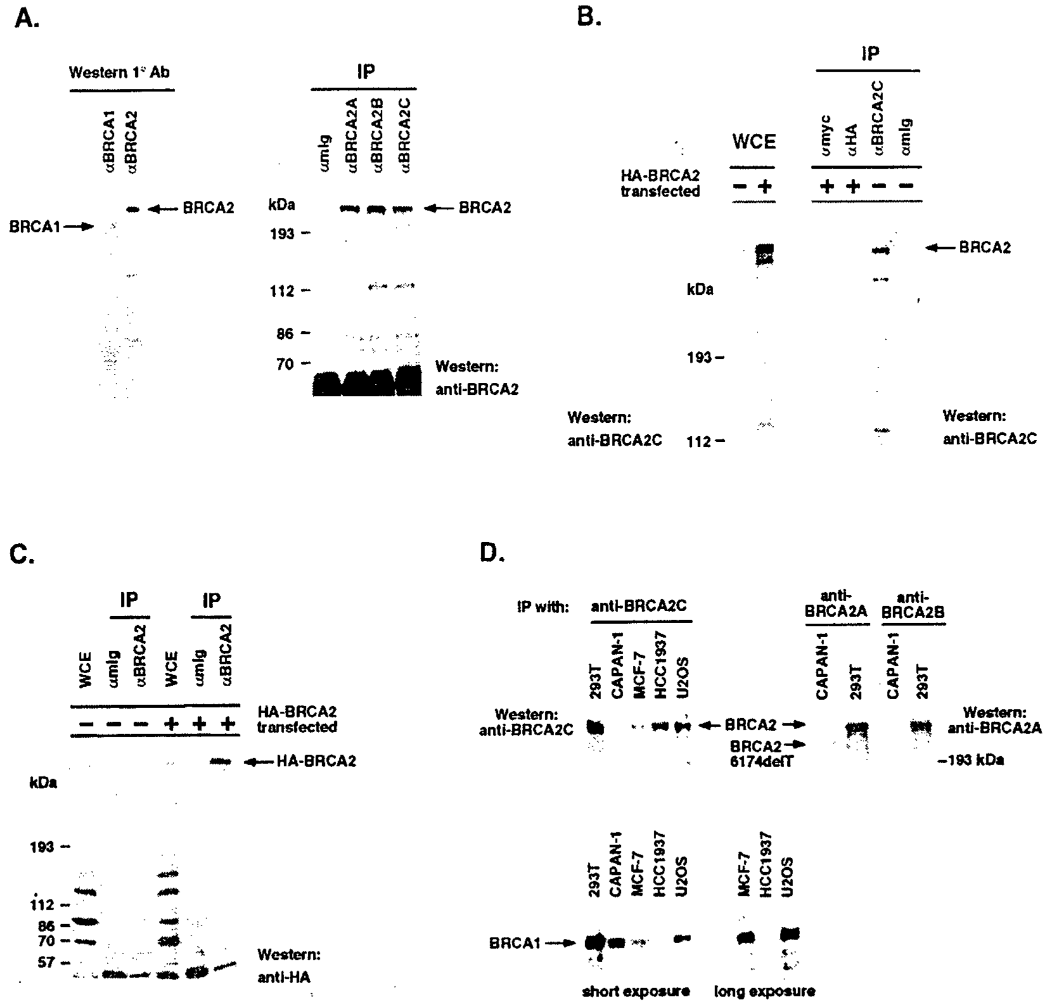

Figure 1. Characterization of Anti-BRCA2 Antibodies

(A) Left, whole-cell extracts of U2OS cells were separated by SDS-PAGE and immunoblotted with either anti-BRCA1 mAb MS110 or anti-BRCA2C antibody. Right, 293T cell extracts were subjected to immunoprecipitation (IP) with control antibody (rabbit anti-mouse IgG) or three independent anti-BRCA2 antibodies (A, B, and C), and the immunoblot was probed with anti-BRCA2C antibody.
(B) Aliquots of whole-cell extract (WCE, 50 μg/lane) from untransfected 293T (−) cells or cells transfected with expression plasmids encoding HA-BRCA2 (+) were separated by SDS-PAGE and immunoblotted with anti-BRCA2 antibody (left panel). Aliquots of extract from cells transfected with expression plasmids encoding HA-BRCA2 were subjected to immunoprecipitation by a control anti-myc antibody (9E10) or anti-HA mAb 12CA5, and extracts of untransfected 293T cells were subjected to immunoprecipitation with anti-BRCA2C antibody or a control rabbit anti-mouse IgG Ab. Immunoblotting was performed with anti-BRCA2C antibody (right panel).
(C) Whole-cell extracts (50 mcg) of untransfected 293T cells (−) or 293T cells transfected with an HA-BRCA2 expression plasmid (+) were subjected to immunoprecipitation with control (anti-mouse IgG) or anti-BRCA2C antibodies, separated by SDS-PAGE, and immunoblotted using anti-HA antibody (12CA5).
(D) Top, extracts of 293T, CAPAN-1, MCF-7, HCC1937, and U2OS cells were immunoprecipitated and immunoblotted with anti-BRCA2C antibody (left panel). Extracts of 293T and CAPAN-1 cells were immunoprecipitated with anti-BRCA2A or anti-BRCA2B antibodies and immunoblotted with anti-BRCA2A (right panel). Bottom, extracts of 293T, CAPAN-1, MCF-7, HCC1937, and U2OS cells were immunoprecipitated with an affinity-purified, polyclonal anti-BRCA1 antibody (raised against residues 758–1313 of BRCA1) and immunoblotted with a monoclonal anti-BRCA1 antibody, MS110. A longer exposure in the lower panel is shown here to illustrate the truncated BRCA1 protein present in HCC1937 cells.

2B). This is in agreement with the above-noted finding that extreme C terminus of BRCA1 is not required for BRCA1/BRCA2 coprecipitation. These data indicate that authentic, clonal BRCA1 and BRCA2 can interact in vivo.

Finally, reciprocal immunoprecipitation experiments were performed with anti-BRCA2 antibodies raised against three different regions of BRCA2. Both BRCA1 and RAD51 were detected in all three anti-BRCA2 immunoprecipitates from naive MCF7 or 293T cells (Figures 3A and 3B, and data not shown), confirming that BRCA1 and BRCA2 interact in unperturbed cells. Anti-RAD51 immunoprecipitates generated from an extract of MCF7 cells contained both BRCA1 and BRCA2 (Figure 3A, left panel). To determine whether anti-BRCA2 Abs cross-react with BRCA1, we repeated these experiments in

MASTER PROOF

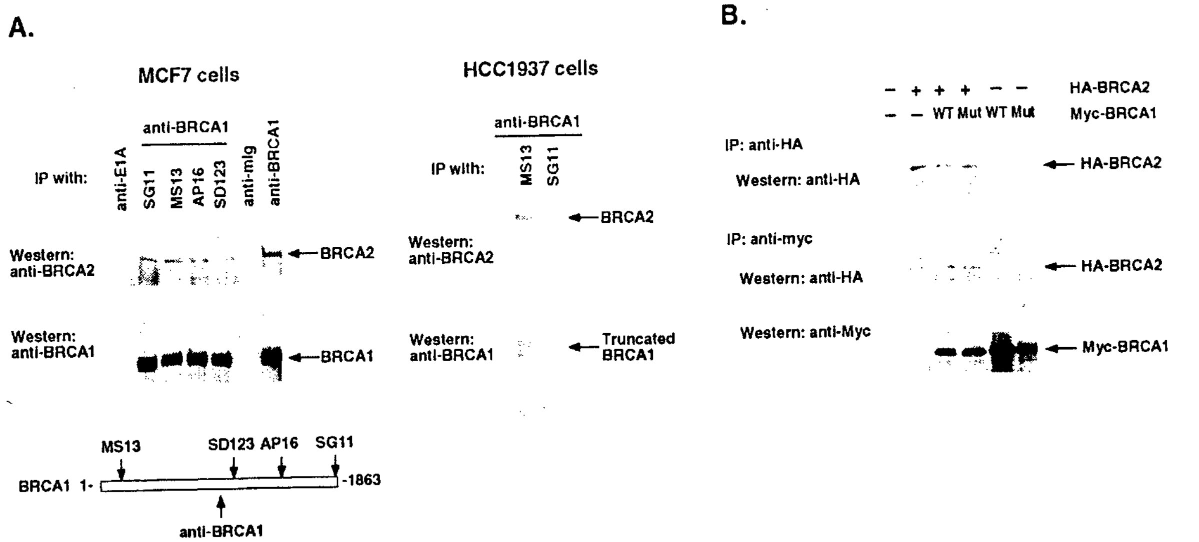

Figure 2. Coimmunoprecipitation of BRCA2 and BRCA1

(A) Left, extracts of MCF-7 cells were subjected to immunoprecipitation with control anti-E1A mAb M73, anti-BRCA1 mAbs SG11, MS13, AP16, and SD123, a control rabbit antibody (anti-mIg), or with an affinity-purified anti-BRCA1 rabbit polyclonal Ab. Right, extracts of HCC1937 cells were subjected to immunoprecipitation with N-terminal-specific BRCA1 mAb MS13 or with mAb SG11 (raised against a peptide corresponding to the C-terminal 17 amino acids of BRCA1) and immunoblotted with either anti-BRCA1 mAb MS110 or anti-BRCA2C Ab. The locations of the epitopes recognized by each of the BRCA1 antibodies used in these immunoprecipitation experiments are shown below.

(B) 293T cells were transfected with a plasmid encoding HA-BRCA2, a plasmid encoding myc-BRCA1 (WT), a plasmid encoding myc-BRCA1Y1853term (Mut), or plasmids encoding HA-BRCA2 and myc-BRCA1 (WT or Mut). Top, extracts were subjected to immunoprecipitation with anti-HA antibody and immunoblotting with anti-HA mAb 12CA5 to indicate the synthesis of HA-BRCA2. Middle and bottom, extracts were subjected to immunoprecipitation with anti-myc mAb 9E10. Immunoprecipitates were separated by SDS-PAGE and immunoblotted with either anti-HA mAb 12CA5 to illustrate the associated HA-BRCA2 (middle) or anti-myc mAb 9E10 to indicate the synthesis of myc-BRCA1 (WT or MUT; lower panel).

CAPAN-1 cells. As noted above, CAPAN-1 cells lack the epitopes against which anti-BRCA2C Ab was raised, and anti-BRCA2C Ab failed to immunoprecipitate BRCA1, BRCA2, or RAD51 from extracts of these cells (Figure 3A right panel), implying that anti-BRCA2C Ab does not cross-react with BRCA1 or RAD51.

The anti-BRCA2A epitope should be still present in the truncated BRCA2 species present in CAPAN-1 cells. Indeed, anti-BRCA2A immunoprecipitated a 230 kDa BRCA2 species from CAPAN-1 cells (Figure 3B, right panel; also see Figure 1D), along with both BRCA1 and RAD51 (Figure 3B, right panel). The presence of complexes containing BRCA1 and a BRCA2 species truncated at residue 1981 suggests that BRCA1 interacts with sequences present in the N-terminal half of BRCA2.

Sequences Adjacent to, but Not at the Extreme C Terminus of, BRCA1 Mediate BRCA2 Binding

We generated six overlapping BRCA1 fragments spanning the entire BRCA1 primary sequences as GST fusion proteins (Figure 4A; also see Scully et al., 1997a) and used them to determine whether there are discrete regions of the BRCA1 structure that mediate BRCA2 binding. It has already been shown that GST-BRCA1 fragment #4 (GST-B1F4), which contains BRCA1 residues 758–1064, can bind to RAD51 in vitro (Scully et al., 1997a). Since RAD51 interacts with both BRCA1 and BRCA2 (Figure 3A; also see review Zhang et al., 1998), one might imagine that RAD51 mediates the interaction between BRCA1 and BRCA2. We tested this hypothesis by employing the same ligand affinity binding assay used to define the RAD51/BRCA1 interaction (Scully et al., 1997a). If RAD51 mediates the interaction between BRCA1 and BRCA2, then GST-B1F4, the fragment of BRCA1 that interacts with RAD51, should also bind to BRCA2. Equivalent quantities of each fusion protein, bound to glutathione-sepharose beads, were incubated with extracts of MCF7 cells. Proteins bound to the beads were recovered, separated electrophoretically, and immunoblotted with either anti-RAD51 or anti-BRCA2 antibodies. While RAD51 again bound to GST-B1F4 (Figure 4B, lower panel), BRCA2 did not. Instead, it bound to GST-B1F6 (Figure 4B, upper panel). Identical results were obtained with extracts of CV-1P and DU-145 cells (data not shown).

As a test of the significance of this observation, we generated mammalian expression vectors encoding the six BRCA1 fragments, noted above. In this instance, the GST moiety at the N terminus of each was substituted with an amino-terminal myc epitope and a nuclear localization sequence when necessary. B1F2 and B1F3 have their own nuclear localization sequences. After transient transfection into 293T cells, myc-tagged BRCA1 fragments were recovered by anti-myc immunoprecipitation, and any bound BRCA2 was sought by immunoblotting with anti-BRCA2 antibody. As a positive control, full-length BRCA1 was also tested, and, as expected, it interacted with BRCA2. Moreover, the only BRCA1 fragment that interacted with BRCA2 was B1F6, the

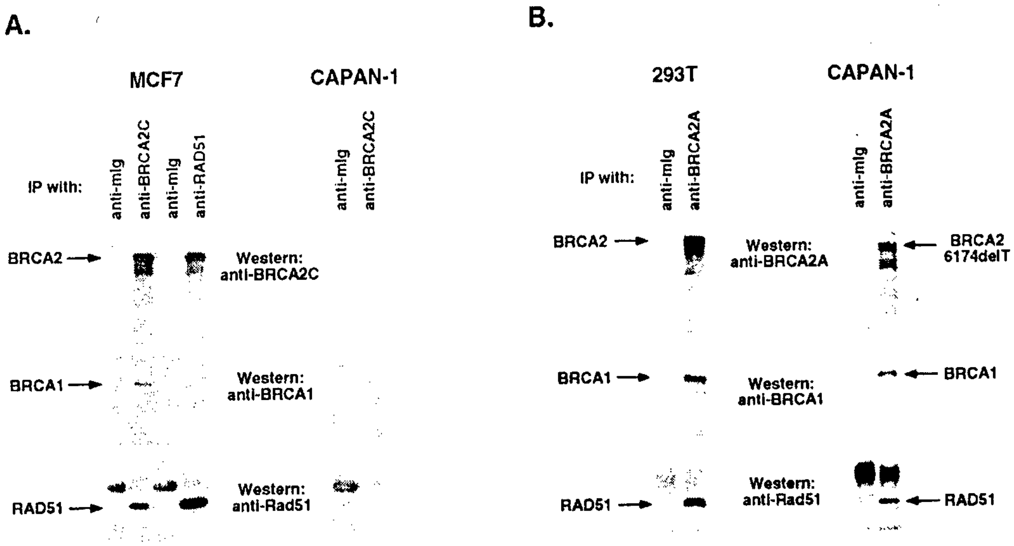

Figure 3. Association of BRCA1 and RAD51 with BRCA2

(A) Left, extracts of MCF-7 cells were subjected to immunoprecipitation with control (anti-mIg), anti-BRCA2C, or anti-RAD51 antibodies. Right, extracts of CAPAN-1 cells were subjected to immunoprecipitation with control (anti-mIg) or anti-BRCA2C Abs. All immunoprecipitates were immunoblotted with anti-BRCA1 mAb MS110, anti-BRCA2C Ab, or anti-RAD51 Ab.
(B) Extracts of 293T or CAPAN-1 cells were immunoprecipitated with anti-mIg Ab or with anti-BRCA2A. Immunoprecipitates were immunoblotted with anti-BRCA1 mAb MS110, anti-BRCA2A Ab, or anti-RAD51 Ab.

same segment that bound to BRCA2 in vitro (Figure 4C). In keeping with these results, a mutant BRCA1 species (BRCA1ΔBAMH I) deleted for residues 1314–1863, the residues present in B1F6, failed to bind BRCA2 (Figure 4D, right panel). These results strongly suggest that RAD51 does not serve as an essential bridge between BRCA1 and BRCA2. On the other hand, sequences at or near the BRCA1 C terminus are important for BRCA1/BRCA2 complex formation.

Colocalization of BRCA1 and BRCA2 in S Phase Nuclear Foci

BRCA1 and RAD51 colocalize in nuclear dots in S and G2 cells (Scully et al., 1997a, 1997c). Since BRCA2 interacted with and coprecipitated with both BRCA1 and RAD51, we asked whether nuclear dots detected by anti-BRCA1 or anti-RAD51 staining also contain BRCA2. Two-color immunostaining was performed using anti-BRCA1 and anti-BRCA2 Abs and visualized by confocal microscopy. BRCA2 immunostaining revealed a nuclear dot pattern, consistent with previous work suggesting that BRCA2 is a nuclear protein (Bertwistle et al., 1997; Chen et al., 1998). Figure 5A shows the results of an experiment using the BRCA1 mAb, SD118 (green), and anti-BRCA2C Ab (red) in DU145 cells. Extensive colocalization of BRCA1 and BRCA2 in nuclear dot structures is apparent (Figure 5A). Anti-BRCA2C staining was blocked by preincubation with the GST-BRCA2 fusion protein against which anti-BRCA2C was raised, but not by preincubation with GST (data not shown). Similar colocalization results were obtained in other cell lines (MCF-7, SaOS2, and CV1-P) and with each of the three affinity-purified anti-BRCA2 antibodies (data not shown).

To test whether affinity-purified BRCA2 antibody recognizes endogenous BRCA2 and not any cross-reacting protein(s), we repeated the aforementioned experiments in CAPAN-1 cells. CAPAN-1 cells contain only a truncated form of BRCA2 that has lost the epitopes recognized by anti-BRCA2C (see above). In these cells, anti-BRCA2C did not produce a signal, unlike anti-BRCA1, which revealed the previously described BRCA1 dot pattern (data not shown).

The BRCA1 S-phase dot pattern undergoes dynamic changes after DNA damage (Scully et al., 1997c). When S phase cells were treated with hydroxyurea (HU), most lost their punctate BRCA1 immunostaining. Only in late S phase cells, where PCNA immunostaining is punctate, did BRCA1 immunostaining remain punctate, and it now colocalized with these PCNA-containing replication centers (Scully et al., 1997c). We asked whether BRCA2 immunostaining undergoes similar changes. As shown in Figure 5B, there was very limited overlap between the PCNA staining pattern and the BRCA2 dot pattern before HU treatment. However, after exposure to HU for 1 hr, extensive colocalization of BRCA2 and PCNA was apparent (Figure 5B).

Colocalization of BRCA1 and BRCA2 on Meiotic Chromosomes

Colocalization of BRCA1 and RAD51 has also been detected on human meiotic chromosomes (Scully et al., 1997a). *BRCA2* and *BRCA1* mRNA expression is coordinately regulated in mitotic and meiotic cells (Rajan et al., 1996; Blackshear et al., 1998). Given the biochemical interactions between BRCA1 and BRCA2 and their colocalization in mitotic cells, we asked whether BRCA2 is concentrated on meiotic chromosomes.

BRCA2 immunostaining of human spermatocyte nuclei was sought using anti-BRCA2B and 2C. While the

2

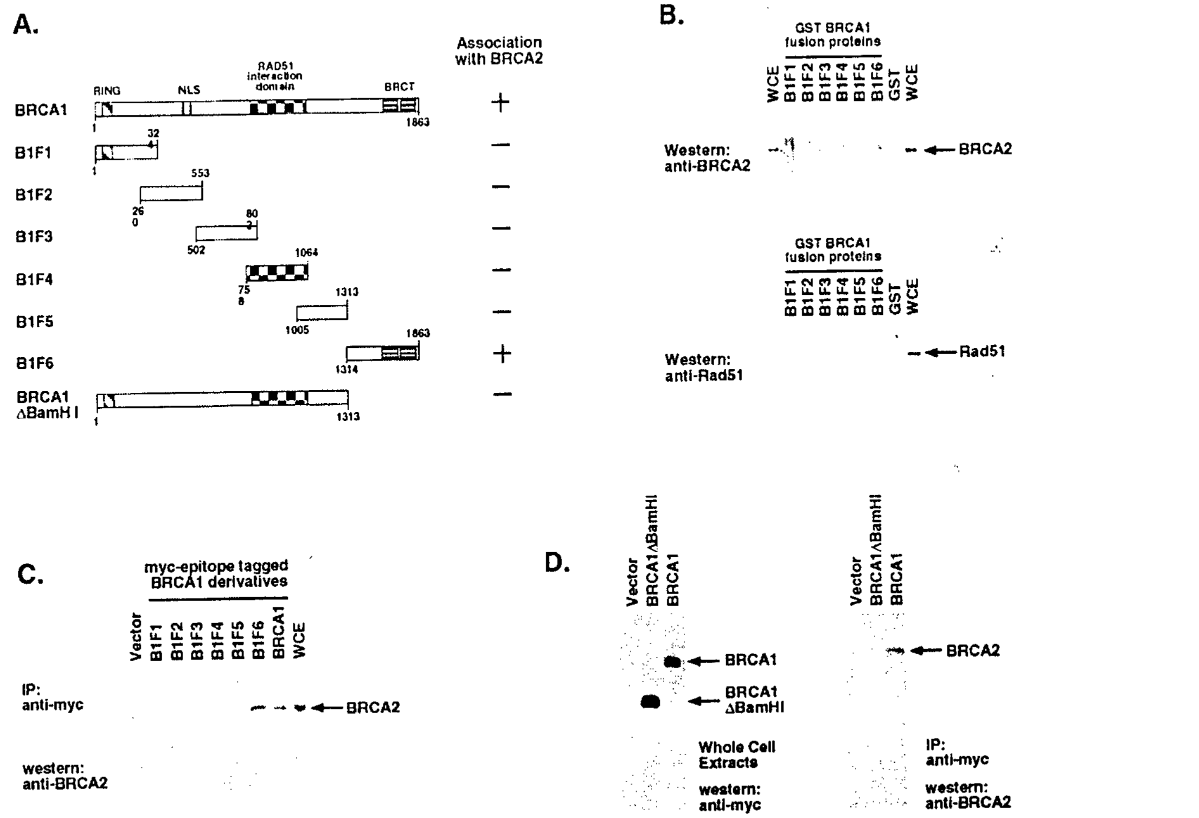

Figure 4. The C Terminus of BRCA1 Associates with BRCA2

(A) Schematic diagram of BRCA1 and its derivatives. Ring domain, two nuclear localization sequences (NLS), the RAD51 interaction domain, and the two BRCT repeats are indicated. Corresponding BRCA1 residues are marked.

(B) Top, beads coated with GST-BRCA1 fusion proteins were incubated with aliquots of an MCF-7 cell extract. Proteins bound to the beads were washed, eluted, separated by SDS-PAGE, and immunoblotted using anti-BRCA2C Ab. The smudges on the top of the gel are nonspecific signals resulting from the GST fusion protein preparation. Bottom, the same ligand affinity binding assay was repeated, and immunoblotting was performed using anti-RAD51 antibody.

(C) 293T cells were transfected with either vector plasmids or plasmids encoding myc-BRCA1 or myc-BRCA1 fragments (B1F1-B1F6). Extracts were subjected to immunoprecipitation with anti-myc mAb 9E10, separated by SDS-PAGE, and immunoblotted with anti-BRCA2C Ab.

(D) 293T cells were transfected with either vector plasmids or plasmids encoding myc-BRCA1 or myc-BRCA1ΔBAMH I (deleted for residues 1314–1863, the residues present in B1F6). Left, whole-cell extracts from transfected cells were separated by SDS-PAGE and immunoblotted using anti-myc mAb 9E10 to examine the synthesis of myc-epitope-tagged proteins. After transfection, both myc-BRCA1 and myc-BRCA1Δ BAMH I localized in nuclei (data not shown). Right, extracts were subjected to immunoprecipitation with the anti-myc mAb 9E10, separated by SDS-PAGE, and immunoblotted with anti-BRCA2C Ab.

2B Ab gave a stronger signal, both antibodies elicited nuclear staining. Cells were costained with anti-BRCA2B (red) and antibody to the axial element protein, SCP3 (white). In early zygonema nuclei, there was BRCA2 staining at discrete sites on unsynapsed axial elements (data not shown). Figure 6A shows a late zygonema–early pachynema nucleus where the majority of axes have synapsed. Although there was no BRCA2 detected on synapsed axes, significant staining was detected on the unsynapsed axial element (arrow head–bubble area). BRCA2 staining also was detected on the unpaired X and Y chromosomes (arrow on X chromosome). Since X and Y have no homologs, they remain unsynapsed throughout pachynema. These data indicate that, like BRCA1, BRCA2 is present on unsynapsed axial elements.

The specificity of anti-BRCA2B and anti-BRCA2C for BRCA2 recognition was analyzed by preincubating each Ab with its respective GST-fused antigen and then testing the axial element staining capabilities of the adsorbed serum. The relevant BRCA2 segment blocked its cognate antibody from staining unsynapsed axial elements (data not shown). In contrast, preincubation of anti-BRCA2 antibodies with an unrelated GST-fusion protein or GST failed to block anti-BRCA2 antibodies from staining axial elements (data not shown). Therefore, the anti-BRCA2 antibodies revealed the localization of BRCA2 protein.

BRCA1 and RAD51 colocalize on unsynapsed axial elements (Scully et al., 1997a). Given the above-noted results on BRCA2 and the physical association of BRCA2 with BRCA1 and RAD51, we asked whether BRCA2 colocalizes with BRCA1 and RAD51 on meiotic chromosomes. Human spermatocytes were costained with a BRCA1 mAb (green) and affinity-purified anti-BRCA2B antibody (red). As shown in Figure 6B, there is

MASTER PROOF SH

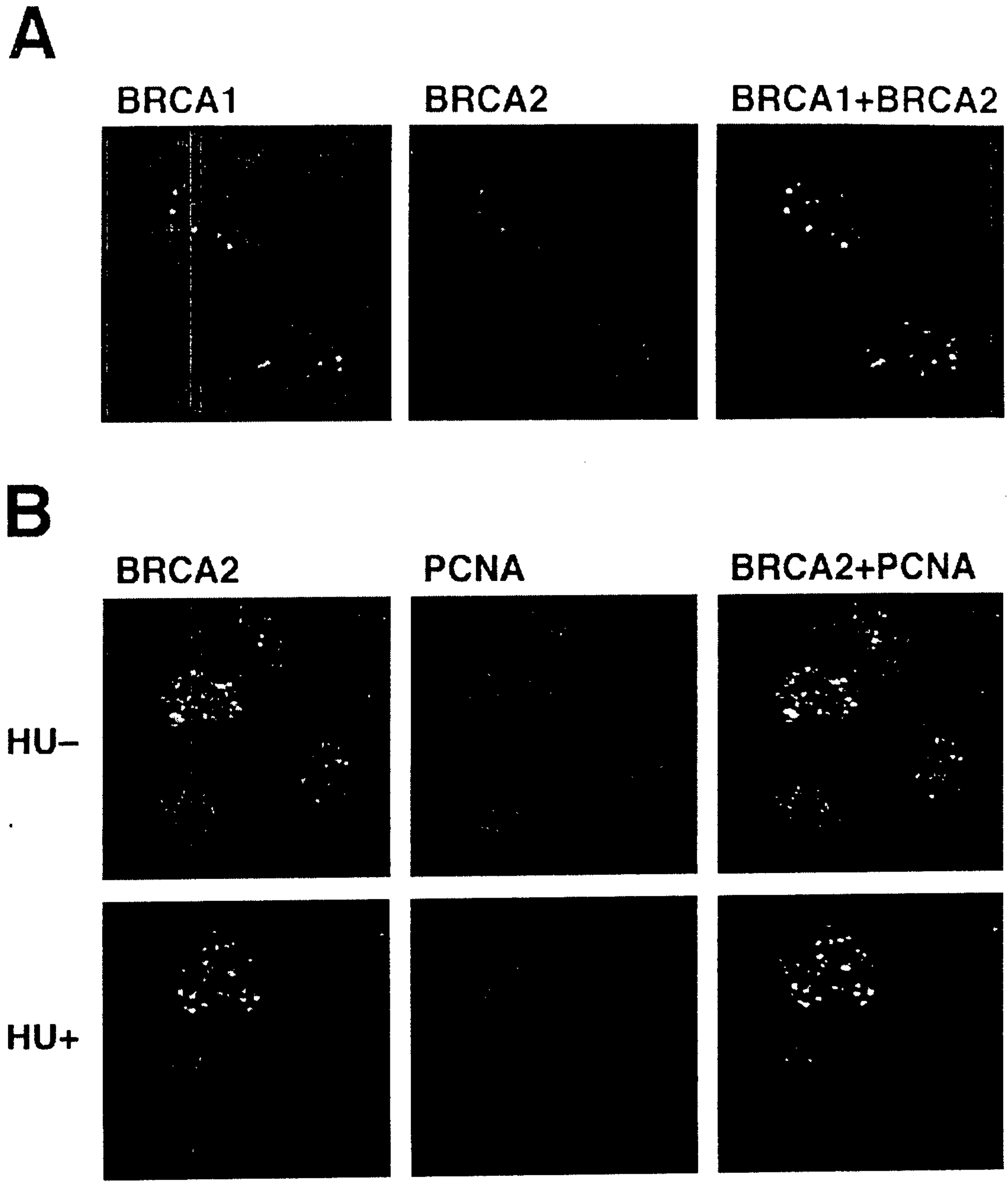

Figure 5. Colocalization of BRCA1 and BRCA2 in Somatic Cells

(A) Colocalization of BRCA1 and BRCA2 in discrete nuclear dots. DU145 cells were prepared as described in Experimental Procedures, stained with anti-BRCA1 mAb SD118 (green) and affinity-purified anti-BRCA2C Ab (red), and imaged by confocal microscopy. Where green and red signals overlap, a yellow pattern is observed, indicating the colocalization of BRCA1 and BRCA2.

(B) Recruitment of BRCA2 to replication foci following hydroxyurea (HU) treatment. MCF-7 cells were double-stained with anti-BRCA2C Ab (green) and anti-PCNA antiserum (AK serum, red). In untreated cells, BRCA2 dots (green) did not overlap significantly with PCNA foci (red). In HU-treated cells, there was extensive colocalization of BRCA2 (green) and PCNA (red) as indicated by yellow signals in the composite picture.

extensive colocalization of BRCA1 and BRCA2. RAD51 also colocalized with BRCA2 on unsynapsed axial elements (data not shown). The colocalization of BRCA1, BRCA2, and RAD51 on synaptonemal complexes further suggests that complexes containing BRCA1, BRCA2, and RAD51 participate in one or more signaling pathways.

Discussion

The results presented here reveal a specific physical association between the products of the two major hereditary breast cancer genes, *BRCA1* and *BRCA2*. This interaction was revealed by coimmunoprecipitation of

08-19-98 16:24:23 0808415114

A BRCA2+SCP3

4/C
FPO

B BRCA1 BRCA2 BRCA1+BRCA2

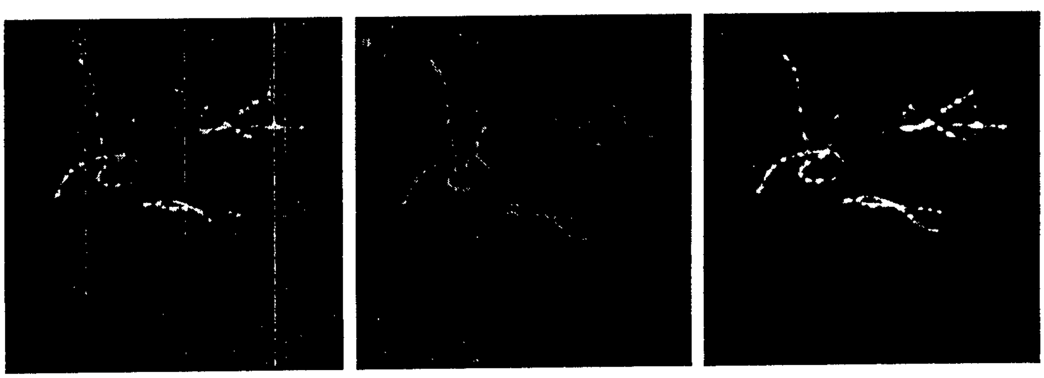

Figure 6. Colocalization of BRCA2 and BRCA1 on Meiotic Chromosomes
(A) A late human zygotene/early pachytene nucleus was costained with anti-BRCA2B Ab (red) and anti-SCP3 antibody (white). BRCA2 (red) localized to unsynapsed regions of a synapsing axial element (indicated by arrowhead) and the unsynapsed X (indicated by arrow) and Y chromosomes.
(B) Meiotic cells were stained with anti-BRCA1 mAb MS110 (green) and affinity-purified anti-BRCA2B Ab (red). Where green and red foci overlap, a yellow signal is observed, confirming the colocalization of BRCA1 and BRCA2.

the two proteins from untransfected cells, using antibodies specific for BRCA1 to coprecipitate BRCA2, and antibodies specific for BRCA2 to coprecipitate BRCA1. Moreover, RAD51 antibodies coimmunoprecipitated both BRCA1 and BRCA2.

In mitotic cells, we found that BRCA2 and BRCA1 coexist in nuclear dot structures before DNA damage, and in PCNA-containing replicating structures thereafter, implying that their physical association is linked to their joint performance of certain form(s) of biological work. In this regard, they were also found to codecorate synaptonemal complexes, further extending the repertoire of their conjoint activities to meiotic cells. Whether there is a unique species of complex containing all three

MASTER PROOF

proteins or whether there are multiple complexes containing BRCA1/BRCA2/RAD51 and yet other proteins is unclear.

The structural basis for the various protein/protein contacts within these multiprotein complexes is not fully understood. However, it would appear that the C-terminal segment of BRCA1 has an intrinsic ability to interact with BRCA2. The actual sequences within these 550 residues (aa 1314–1863) that are responsible for this interaction have not yet been identified. Intact BRCT repeats are not essential for the interaction, because one of them is deleted in the mutant BRCA1 of HCC1937 cells, which coimmunoprecipitated normally with BRCA2. Furthermore, data presented above indicate that a mutant form of BRCA1 (Y1853term), possibly affecting one of the two BRCT domains and rendering BRCA1 transactivation-defective (Chapman and Verma, 1996; Monteiro et al., 1996), bound BRCA2 in transient transfection assays. Unlike wild-type BRCA1, the same mutant also failed to bind the RNA polymerase II holoenzyme (Scully et al., 1997b). These results suggest that the transactivation function of BRCA1 is not required for its interaction with BRCA2. They similarly dissociate BRCA2 binding to BRCA1 and the ability of BRCA1 to copurify with RNA polymerase II holoenzyme. Thus, the relevant BRCA2 binding domain can be localized within a 440 residue segment (residues 1314–1756) at the N-terminal end of B1F6 (Figure 4A). The fact that a specific, C-terminal BRCA1 fragment can interact with BRCA2 in vitro and in vivo reinforces the impression that BRCA2 binding directly or indirectly is an intrinsic property of BRCA1. In a similar vein, although RAD51 does not appear to be the bridge between BRCA1 and BRCA2, data presented here (anti-RAD51 coprecipitation of endogenous BRCA1 [Figure 3A]) reinforce the view that RAD51 and BRCA1 interact, although it is still not clear whether the interaction is direct or indirect.

ED: C OK, as done?

The detailed stoichiometry of the BRCA1/BRCA2/RAD51 interaction is not yet clear. It is apparent, however, that anti-RAD51 antibodies were as efficient as anti-BRCA2 antibodies in immunoprecipitating BRCA2. Thus, it is possible that BRCA2 is quantitatively bound to RAD51 in the cell. The reverse relationship is apparently not the case, since there appears to be a pool of cellular RAD51 uncomplexed with BRCA2. Interestingly, RAD51 expression increases as cells undergo immortalization (Xia et al., 1997), and one might speculate that the existence of "free" RAD51 is a manifestation of cell immortalization. However, similar proportions of free and "bound" RAD51 were detected in extracts of primary human diploid fibroblasts (data not shown). Whatever the reason for the rise in RAD51 with immortalization, it is possible that free and "BRCA2-bound" RAD51 have different biochemical functions.

The interaction between BRCA1 and BRCA2 appears to be substoichiometric. Based on a comparison of immunoblot intensities of whole-cell extracts versus coimmunoprecipitated protein, we estimate that 2%–5% of cellular BRCA1 is complexed to BRCA2 and that a similar percentage of BRCA2 is complexed with BRCA1 in MCF-7 cell extracts. It is not yet known whether this reflects a regulated interaction between BRCA1 and BRCA2, whether our current immunopurification strategy is inefficient at preserving these complexes, or whether free and bound BRCA1 and/or BRCA2 behave differently in vivo.

Taken together, these results imply that BRCA1 and BRCA2 function, at least in part, as a biochemical complex together with at least one other protein. One might imagine that such a complex plays a role in one or more DNA damage response pathways, particularly in the control of double-strand break repair and homologous recombination. This is supported by the change of localization of both BRCA1 and BRCA2 following DNA damage in mitotic cells and the presence of both proteins (with RAD51) on the axial elements of developing synaptonemal complexes in meiotic cells. Conceivably, dysfunction of this pathway is required for the evolution of most hereditary breast and ovarian cancers. If so, mutations in another gene(s) involved in such a pathway might also contribute to hereditary breast/ovarian cancer.

Somatic mutation of the *BRCA1* and *BRCA2* genes does not accompany sporadic breast or ovarian cancer. Hence, it is not yet apparent whether the *BRCA1/BRCA2* DNA damage response pathway, described above, is dysfunctional in sporadic breast cancer. However, LOH is commonly observed in the regions of 17q and 13q within which *BRCA1* and *BRCA2* are located, possibly reflecting a role for haploinsufficiency at either or both of these loci in the evolution of certain forms of sporadic breast/ovarian cancer (Futreal et al., 1994; Neuhausen and Marshall, 1994; Cleton-Jansen et al., 1995; Beckmann et al., 1996; Kelsell et al., 1996; Lancaster et al., 1996; Miki et al., 1996; Teng et al., 1996; Bieche et al., 1997; Kerangueven et al., 1997). In addition, new results suggest that the level of BRCA1 is markedly reduced in many high-grade invasive breast cancers (C. Wilson, personal communication). As with the possibility of haploinsufficiency, these findings, too, elicit speculation that there is a role for a reduction in the normal amplitude of BRCA1 and/or BRCA2 function during the evolution of a significant fraction of sporadic breast/ovarian cancers.

Since BRCA1 and BRCA2 colocalize and interact before and after DNA damage, our original speculations on the nature of BRCA1 function, based upon localization data and association with RAD51, can now be extended to BRCA2. In this regard, hydroxyurea or UV treatment of S phase cells may generate persistent regions of parental ssDNA, in close proximity to replication forks. These ssDNA regions or their derivatives (dsDNA breaks) may be recombinogenic—possibly accounting, in part, for the recruitment of RAD51/BRCA1/BRCA2/BARD1 complexes to PCNA-containing sites in these circumstances (see also Scully et al., 1997c). These complexes may, therefore, function in a process analogous to prokaryotic "daughter strand gap repair," an error-free, *RecA*-dependent homologous recombinational response to ssDNA lesions generated during attempted replication across a DNA adduct (Rupp and Howard-Flanders, 1968; Hanawalt et al., 1979). Defects in such a process, possibly arising from insufficient BRCA1 or BRCA2 function, could explain some of the spontaneous anomalies in chromosome structure and sensitivity to DNA adducting agents noted recently in cells of *BRCA2* mutant mouse embryos (Patel et al., 1998). If this homologous recombinational process were

MASTER PROOF

saturable, then either a high "load" to the replication machinery of adducted DNA or a quantitative defect in the homologous recombinational pathway might translate into inefficient gap repair and, hence, increased cancer risk.

The concept of a common, *BRCA1/BRCA2* hereditary breast and ovarian cancer pathway suggests at least one hypothesis for understanding the tissue specificity of BRCA1/BRCA2-linked disease. A potentially "universal" carcinogen can give rise to tissue-specific disease, if it is concentrated in certain specialized cell types (so-called "remote carcinogenesis," reviewed in Friedberg et al., 1995). Conceivably, the breast ductal epithelium accumulates such a carcinogen and, therefore, suffers an unusually high rate of DNA damage of a type that stresses postreplication homologous recombination (such as DNA adduction). Lifetime estrogen exposure is a risk factor in breast cancer. Some estrogen metabolites can adduct DNA, and animal models suggest that they are carcinogens in estrogen-responsive tissue (Liehr et al., 1986; Fishman et al., 1995). Additional, as yet unidentified extrinsic/environmental agents might also be implicated as "remote carcinogens" in the etiology of some breast cancers. In this setting, the tissue specificity of *BRCA1/BRCA2*-linked disease might, in part, reflect an inadequate DNA repair response to tissue-specific DNA adduction.

Experimental Procedures

Plasmids

To generate vectors for the expression of myc epitope-tagged BRCA1 in mammalian cells, sequences encoding the tag were generated by PCR using pA3M (a pcDNA3 derivative vector containing three repeats of sequences that encode the myc epitope; Makela et al., 1995) as a template and the following primers: 5'-CACAAGCTT GGCCGCCAGTGTGCTGGA-3' and 5'-ATAGGATCCATAACCGGTC AAGTCTTCTTC-3'. The product was ligated, in place of the HA-encoding sequences, into the HindIII-BamHI site of pcDNA3β/HA plasmids containing either wild type or the Y1853term mutant of BRCA1 (Scully et al., 1997a, 1997b). A BamHI fragment of BRCA1, encoding residues 1–1313 of BRCA1, was inserted in-frame into a new pcDNA3β-myc vector to generate myc-tagged BRCA1ΔBAMH I (deleting residues 1314–1863 of BRCA1).

BRCA2 full-length cDNA was assembled from fragments derived from five human cDNA libraries—including breast, placenta, thymus and brain. cDNA fragments were ligated to produce a full-length *BRCA2* cDNA. It was sequenced fully and found to be intact before use in the experiments described here. To generate a mammalian expression plasmid encoding HA-tagged full-length BRCA2, a pcDNA3β/HA vector containing wild-type *BRCA1* cDNA was digested with BamHI and XhoI to remove the full-length *BRCA1* sequence. A BamHI-EcoRV-XhoI linker was ligated into this cleaved/excised vector to generate a new mammalian expression vector termed pcDNA3β/HA-2. A 10 Kb SalI fragment containing the sequences encoding the full-length BRCA2 was inserted in-frame into the XhoI site of the pcDNA3β/HA-2 to generate an expression plasmid encoding HA-tagged BRCA2.

To generate plasmids encoding myc epitope-tagged BRCA1 fragments #1–#6, which correspond to the previously described GST-BRCA1 #1–#6 (Scully et al., 1997a), BamHI-EcoRI fragments encoding, respectively, BRCA1 fragments #1–#6 were individually ligated, in parallel, into pcDNA3 digested with HindIII and EcoRI, along with the HindIII-BamHI fragment encoding the myc epitope tag from pcDNA3β-myc-BRCA1. BRCA1 fragments #2 and #3 contain nuclear localization sequences and localized to the nucleus when synthesized in vivo. To ensure that BRCA1 fragment #1, #4, #5, and #6 also localized to nuclei, the SV40 nuclear localization sequence was inserted between the sequence encoding the myc epitope tag and the sequence encoding each relevant BRCA1 fragment.

Antibodies

Some of the anti-BRCA1 mAbs used here were described previously (Scully et al., 1996). SD118 and SD123 are monoclonal antibodies raised against GST fusion proteins encoding residues 758–1313 of BRCA1. Rabbit polyclonal antisera for BRCA1 were raised against GST fusion proteins encoding residues 758–1313 of BRCA1. Rabbit polyclonal antisera for BRCA2, anti-BRCA2A, anti-BRCA2B, and anti-BRCA2C were, respectively, raised against GST-BRCA2 fusion proteins encoding residues 1425–1973, 2422–2976, and 3245–3418. All polyclonal antisera were affinity-purified using an AminoLink kit, as suggested by the manufacturer (Pierce). "AK" anti-PCNA antisera is a generous gift of Dr. Robert L. Ochs (the Scripps Research Institute, La Jolla, CA).

Cell Culture

In general, cells were grown in DMEM supplemented with 10% fetal bovine serum. CAPAN-1 and HCC1937 were cultivated in RPMI supplemented with 10% fetal bovine serum. For transfection, the standard calcium phosphate precipitation method was used. Cells were collected 48 hr after transfection.

Immunoprecipitation and Immunoblotting

NETN buffer (150 mM NaCl, 1 mM EDTA, 20 mM Tris [pH 8.0], 0.5% NP-40) was normally used for cell lysis. For a typical immunoprecipitation reaction, 1–2 mg of whole-cell extract was incubated with 1 μg of antibody and 20 μl of protein A Sepharose beads (1:1) at 4°C for 1–2 hr. Beads were washed four times in 1 ml of NETN buffer. Proteins bound to the beads were eluted by boiling in SDS gel sample buffer, separated by SDS-PAGE, and transferred to Immobilon-P (Millipore). Immunoblotting was performed using the ECL kit as suggested by the manufacturer (Amersham). The primary antibodies were routinely used at a concentration of 1 μg/ml, and the HRP-conjugated secondary antibodies were used either at 1:2000 (HRP-conjugated protein A; Amersham) or 1:5000 dilution (HRP-conjugated goat anti-mouse Ig; Jackson ImmunoResearch laboratories, Inc.).

Immunostaining

Cells were fixed and permeabilized as described previously (Scully et al., 1997a). Monoclonal anti-BRCA1 antibodies were used at a 1:10 to 1:50 dilution of the hybridoma culture supernatant. Affinity-purified anti-BRCA2 antibodies were used at a concentration of 1–2 μg/ml. The preparation and immunostaining of human spermatocytes, antibody incubation, and detection were performed according to Wessel and McClay (1986), or as described previously (Scully et al., 1997a). Fluorochrome-conjugated secondary antibodies were obtained from Jackson Immunoresearch or Pierce, and were used according to the manufacturer's instructions.

Acknowledgments

We are grateful to Matt Fred for his expert technical assistance, Dr. David Hill for his gift of the CAPAN-1 cell line, Dr. Robert L. Ochs for anti-PCNA AK sera, Dr. James A. Decaprio and Jianmin Gan for their help in generating monoclonal antibodies, and Dr. Sean V. Tavtigian and Albert Wong for providing reagents. In addition, we are grateful to all of our laboratory and divisional colleagues for many helpful and stimulating conversations. J. C. was supported by NIH training grant. R. S. was supported by DOD IDEA award. This work was supported by grants from DOD IDEA award and the National Cancer Institute to D. M. L.

Received May 19, 1998; revised August 3, 1998.

References

Baumann, P., Benson, F.E., and West, S.C. (1996). Human Rad51 protein promotes ATP-dependent homologous pairing and strand transfer reactions in vitro. Cell *87*, 757–766.

Beckmann, M.W., Picard, F., An, H.X., Van Roeyen, C.R.C., Dominik,

08-19-98 16:24:23 0808415114

S.I., et al. (1996). Clinical impact of detection of loss of heterozygosity of BRCA1 and BRCA1 markers in sporadic breast cancer. Br. J. Cancer *73*, 1220–1226.

Bertwistle, D., Swift, S., Marston, N.J., Jackson, L.E., Crossland, S., et al. (1997). Nuclear location and cell cycle regulation of the BRCA2 protein. Cancer Res. *57*, 5485–5488.

Bieche, I., Nogues, C., Rivoilan, S., Khodja, A., Latil, A., and Lidereau, R. (1997). Prognostic value of loss of heterozygosity at BRCA2 in human breast carcinoma. Br. J. Cancer *76*, 1416–1418.

Blackshear, P.E., Goldsworthy, S.M., Foley, J.F., McAllister, K.A., Bennett, L.M., et al. (1998). Brca1 and Brca2 expression patterns in mitotic and meiotic cells of mice. Oncogene *16*, 61–68.

Bork, P., Hofmann, K., Bucher, P., Neuwald, A.F., Altschul, S.F., and Koonin, E.V. (1997). A superfamily of conserved domains in DNA damage-responsive cell cycle checkpoint proteins. FASEB J. *11*, 68–76.

Callebaut, I., and Mornon, J.P. (1997). From BRCA1 to RAP1: a widespread BRCT module closely associated with DNA repair. FEBS Lett. *400*, 25–30.

Chapman, M.S., and Verma, I.M. (1996). Transcriptional activation by BRCA1. Nature *382*, 678–679.

Chen, F., Nastasi, A., Shen, Z., Brenneman, M., Crissman, H., and Chen, D.J. (1997). Cell cycle-dependent protein expression of mammalian homologs of yeast DNA double-strand break repair genes *Rad51* and *Rad52*. Mutat. Res. *384*, 205–211.

Chen, P.L., Chen, C.F., Chen, Y., Xiao, J., Sharp, Z.D., and Lee, W.H. (1998). The BRC repeats in BRCA2 are critical for RAD51 binding and resistance to methyl methanesulfonate treatment. Proc. Natl. Acad. Sci. USA *95*, 5287–5292.

Claus, E.B., Risch, N., and Thompson, W.D. (1991). Genetic analysis of breast cancer in the cancer and steroid hormone study. Am. J. Hum. Genet. *48*, 232–241.

Cleton-Jansen, A.M., Collins, N., Lakhani, S.R., Weissenbach, J., Devilee, P., et al. (1995). Loss of heterozygosity in sporadic breast tumours at the BRCA2 locus on chromosome 13q12-q13. Br. J. Cancer *72*, 1241–1244.

Connor, F., Bertwistle, D., Mee, P.J., Ross, G.M., Swift, S., et al. (1997). Tumorigenesis and a DNA repair defect in mice with a truncating Brca2 mutation. Nat. Genet. *17*, 423–430.

Fishman, J., Osborne, M.P., and Telang, N.T. (1995). The role of estrogen in mammary carcinogenesis. Ann. N Y Acad. Sci. *768*, 91–100.

Friedberg, E.C., Walker, G.C., and Siede, W. (1995). DNA repair and mutagenesis. (Washington, DC: ASM Press).

Futreal, P.A., Liu, Q., Shattuck-Eidens, D., Cochran, C., Harshmann, K., et al. (1994). BRCA1 mutations in primary breast and ovarian carcinomas. Science *266*, 120–122.

Goggins, M., Schutte, M., Lu, J., Moskaluk, C.A., Weinstein, C.L., et al. (1996). Germline *BRCA2* gene mutations in patients with apparently sporadic pancreatic carcinomas. Cancer Res. *56*, 5360–5364.

Gowen, L.C., Johnson, B.L., Latour, A.M., Sulik, K.K., and Koller, B.H. (1996). BRCA1 deficiency results in early embryonic lethality characterized by neuroepithelial abnormalities. Nat. Genet. *12*, 191–194.

Gudas, J.M., Nguyen, H., Li, T., and Cowan, K. (1995). Hormone-dependent regulation of BRCA1 in human breast cancer cells. Cancer Res. *55*, 4561–4565.

Gudas, J.M., Li, T., Nguyen, H., Jensen, D., Rauscher, F.J.I., and Cowan, K.H. (1996). Cell cycle regulation of BRCA1 messenger RNA in human breast epithelial cells. Cell Growth Differ. *7*, 717–723.

Hakem, R., de la Pompa, J.L., Sirard, C., Mo, R., Woo, M., Hakem, A., Wakeham, A., Potter, J., Reitmair, A., Billia, F., et al. (1996). The tumor suppressor gene *Brca1* is required for embryonic cellular proliferation in the mouse. Cell *85*, 1009–1023.

Hakem, R., de la Pompa, J.L., Elia, A., Potter, J., and Mak, T.W. (1997). Partial rescue of Brca1 (5–6) early embryonic lethality by p53 or p21 null mutation. Nat. Genet. *16*, 298–302.

Hall, J.M., Lee, M.K., and Newmann, B. (1990). Linkage of early-onset breast cancer to chromosome 17q21. Science *250*, 1684–1689.

Hanawalt, P.C., Cooper, P.K., Ganesan, A., and Smith, C.A. (1979). DNA repair in bacteria and mammalian cells. Annu. Rev. Biochem. *48*, 783–836.

Kelsell, D.P., Spurr, N.K., Barnes, D.M., Gusterson, B., and Bishop, D.T. (1996). Combined loss of BRCA1/BRCA2 in grade 3 breast carcinomas. Lancet *347*, 1554–1555.

Kerangueven, F., Eisinger, F., Noguchi, T., Allione, F., Wargniez, V., et al. (1997). Loss of heterozygosity in human breast carcinomas in the ataxia telangiectasia, Cowden disease and *BRCA1* gene regions. Oncogene *14*, 339–347.

Koonin, V.F., Altschul, S.F., and Bork, P. (1996). BRCA1 protein products: functional motifs. Nat. Genet. *13*, 266–267.

Lancaster, J.M., Wooster, R., Mangion, J., Phelan, C.M., Cochran, C., et al. (1996). BRCA2 mutations in primary breast and ovarian cancers. Nat. Genet. *13*, 238–240.

Lane, T.F., Deng, C., Elson, A., Lyu, M.S., Kozak, C.A., and Leder, P. (1995). Expression of BRCA1 is associated with terminal differentiation of ectodermally and mesodermally derived tissues in mice. Genes Dev. *9*, 2712–2722.

Liehr, J.G., Avitts, T.A., Randerath, E., and Randerath, K. (1986). Estrogen-induced endogenous DNA adduction: possible mechanism of hormonal cancer. Proc. Natl. Acad. Sci. USA *83*, 5301–5305.

Lim, D.S., and Hasty, P. (1996). A mutation in mouse rad51 results in an early embryonic lethal that is suppressed by a mutation in p53. Mol. Cell. Biol. *16*, 7133–7143.

Liu, C.Y., Flesken-Nikitin, A., Li, S., Zeng, Y., and Lee, W.-H. (1996). Inactivation of the mouse *Brca1* gene leads to failure in the morphogenesis of the egg cylinder in early postimplantation development. Genes Dev. *10*, 1835–1843.

Ludwig, T., Chapman, D.L., Papaioannou, V.E., and Efstratiadis, A. (1997). Targeted mutations of breast cancer susceptibility gene homologs in mice: lethal phenotypes of Brca1, Brca2, Brca1/Brca2, Brca1/p53, and Brca2/p53 nullizygous embryos. Genes Dev. *11*, 1226–1241.

Makela, T.P., Parvin, J.D., Kim, J., Huber, L.J., Sharp, P.A., and Weinberg, R.A. (1995). A kinase-deficient transcription factor TFIIH is functional in basal and activated transcription. Proc. Natl. Acad. Sci. USA *92*, 5174–5178.

Marcus, J.N., Watson, P., Page, D.L., Narod, S.A., Lenoir, G., et al. (1996). Hereditary breast cancer: pathobiology, prognosis, and *BRCA1* and *BRCA2* gene linkage. Cancer *77*, 697–709.

Marquis, S.T., Rajan, J.V., Wynshaw-Boris, A., Xu, J., and Yin, G.-Y. (1995). The developmental pattern of BRCA1 expression implies a role in differentiation of the breast and other tissues. Nat. Genet. *11*, 17–26.

Miki, Y., Swensen, J., Shattuck-Eidens, D., Futreal, P.A., Harshman, K., et al. (1994). A strong candidate for the breast and ovarian cancer susceptibility gene *BRCA1*. Science *266*, 66–71.

Miki, Y., Katagiri, T., Kasumi, F., Yoshimoto, T., and Nakamura, Y. (1996). Mutation analysis in the *BRCA2* gene in primary breast cancers. Nat. Genet. *13*, 245–247.

Monteiro, A.N.A., August, A., and Hanafusa, H. (1996). Evidence for a transcriptional activation function of BRCA1 C-terminal region. Proc. Natl. Acad. Sci. USA *93*, 13595–13599.

Narod, S.A., Feunteun, J., Lynch, H.T., Watson, P., Conway, T., Lynch, J., and Lenoir, G. (1991). Familial breast-ovarian cancer locus on chromosome 17q12-23. Lancet *338*, 82–83.

Neuhausen, S.L., and Marshall, C.J. (1994). Loss of heterozygosity in familial tumors from three BRCA1-linked kindreds. Cancer Res. *54*, 6069–6072.

Newman, B., Austin, M.A., Lee, M., and King, M.-C. (1988). Inheritance of breast cancer: evidence for autosomal dominant transmission in high risk families. Proc. Natl. Acad. Sci. USA *85*, 1–5.

Patel, K.J., Yu, V.P.C.C., Lee, H., Corcoran, A., Thistlethwaite, F.C., Evans, M.J., Colledge, W.H., Friedman, L.S., Ponder, B.A.J., and Venkitaraman, A.R. (1998). Involvement of Brca2 in DNA repair. Mol. Cell *1*, 347–357.

Radding, C.M. (1991). Helical interactions in homologous pairing and strand exchange driven by RecA protein. J. Biol. Chem. *266*, 5355–5358.

MASTER PROOF

08-19-98 16:24:23 0808415114

Rajan, J.V., Wang, M., Marquis, S.T., and Chodosh, L.A. (1996). Brca2 is coordinately regulated with Brca1 during proliferation and differentiation in mammary epithelial cells. Proc. Natl. Acad. Sci. USA *93*, 13078–13083.

Rajan, J.V., Marquis, S.T., Gardner, H.P., and Chodosh, L.A. (1997). Developmental expression of Brca2 colocalizes with Brca1 and is associated with proliferation and differentiation in multiple tissues. Dev. Biol. *184*, 385–401.

Rupp, W.D., and Howard-Flanders, P. (1968). Discontinuities in the DNA synthesised in an excision-defective strain of *Escherichia coli* following ultraviolet irradiation. J. Mol. Biol. *31*, 291–304.

Scully, R., Ganesan, S., Brown, M., DeCaprio, J.A., Cannistra, S.A., Feunteun, J., Schnitt, S., and Livingston, D.M. (1996). Location of BRCA1 in human breast and ovarian cell lines. Science *272*, 123–125.

Scully, R., Chen, J., Plug, A., Xiao, Y., Weaver, D., Feunteun, J., Ashley, T., and Livingston, D.M. (1997a). Association of BRCA1 with Rad51 in mitotic and meiotic cells. Cell *88*, 265–275.

Scully, R., Anderson, S.F., Chao, D.M., Wei, W., Ye, L., Young, R.A., Livingston, D.M., and Parvin, J.D. (1997b). BRCA1 is a component of the RNA polymerase II holoenzyme. Proc. Natl. Acad. Sci. USA *94*, 5605–5610.

Scully, R., Chen, J., Ochs, R.L., Keegan, K., Hoekstra, M., Feunteun, J., and Livingston, D.M. (1997c). Dynamic changes of BRCA1 subnuclear location and phosphorylation state are initiated by DNA damage. Cell *90*, 425–435.

Sharan, S.K., Morimatsu, M., Albrecht, U., Lim, D.-S., Regel, E., et al. (1997). Embryonic lethality and radiation hypersensitivity mediated by Rad51 in mice lacking BRCA2. Nature *386*, 804–810.

Shinohara, A., Ogawa, H., and Ogawa, T. (1992). Rad51 protein involved in repair and recombination in *Saccharomyces cerevisiae* is a RecA-like protein. Cell *69*, 457–470.

Sung, P. (1994). Catalysis of ATP-dependent homologous DNA pairing and strand exchange by yeast Rad51 protein. Science *265*, 1241–1243.

Sung, P., and Robberson, D.L. (1995). DNA strand exchange mediated by a Rad51-ssDNA nucleoprotein filament with polarity opposite to that of RecA. Cell *82*, 453–461.

Suzuki, A., de la Pompa, J.L., Hakem, R., Elia, A., Yoshida, R., et al. (1997). Brca2 is required for embryonic cellular proliferation in the mouse. Genes Dev. *11*, 1242–1252.

Tavtigian, S.V., Simard, J., Rommens, J., Couch, F., Shattuck-Eidens, D., et al. (1996). The complete *BRCA2* gene and mutations in chromosome 13q-linked kindreds. Nat. Genet. *12*, 333–337.

Teng, D.H., Bogden, R., Mitchell, J., Baumgard, M., Bell, R., et al. (1996). Low incidence of BRCA2 mutations in breast carcinoma and other cancers. Nat. Genet. *13*, 241–244.

Tsuzuki, T., Fujii, Y., Sakumi, K., Tominaga, Y., Nakao, K., et al. (1996). Targeted disruption of the *Rad51* gene leads to lethality in embryonic mice. Proc. Natl. Acad. Sci. USA *93*, 6236–6240.

Vaughn, J.P., Davis, P.L., Jarboe, M.D., Huper, G., Evans, A.C., et al. (1996). BRCA1 expression is induced before DNA synthesis in both normal and tumor-derived breast cells. Cell Growth Differ. *7*, 711–715.

Wessel, G.M., and McClay, D.R. (1986). Two embryonic, tissue-specific molecules identified by a double-label immunofluorescence technique for monoclonal antibodies. J. Histochem. Cytochem. *34*, 703–706.

Wooster, R., Neuhausen, S.L., Mangion, J., Quirk, Y., Ford, D., et al. (1994). Localization of a breast cancer susceptibility gene, *BRCA2*, to chromosome 13q12–13. Science *265*, 2088–2090.

Wooster, R., Bignell, G., Lancaster, J., Swift, S., Seal, S., et al. (1995). Identification of the breast cancer susceptibility gene *BRCA2*. Nature *378*, 789–792.

Xia, S.J., Shammas, M.A., and Reis, R.J. (1997). Elevated recombination in immortal human cells is mediated by HsRAD51 recombinase. Mol. Cell. Biol. *17*, 7151–7158.

Zhang, H., Tombline, G., and Weber, B.L. (1998). BRCA1, BRCA2, and DNA damage response: collision or collusion? Cell *92*, 433–436.

MASTER PROOF

SW

Figure 1A

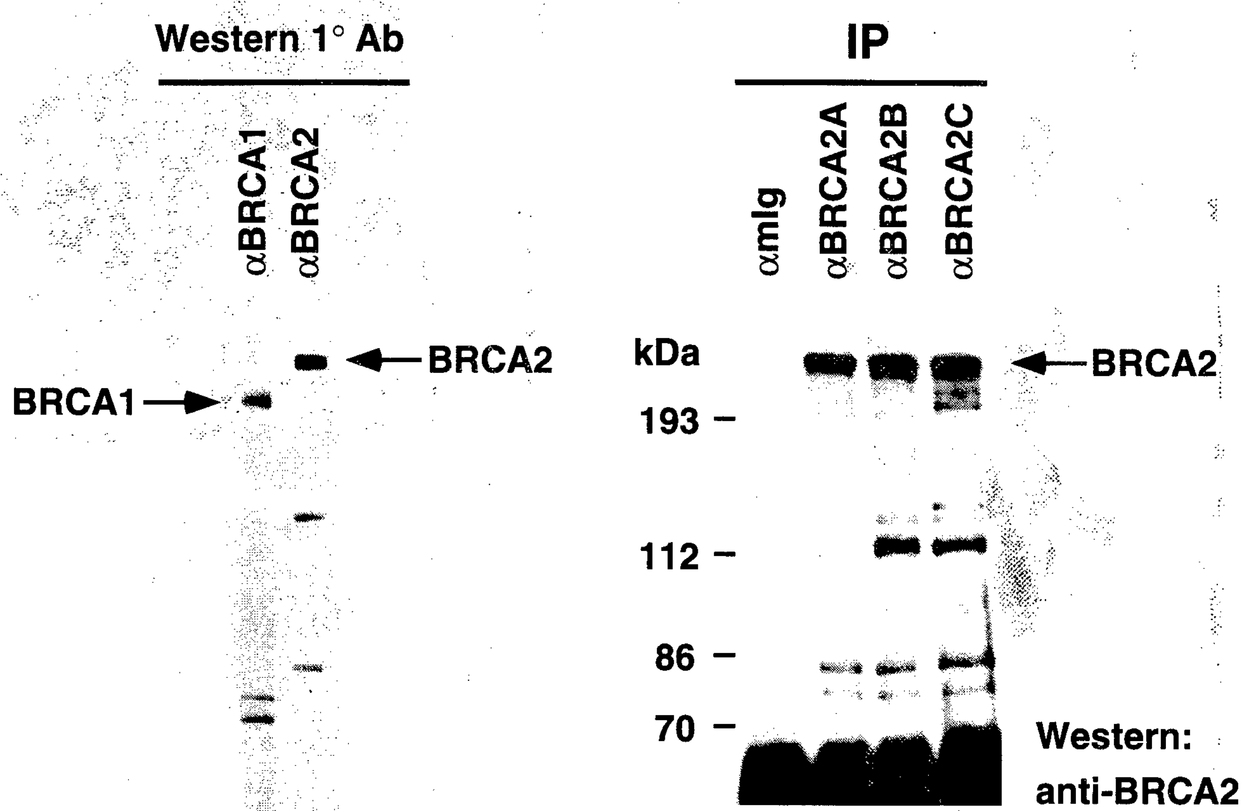
Western 1° Ab
αBRCA1
αBRCA2
BRCA1
BRCA2
IP
αmIg
αBRCA2A
αBRCA2B
αBRCA2C
kDa
BRCA2
193
112
86
70
Western:
anti-BRCA2

Figure 1B

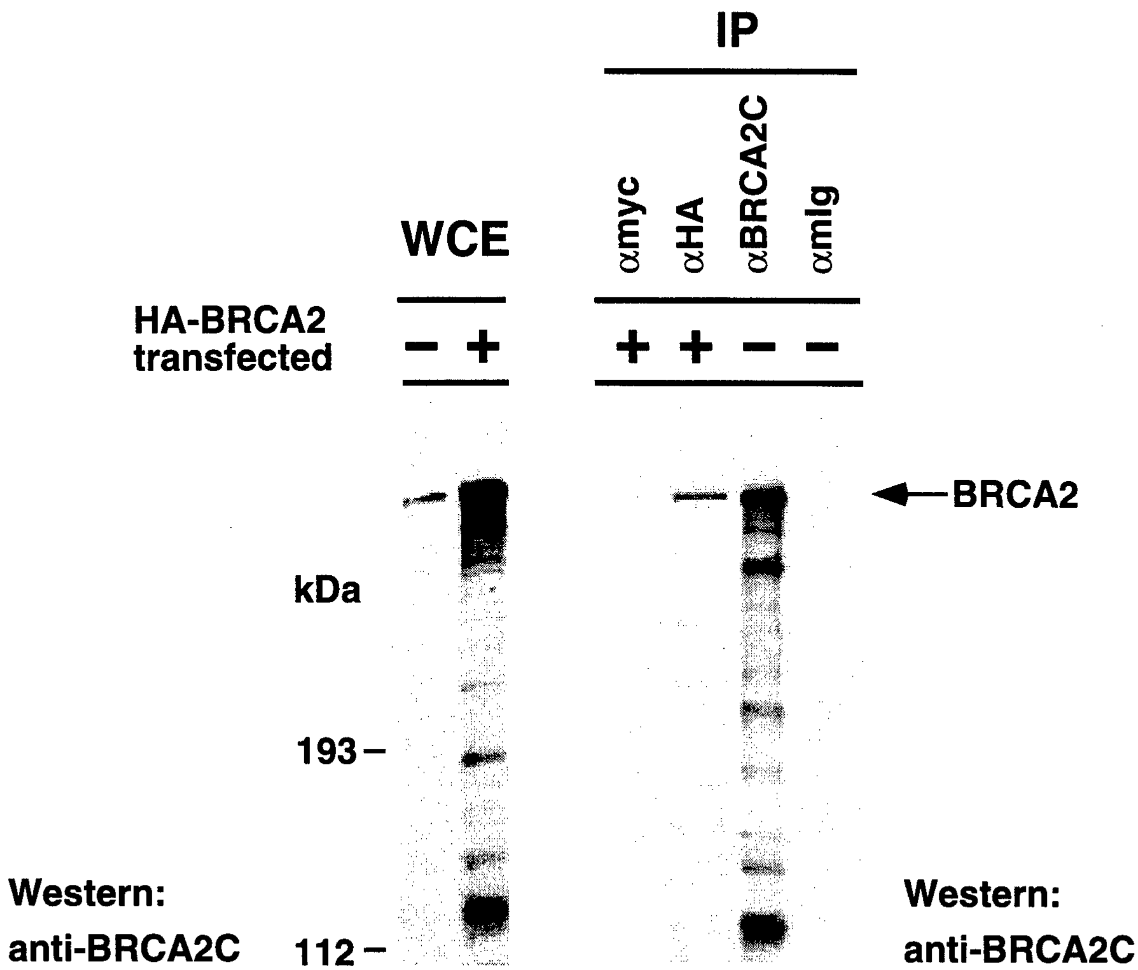
IP
αmyc
αHA
αBRCA2C
αmIg
WCE
HA-BRCA2
transfected
− +
+ + − −
BRCA2
kDa
193
112
Western:
anti-BRCA2C
Western:
anti-BRCA2C

Figure 1C

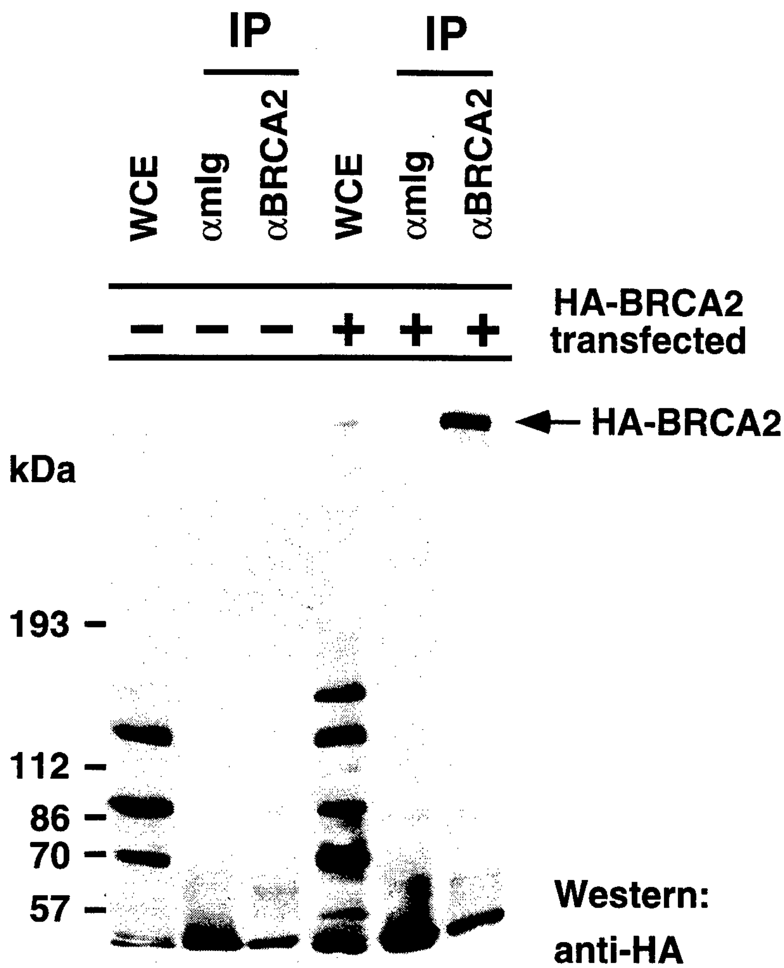
IP
IP
WCE
αmIg
αBRCA2
WCE
αmIg
αBRCA2
HA-BRCA2 transfected
– – – + + +
HA-BRCA2
kDa
193
112
86
70
57
Western: anti-HA

Figure 1D

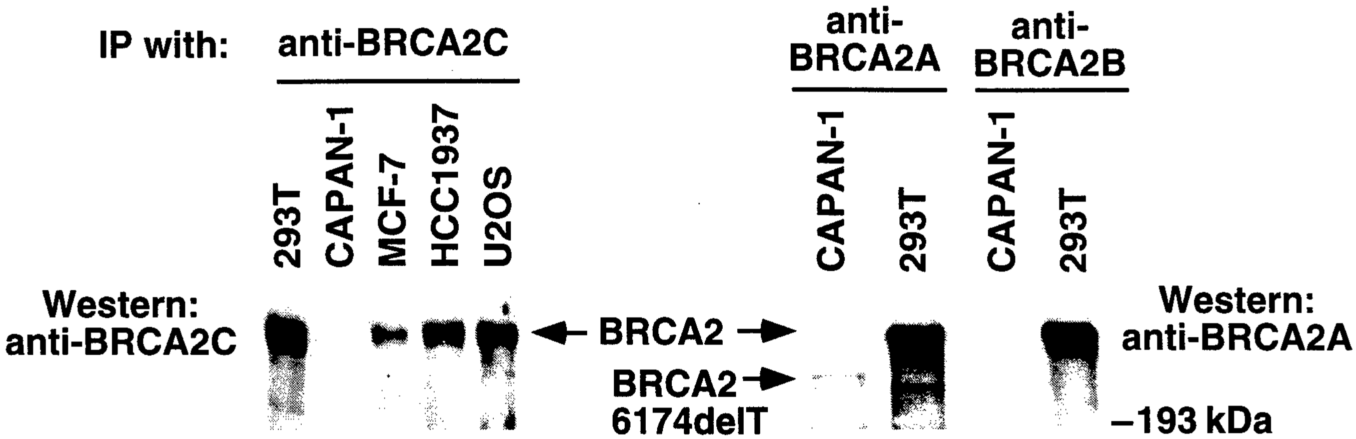

IP with:
anti-BRCA2C
anti-BRCA2A
anti-BRCA2B
293T
CAPAN-1
MCF-7
HCC1937
U2OS
CAPAN-1
293T
CAPAN-1
293T
Western: anti-BRCA2C
BRCA2
BRCA2 6174delT
Western: anti-BRCA2A
–193 kDa

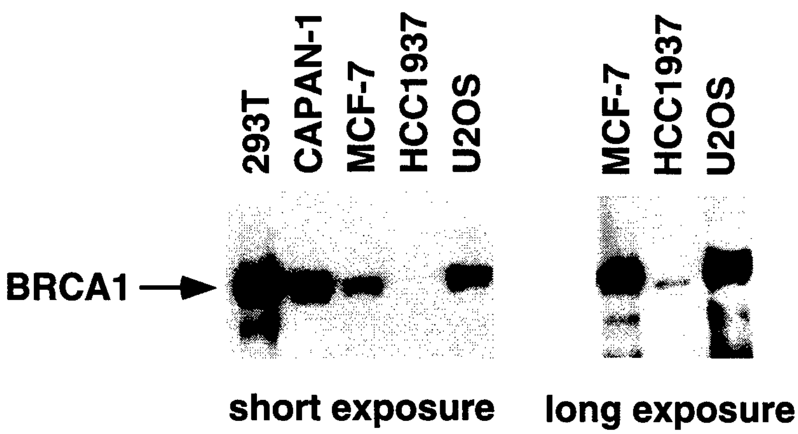

293T
CAPAN-1
MCF-7
HCC1937
U2OS
MCF-7
HCC1937
U2OS
BRCA1
short exposure
long exposure

Figure 2A

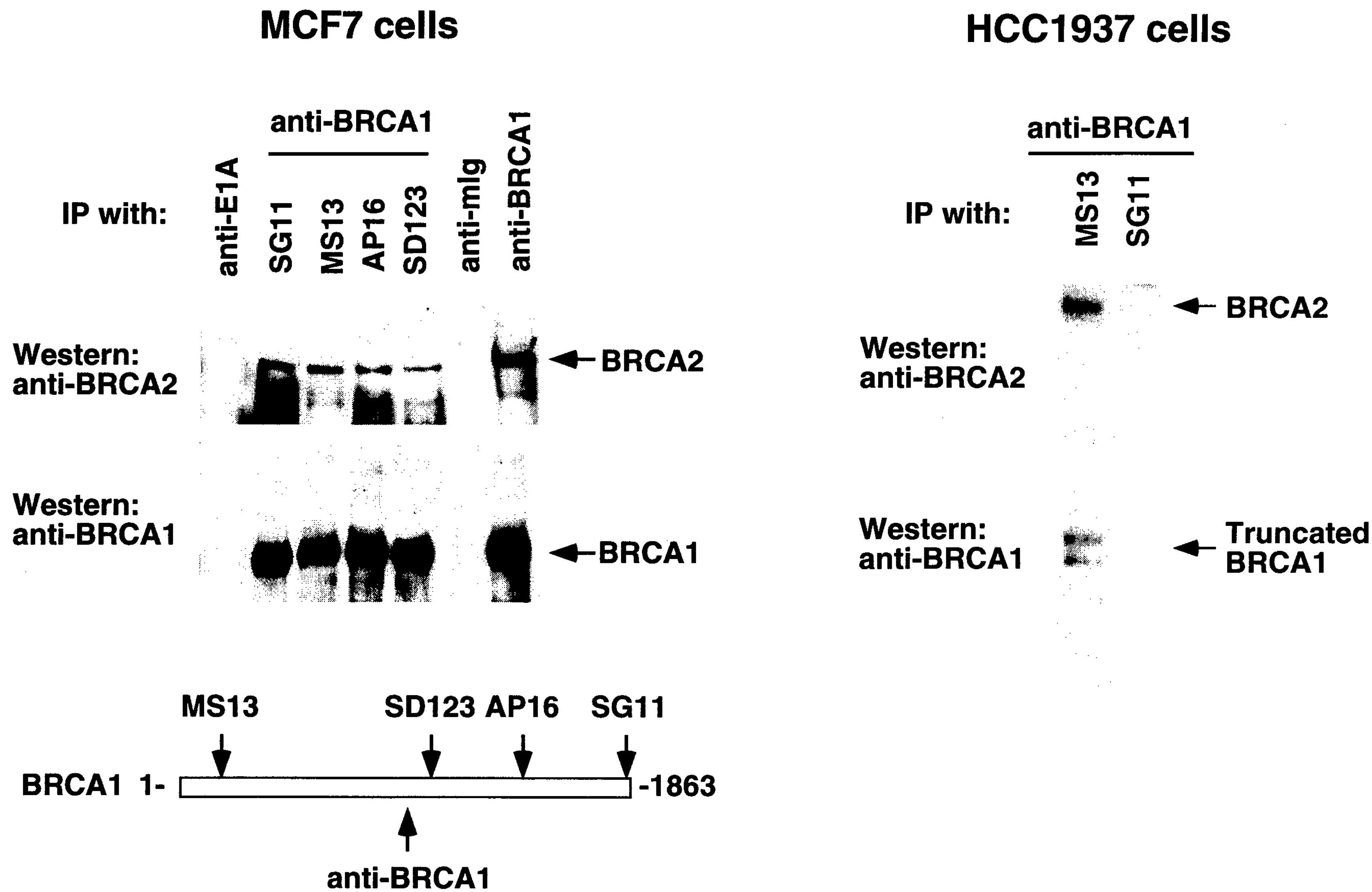
MCF7 cells
HCC1937 cells
IP with:
anti-BRCA1
anti-E1A
SG11
MS13
AP16
SD123
anti-mIg
anti-BRCA1
Western: anti-BRCA2
Western: anti-BRCA1
BRCA2
BRCA1
IP with:
anti-BRCA1
MS13
SG11
Western: anti-BRCA2
Western: anti-BRCA1
BRCA2
Truncated BRCA1
MS13
SD123
AP16
SG11
BRCA1 1-
-1863
anti-BRCA1

Figure 2B

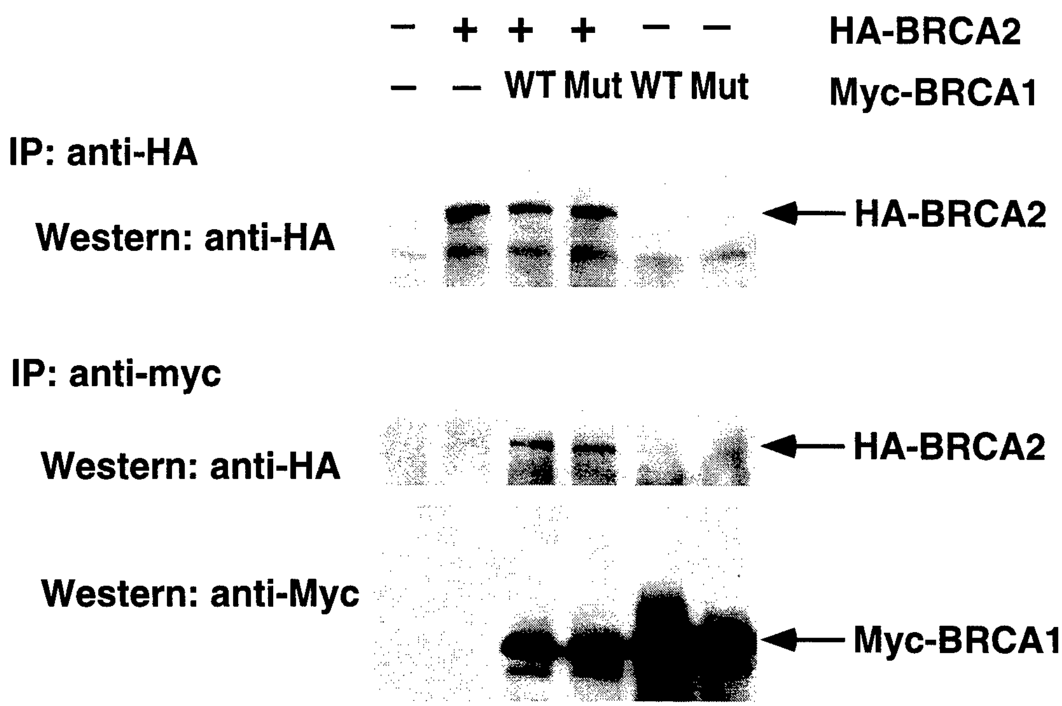
– + + + – – HA-BRCA2
– – WT Mut WT Mut Myc-BRCA1
IP: anti-HA
Western: anti-HA
HA-BRCA2
IP: anti-myc
Western: anti-HA
HA-BRCA2
Western: anti-Myc
Myc-BRCA1

Figure 3A

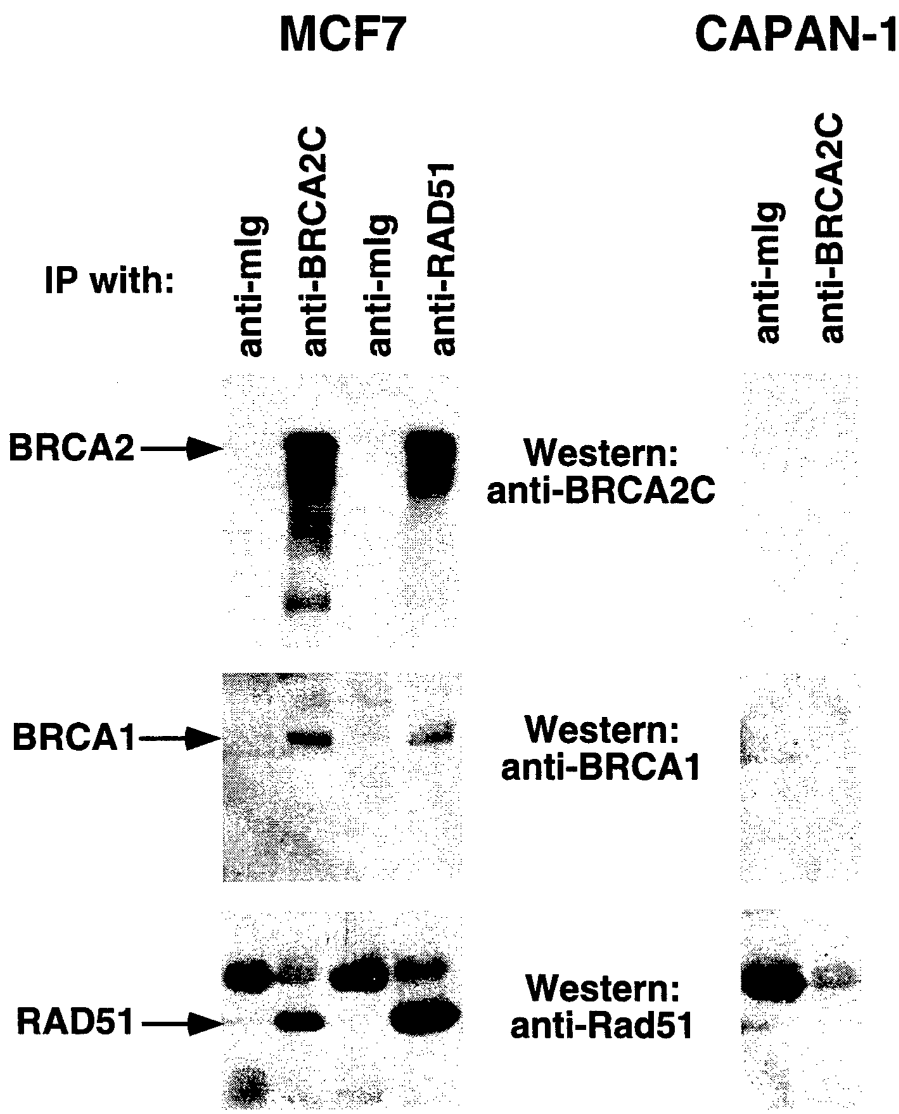
MCF7
CAPAN-1
IP with:
anti-mIg
anti-BRCA2C
anti-mIg
anti-RAD51
anti-mIg
anti-BRCA2C
BRCA2
Western: anti-BRCA2C
BRCA1
Western: anti-BRCA1
RAD51
Western: anti-Rad51

Figure 3B

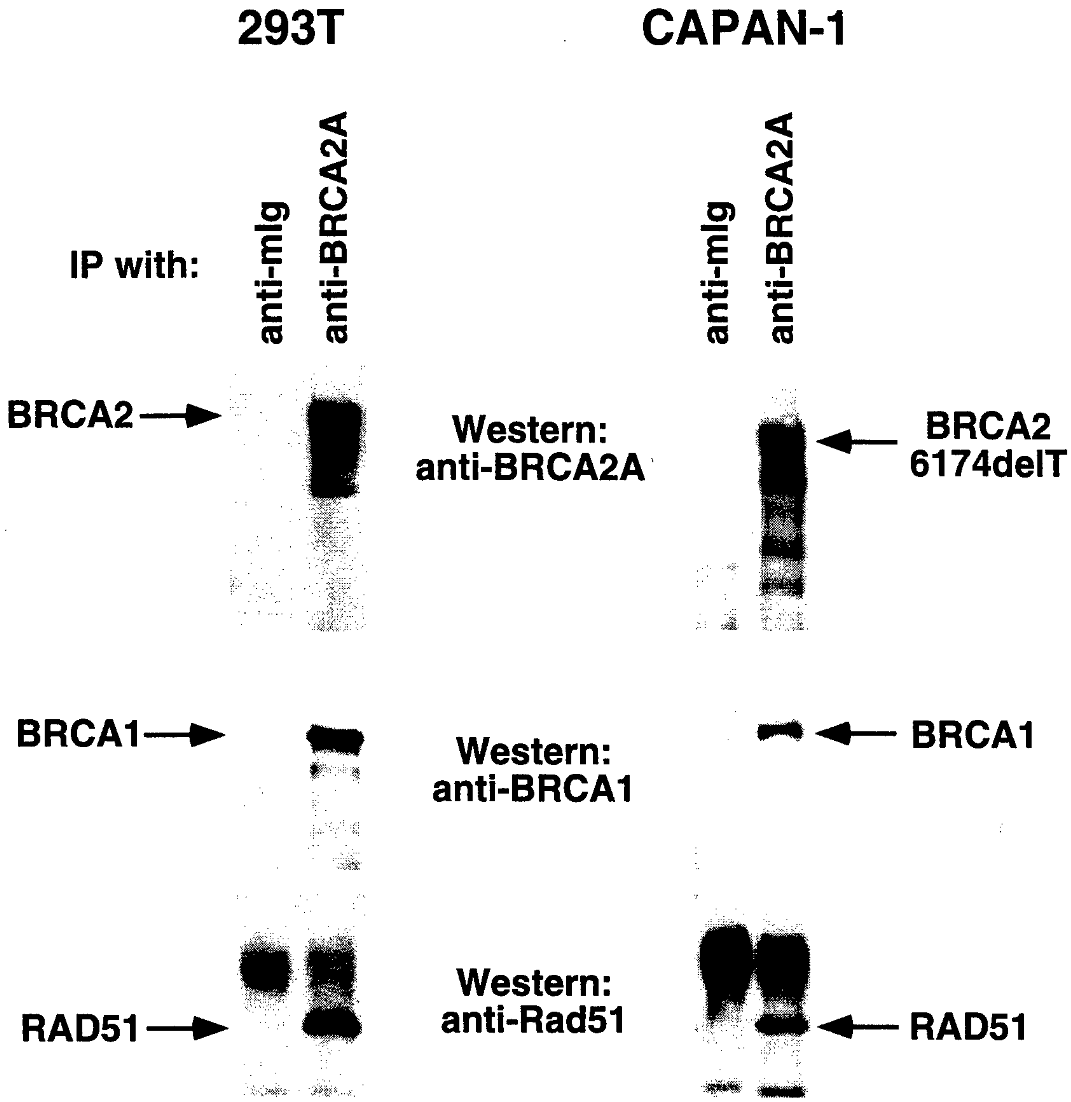
293T
CAPAN-1
IP with:
anti-mIg
anti-BRCA2A
anti-mIg
anti-BRCA2A
BRCA2
Western:
anti-BRCA2A
BRCA2
6174delT
BRCA1
Western:
anti-BRCA1
BRCA1
RAD51
Western:
anti-Rad51
RAD51

Figure 4A

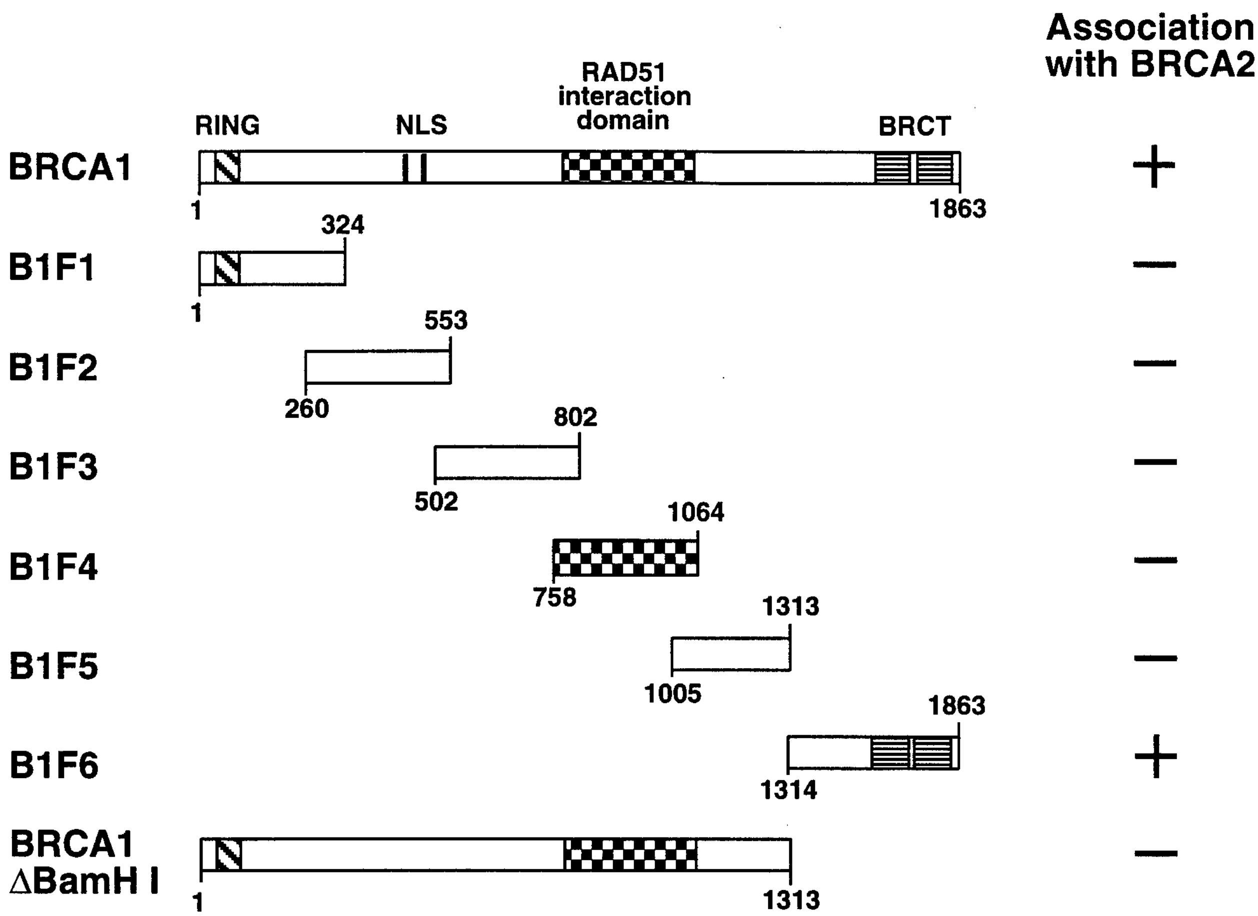

Association with BRCA2
RAD51 interaction domain
RING
NLS
BRCT
BRCA1
1
1863
+
B1F1
324
1
−
B1F2
553
260
−
B1F3
802
502
−
B1F4
1064
758
−
B1F5
1313
1005
−
B1F6
1863
1314
+
BRCA1 ΔBamH I
1
1313
−

Figure 4B

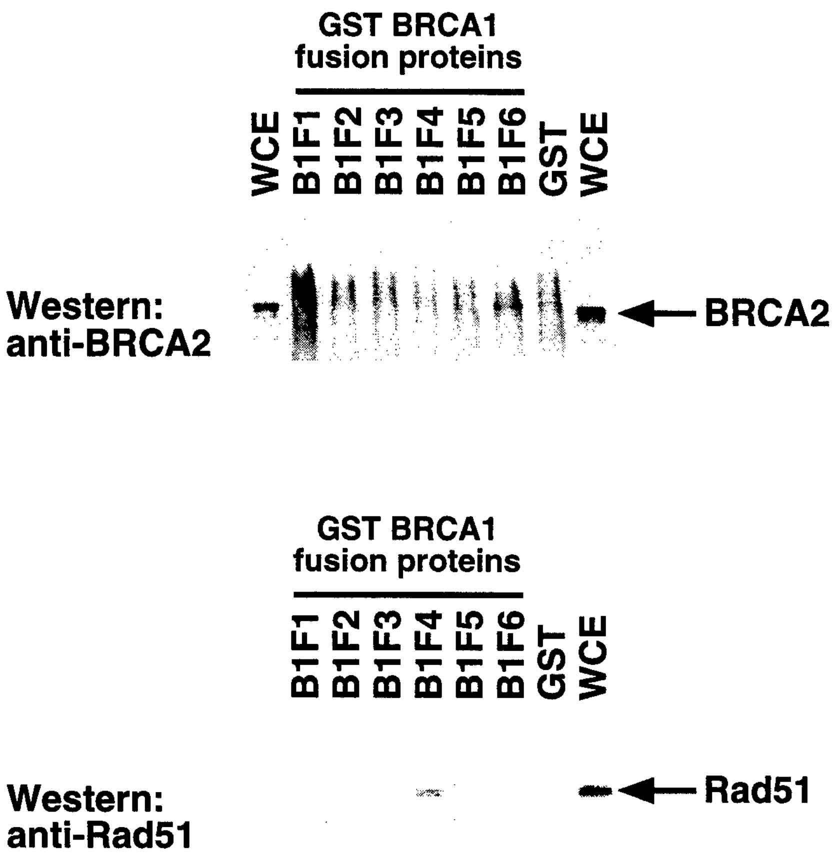
GST BRCA1
fusion proteins
WCE
B1F1
B1F2
B1F3
B1F4
B1F5
B1F6
GST
WCE
Western:
anti-BRCA2
BRCA2
GST BRCA1
fusion proteins
B1F1
B1F2
B1F3
B1F4
B1F5
B1F6
GST
WCE
Western:
anti-Rad51
Rad51

Figure 4C

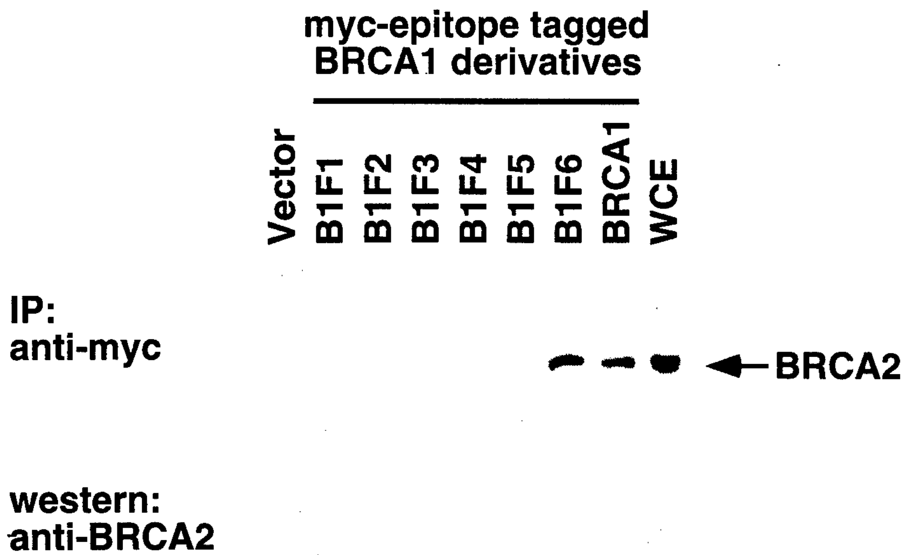
myc-epitope tagged
BRCA1 derivatives
Vector
B1F1
B1F2
B1F3
B1F4
B1F5
B1F6
BRCA1
WCE
IP:
anti-myc
BRCA2
western:
anti-BRCA2

Figure 4D

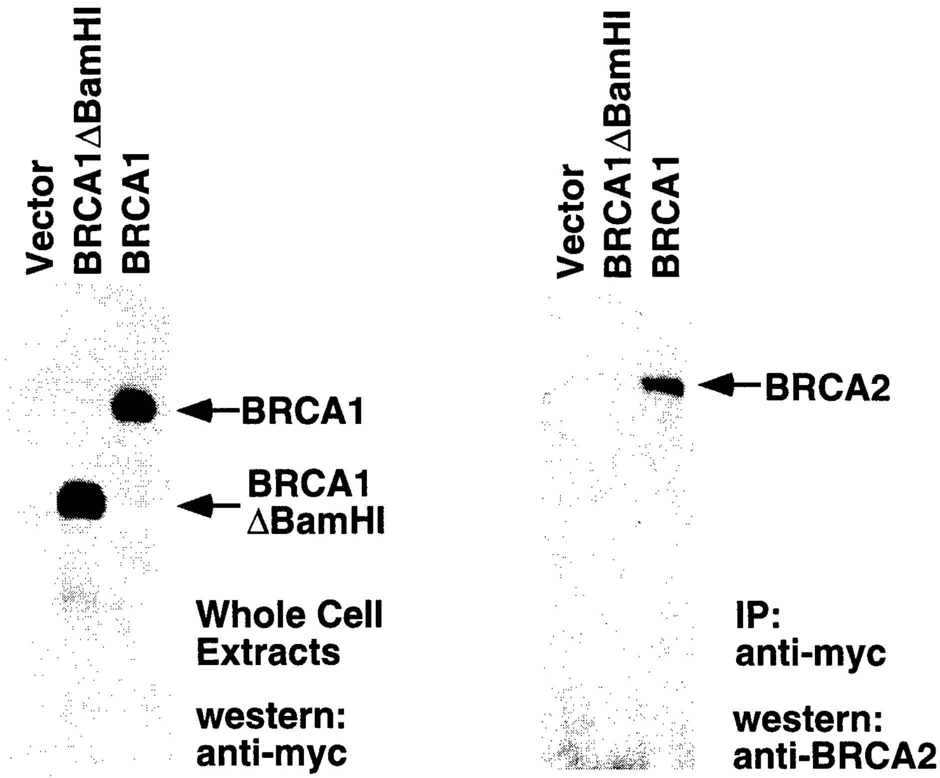
Vector
BRCA1ΔBamHI
BRCA1
BRCA1
BRCA1
ΔBamHI
Whole Cell
Extracts
western:
anti-myc
Vector
BRCA1ΔBamHI
BRCA1
BRCA2
IP:
anti-myc
western:
anti-BRCA2

Figure 5

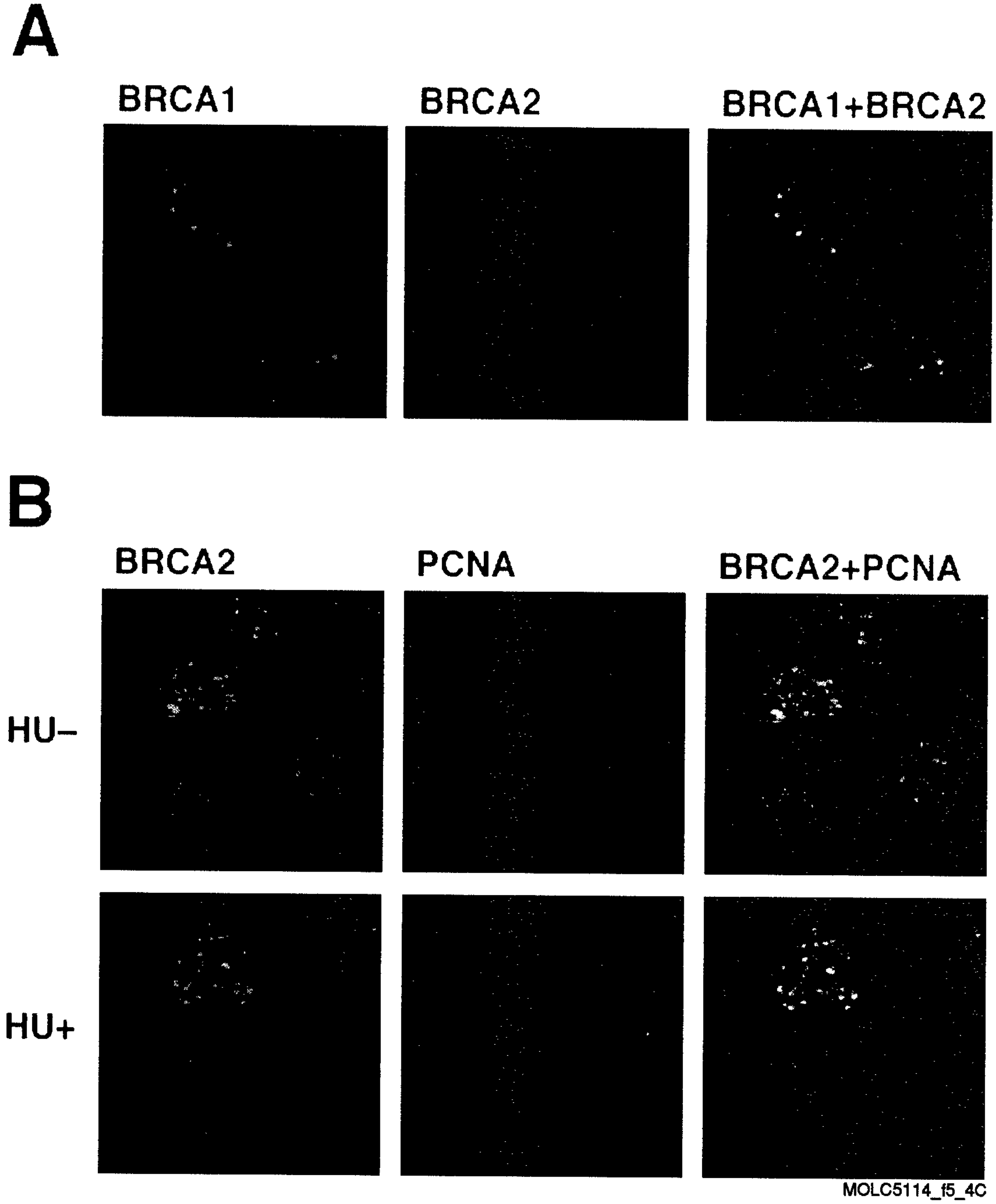
A
BRCA1
BRCA2
BRCA1+BRCA2
B
BRCA2
PCNA
BRCA2+PCNA
HU–
HU+
MOLC5114_f5_4C

Figure 6

A BRCA2+SCP3

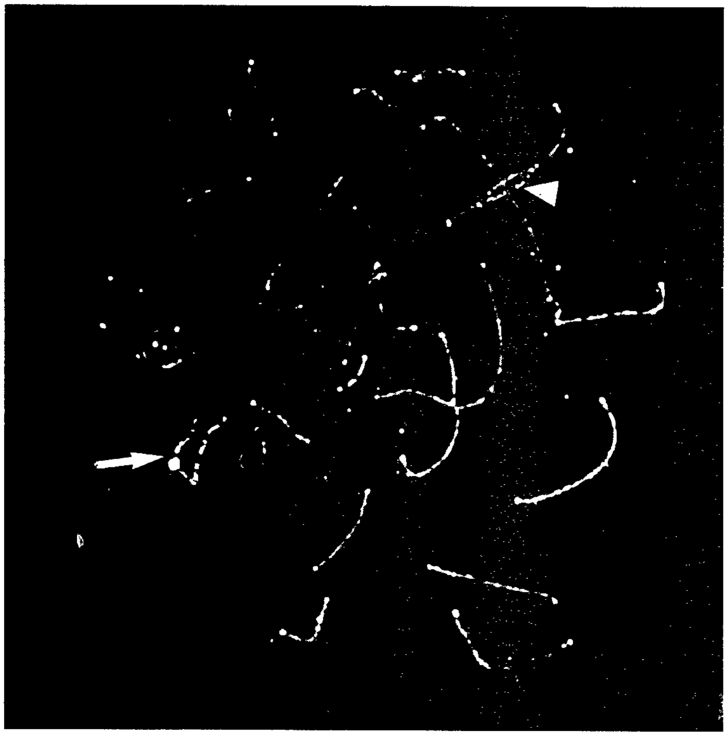

B BRCA1 BRCA2 BRCA1+BRCA2